



HUNGARIAN
ACADEMY
OF SCIENCES

Hungarian Agricultural Engineering

N^o 33/2018

Editors-in-Chief:

Dr László TÓTH
Dr. László KÁTAI

Managing Editor:

Dr. Csaba FOGARASSY

Secretary of Editorial board:

Dr. László MAGÓ

Editorial Board:

Dr. David C. FINGER

Dr. György SITKEI

Dr. Gábor KESZTHELYI-SZABÓ

Dr. László TÓTH

Dr. János BEKE

Dr. István SZABÓ

Dr. István J. JÓRI

Dr. Béla HORVÁTH

Dr. Péter SEMBERY

Dr. László FENYVESI

Dr. Csaba FOGARASSY

Dr. Zoltán BÁRTFAI

Dr. László MAGÓ

Dr. Bahattin AKDEMIR

Dr. R. Cengiz AKDENIZ

Dr. József NYERS

Dr. Mičo V. OLJAČA

Dr. Zdenek PASTOREK

Dr. Vijaya G.S. RAGHAVAN

Dr. Lazar SAVIN

Dr. Bart SONCK

Dr. Goran TOPISIROVIĆ

Dr. Valentin VLADUT

**PERIODICAL OF THE COMMITTEE OF
AGRICULTURAL ENGINEERING OF
THE
HUNGARIAN ACADEMY OF SCIENCES**

Published by

Szent István University, Gödöllő
Faculty of Mechanical Engineering
H-2103 Gödöllő, Páter K. u. 1.



Gödöllő
2018

Published online: <http://hae-journals.org>
HU ISSN 0864-7410 (Print)
HU ISSN 2415-9751(Online)

PREFACE

In the name of the Committee of Agricultural and Biosystem Engineering of the Hungarian Academy of Sciences we would like to welcome everyone who is interested in reading our journal. The Hungarian Agricultural Engineering (HAE) journal was published 30 years ago for the very first time with an aim to introduce the most valuable and internationally recognized Hungarian studies about mechanization in the field of agriculture and environmental protection. In the year of 2014 the drafting committee decided to spread it also in electronic (on-line and DOI) edition and make it entirely international. From this year exclusively the Szent István University's Faculty of Mechanical Engineering took the responsibility to publish the paper twice a year in cooperation with the Hungarian Academy of Sciences. Our goal is to occasionally report the most recent researches regarding mechanization in agricultural sciences (agricultural and environmental technology and chemistry, livestock, crop production, feed and food processing, agricultural and environmental economics and energy production) with the help of several authors. The drafting committee has been established with the involvement of outstanding Hungarian researchers who are recognized on international level as well. All papers are selected by our editorial board and a triple blind review process by prominent experts which process could give the highest guarantee for the best scientific quality. We hope that our journal provides accurate information for the international scientific community and serves the aim of the Hungarian agricultural and environmental engineering research.

Gödöllő, 01.08.2018.



Dr. László KÁTAI
editor in chief



Dr. László TÓTH
editor in chief



ANALYSIS OF THE TOWED AGRICULTURAL MACHINERY MANUFACTURERS IN EUROPE

Author(s):P. Kiss¹ – J. Hajdú² – L. Máthé¹ – J. Dobos¹ – L. Magó¹**Affiliation:**¹Szent István University, Faculty of Mechanical Engineering,²NARIC, Institute of Agricultural Engineering**Email address:**

kiss.peter@gek.szie.hu, mathe.laszlo@gek.szie.hu, mago.laszlo@gek.szie.hu, jozsef@hajdu.co.hu

Abstract

The purpose of our analysis was to gather data on suspension manufacturers and users and to determine their market shares, using the databases of major agricultural machinery exhibitions. To carry out this work, we developed a methodology to examine and analyse the databases of the four largest European agricultural machinery exhibitions. We particularly endeavoured to distinguish manufacturers and distributors of the machinery, and to eliminate duplicates. The market for agricultural trailers and machinery built on trailer superstructures is highly diverse and complex, posing serious difficulties for evaluation and statistical analysis of the data and for determination of actual sales figures.

Keywords

suspension, trailer, agricultural machinery, machinery manufacture, statistics

Introduction

Trailed machinery and transporters with various types of suspension account for a large proportion of the manufacture and sale of agricultural machinery in Europe. These trailed vehicles cover a wide functional range: agricultural trailers, tanker trailers, trailed fertilisers and manure spreaders, sprayers and fodder mixing wagons. They also have many different types of suspension: tandem, tridem, sprung, rigid, steered, etc.

About 40 companies worldwide make round balers, which come in of various constructions and sizes. Total annual sales have been typically between 30,000 and 35,000 units in recent years. Round balers have the common feature of being towed and driven by tractor. All have either a single-axle or – the versions combined with a bale wrapper – twin or tandem axle suspensions. The latter, owing to their weight and towing speed, which is maximised at up to 40–50 km/h, generally require braked axles.

There are considerably fewer companies – 13 or 14 worldwide – that make the more complicated large square balers. Europe has the greatest concentration of production, with nine manufacturers. There are about 3500–3700 large square balers sold annually worldwide.

More than 80 companies worldwide make sprayers. They are made in a wide range of constructions (suspended, liftmounted, trailed and self-propelled) and sizes. In Europe, some 55 manufactures make sprayers (field flat and axial fan, directed

nozzle, tunnel, etc.). Most of them make trailed sprayers with single and double axle suspension, with tanks ranging in size from 1000 to 12,000 litres.

Fertiliser spreaders are also made in various constructions. Most widespread in Europe are tractor-mounted spinning disc types with tank capacities of between 400 and 3000 litres. Trailed spreaders, with tank capacities of between 3500 and 10,000 litres, are used mainly on large farms and are made in much smaller quantities. [1, 2]

To our knowledge, there are no continental statistical surveys regarding the distribution of this machinery, its market and the manufacturers involved, and neither are national statistics available in every case. In an attempt to fill this gap, we put questions to the agricultural machinery manufacturers and traders of each country to find answers to our questions, but our enquiries were only partially successful. This prompted us to take a new approach, using data available on exhibitors at the four largest European agricultural exhibitions to survey the number of European makers and users of suspensions, their capacities and where possible, their market shares.

Here we present the results of systematically gathering data from each exhibitor's internet catalogue and carrying out analysis and data processing over a period of several months.

2. Material and Method**Components of the research work**

1. Target area: the countries of Europe (without CIS)
2. Product types:
 - a. Agricultural vehicles (standard trailers, tippers, trailed tankers, manure spreaders, forage transport wagons etc.)
 - b. Components by type (tridem, boogie, steerable and rigid)
3. Period:
 - a. 2014, 2015 and 2016

Countries and Exhibitions covered by the project

We included the following countries in our market research:

1. Austria
2. Belgium
3. Czech Republic
4. Denmark
5. Estonia
6. Finland

- 7. France
- 8. Netherlands
- 9. Poland
- 10. Latvia
- 11. Lithuania
- 12. Luxembourg
- 13. Hungary
- 14. Great Britain
- 15. Germany
- 16. Italy
- 17. Portugal
- 18. Spain
- 19. Slovenia
- 20. Ukraine
- 21. Sweden

- Brno 2016
- Paris/SIMA 2015

From our experience, we know that these exhibitions cover almost all the products of agricultural machinery manufacturers. We also involved further companies in the study, mainly those in Finland, from agricultural journals.

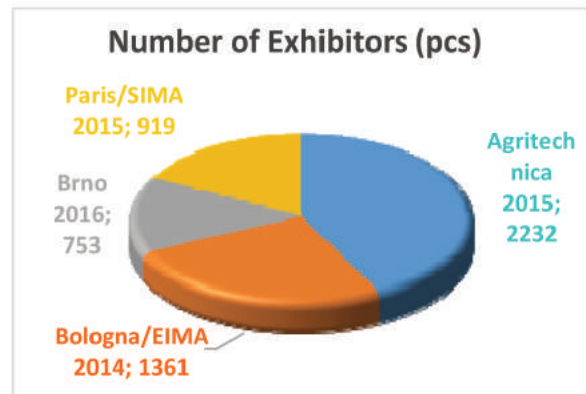


Figure 1. Numbers of companies/exhibitors at the exhibitions

Table 1. The number of companies enumerated per country and per exhibition

exhibition / country	Austria	Belgium	Czech Republic	Denmark	Estonia	Finland	France	Netherlands	Poland	Latvia
Agritechnica 2015	71	23	24	48	2	37	98	125	65	1
Bologna/EIMA 2014	18	12	3	4	0	3	51	14	10	0
Brno 2016	18	19	626	1	0	0	1	7	19	0
Paris/SIMA 2015	14	19	7	9	1	6	530	33	25	0

Table 1. Continued

Lithuania	Luxembourg	Hungary	Great Britain	Germany	Italy	Portugal	Spain	Slovenia	Ukraine	Total
6	5	9	43	1208	390	5	45	17	10	2232
0	0	1	13	57	1100	4	63	8	0	1361
0	0	20	3	24	12	0	1	0	2	753
3	6	2	18	67	129	7	33	4	6	919

Total: 5265

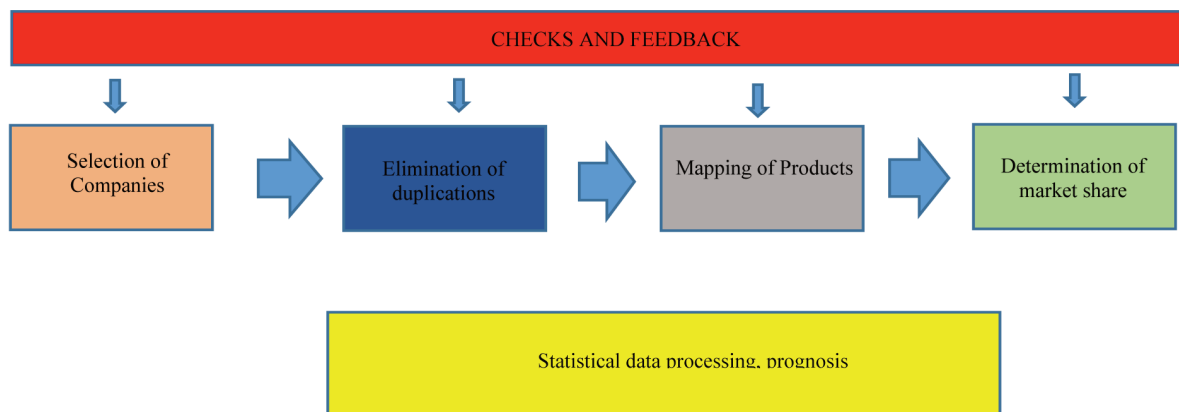


Figure 2. Method of determining relevant companies and their market shares

Table 1 shows that Agritechnica hosted the largest number of companies (2232), followed by the Bologna/EIMA exhibition (Italy). In third place was SIMA in Paris, and in fourth, Brno in the Czech Republic. These figures are distorted, however, by the large numbers of small exhibitors from the host countries. There were 1100 Italian exhibitors at EIMA, for example, and 626 Czech companies at Brno, many of the latter being sales operations with no manufacturing capacity.

Figure 1 shows the number of exhibitors on a pie chart.

Taking account of the international nature of the exhibitions and the numbers of exhibitors there, the ranking is as follows:

From international agricultural journals, we examined a further 25–30 companies, bringing the total to about 5300 companies. There were of course many repetitions among the companies enumerated corresponding to presence at more than one exhibition.

Research methods

Figure 2 shows the methodology we developed to enumerate the relevant companies and determine their market shares.

3. Results and Discussion

We grouped the enumerated companies by the countries listed in the introduction and eliminated the duplicates. A total of 513 relevant companies remained. This is the number of companies in these countries of Europe which manufacture, use and sell agricultural suspensions. The distribution of relevant companies by country is given in Table 2.

Table 2. Countries and relevant companies

Countries	Number of relevant companies (pcs)
Austria	17
Belgium	4
Czech Republic	43
Denmark	18
Estonia	1
Finland	26
France	48
Netherlands	31
Poland	19
Latvia	0
Lithuania	5
Luxembourg	0
Hungary	17
Great Britain	19
Germany	106
Italy	139
Portugal	3
Spain	10
Sweden	3
Slovenia	3
Ukraine	2

4. Results

Determination of the market shares of major manufacturers by product category

Most round baler machinery manufacturers are based in Europe, and the largest number of units are made in Germany and Italy.

The two largest manufacturers are Claas and Krone of Germany. They produce the largest range of types and models and alternate in the position of European market leader. Other large manufacturers are the Lely-Welger (German-Dutch), the CNH Agriculture (Italian), the Kuhn (French) and the John Deere (USA). Welger filed the first patent for a fixed-chamber baler and is a dynamic manufacturer and developer within the Lely Group. CNH Agriculture engages in cooperation in the manufacture of balers. Deutz-Fahr of Germany, part of the SDF Group, also makes balers. Kverneland, owned by Kubota, sells balers from its Italian Galignani baler manufacturing base under the names Kverneland, Vicon and Kubota. Most of the remaining manufacturers (Bergam, Ferraboli, Mascar, Maschio, Wollagri etc.) are Italian. See Figure 3.



Figure 3. Market shares of round baler manufacturers

The design of large square balers is based on a machine produced by Hesston (now part of AGCO) of the USA. The two large manufacturers, Claas and Krone, dominate the market in this product group. Claas is the outright market leader, but Krone does not lag it in the range of types and models. Another major manufacturer is CNH Agriculture, which markets several models under both of its brand names, New Holland and Case IH. John Deere recently added large square balers to its product range and is rapidly developing new models. Previously, it sold large square balers made by Krone.

Massey Ferguson has been marketing these products for some time and has recently been joined by Fendt, another AGCO brand. Kuhn also holds a 5% market share. Among the other manufacturers are Deutz-Fahr and several Italian companies, including Supertino and Cicoria. See Figure 4.

Square balers are also tractor-trailed. Depending on size, balers may have single-axle suspension or twin or tandem axle braked suspension, with balloon tyres.

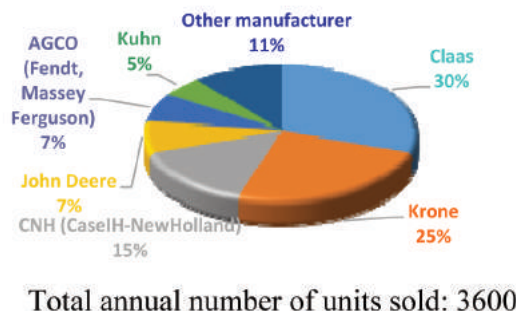


Figure 4. Market shares of square baler manufacturers

Trailed and self-propelled sprayers are dominant in agriculture outside Europe (North and South America, Australia, etc.). About 22,000 trailed field and plantation sprayers are sold each year. The most widespread among European small farms are tractor-mounted sprayers of small capacities (between 400 and 1500 litres). The features of trailed sprayers are of benefit primarily to large and commercial farms and agricultural contractors. The largest worldwide manufacturer of trailed sprayers is the French Exel Group, which owns two previously independent brands, one of which – Hardi – is the clear market leader. Other large manufacturers are Amazone, the Kubota/Kverneland Group, John Deere, the Bergam Group, Caffini, Agrio, the plantation sprayer companies SAE and Unigreen, and more recently Horsch and Lemken. Damman is strong in self-propelled sprayers, but also has a presence with trailed sprayers. See Figure 5.



Figure 5. Market shares of trailed sprayer manufacturers

In large farms outside Europe, particularly in Australia, trailed fertiliser spreaders are in the majority. About 11,000 of them are sold worldwide each year. Most typically, they have a tank of between 5000 and 8000 litres capacity and single-axle braked suspension.



Figure 6. Market shares of trailed fertiliser spreader manufacturers

Those with larger fertiliser tanks have braked twin or tandem axles. In Europe, Amazone of Germany is the largest manufacturer, producing trailed single-axle fertiliser spreaders of capacities between 5500 and 8200 litres. Other large manufacturers are Bredal, Güstrow and the French company Sulky, although the two Polish manufacturers UNIA and ABRZEG also have good positions on European markets. See Figure 6.

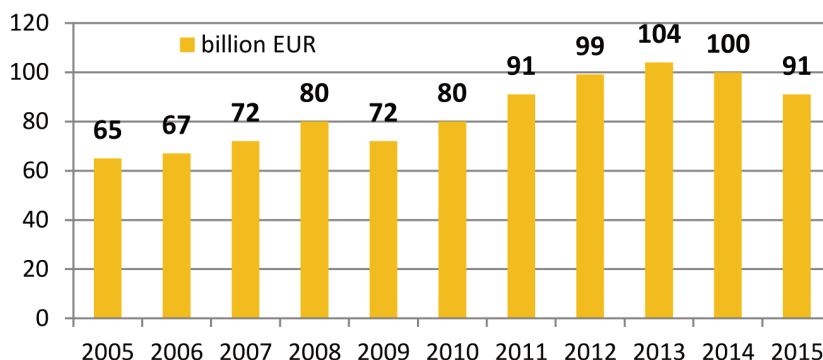


Figure 7. World agricultural machinery turnover between 2005 and 2015. [3, 4, 5]

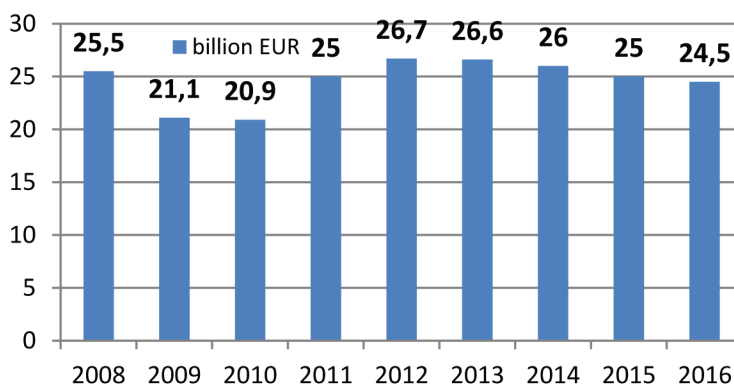


Figure 8. Agricultural machinery turnover in EU countries between 2008 and 2016. [3, 6]

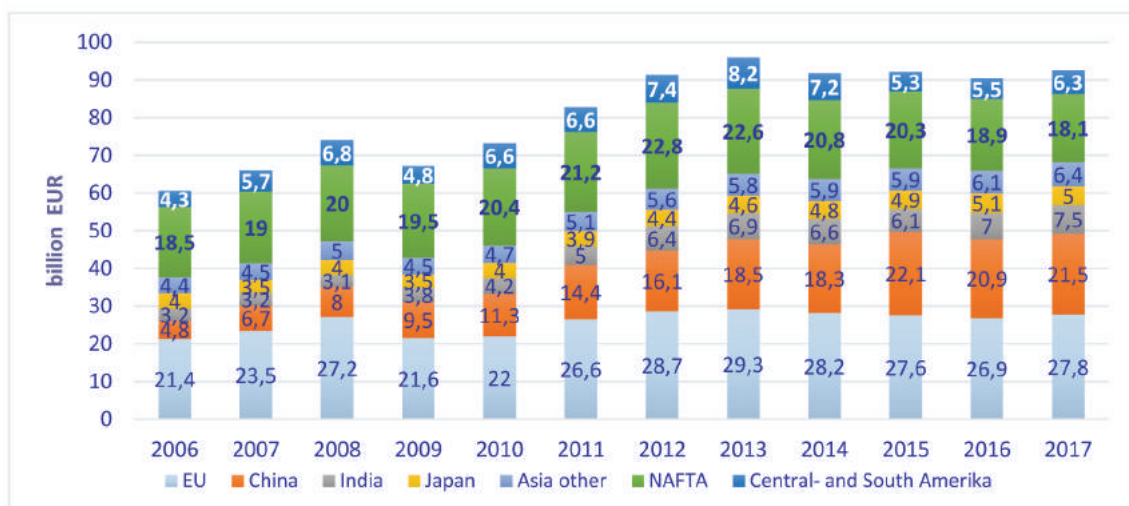


Figure 9. Agricultural machinery manufacturing volume worldwide in billion euros [7, 8]

Global and regional agriculture machinery market trends

There are cyclical variations in agricultural machinery manufacture. This means that the numbers of units of trailed agricultural vehicles increases in some periods and decreases in others [9]. Agriculture is subsidised in every country of Europe. The cycles are to some extent due to the unequal effects of subsidies, but also to the periodic overproduction, cutbacks and increased demand that arise from the laws of the market [10, 11].

Overall, the market in agricultural machinery contracted by 9% worldwide in 2015, as shown on Figure 7. The 91 billion-euro turnover exactly matches that of 2011. The recession is clearly perceptible.

There has been a steady contraction in the EU agricultural machinery market over the last two or three years. This is clear from Figure 8. In 2015, there was a decrease of 8%: the total value of agricultural machinery sales was 23.8 billion euros that year, compared with 26 billion in 2014. The peak was in the post-recession years of 2012 and 2013, when the EU agricultural machinery market swelled to 26.6 and 26.7 billion euros respectively. The figure for 2015 was the lowest for the EU in the period following the economic crisis of 2009–2010. [10, 11]

A good illustration of global trends in the agricultural machinery market is world agricultural machinery production, shown in Figure 9. Following the crisis of 2009, output grew steeply every year until 2013; it then faltered and entered a decreasing trend. There was stagnation until 2016, but preliminary figures show a slightly growing in 2017.

This global trend appears with some phase lag in countries such as Japan and the Asian countries (not including India and China). There, machinery manufacturing continuously grows. Low world price levels are currently being forecast for agricultural commodities, and it can only be hoped that the machinery manufacturing output and the agricultural machinery market will now stabilise.

5. Conclusions and Proposals

The purpose of our analysis was to gather data on suspension manufacturers and users and to determine their market shares, using the databases of major agricultural machinery exhibitions.

To carry out this work, we developed a methodology to examine and analyse the databases of the four largest European agricultural machinery exhibitions. We particularly endeavoured to distinguish manufacturers and distributors of the machinery, and to eliminate duplicates.

The figures showed that German and Italian companies dominate this sector of agricultural machinery manufacturing. More than a hundred manufacturers in these countries incorporate various suspensions into their products. France, the Czech Republic, the Netherlands, Denmark, Finland, the UK, Poland and Austria also have substantial numbers of machinery manufacturers, but most of them serve their domestic markets and have very small shares of the European market in finished products.

Of the product groups under examination, those with the highest levels of sales in terms of number of units were round balers, trailed sprayers and fertiliser spreaders. There is also a substantial market in large square balers, but rather than the number of units, it is the value of machines sold that is significant.

The market for agricultural trailers and machinery built on trailer superstructures is highly diverse and complex, posing serious difficulties for evaluation and statistical analysis of the data and for determination of actual sales figures [12, 13]. Consequently, although we achieved the aim of presenting European manufacturing for this product groups, were unable to fulfil all the objectives of our research.

References

- [1] Hajdú J.: 2016. Big Six = A vezető „Hatok” – A világ vezető hat legnagyobb multinacionális mezőgépgyártójának gazdálkodási mutatói, Mezőgazdasági Technika, 2016. No. 10.
- [2] Heimann J., Haus A.: 2016. Global agricultural machinery markets, VDMA, 2016 January
- [3] Heimann, J., Nonnenmacher P.: 2015. Market Newsletter VDMA, 2015 Oktober
- [4] Boldog V., Bábáné D. E.: 2016. AKI Statisztikai jelentések, Mezőgazdasági gépek forgalma Vol. 26. No. 1. 2016. pp 11.
- [5] Heimann, J.: 2015. European Market Newsletter, VDMA, 2015 March
- [6] CEMA Economic Report.: 2017. European tractor market declined with 6.7% in 2016
- [7] Magó L.: 2015. Agrárpolitika és piacsabályozás a mezőgépi-kereskedelemben – nemzetközi áttekintés, Journal of Central European Green Innovation, Vol. 3, No 2, pp. 83-92.
- [8] Magó L.: 2016. Aktuális mezőgép-, és termény-piaci folyamatok Európában és a világban, Agrárágazat, mezőgazdasági havilap, Vol. 17, No. 5, p. 102-105.
- [9] Borocz M., Szoke L., Horvath B.: 2016. Possible climate friendly innovation ways and technical solutions in the

agricultural sector for 2030. Hungarian Agricultural Engineering, Vol. 29. pp. 55-59. <http://dx.doi.org/10.17676/HAE.2016.29.55>

[10] Kiss P., Hajdú J., Máthé L., Magó L.: 2017. Survey of the European Manufacturers of Towed Agricultural Vehicles and Machinery and Their Market, Conference Proceedings of the 19th International & 14th European-African Regional Conference of the ISTVS, Budapest, September 25–27, 2017.

[11] Magó L.: 2013. Examination of the Agricultural Machine Distribution in Hungary, Hungarian Agricultural Engineering, Periodical of the Committee of Agricultural Engineering of the Hungarian Academy of Sciences, Vol. 25/2013. pp. 9-12. – HU ISSN 0864-7410

[12] Bártfai Z., Blahunka Z., Faust D., Ilosvai P., Nagy B., Szentpétery Zs., Lefánti R. 2009: Synergic Effects in the Technical Development of the Agricultural Production. Mechanical Engineering Letters 2009. Vol. 3., SZIE GÉK, pp. 142-147.

[13] Hajdú J.: Mezőgazdasági tehergépkocsik, Mezőgazdasági Technika, 2016. No. 3.



ALTERNATIVE UTILIZATION OPTIONS IN MULTI-FUNCTION COMPOSTING TECHNIQUES

Author(s):

M. Czikkely¹ – Zs. Tóth² – Cs. Fogarassy³

Affiliation:

¹Assistant lecturer, Doctoral candidate, Climate Change Economics Research Centre, Faculty of Economics and Social Sciences, Szent István University, Hungary

²Faculty of Economics and Social Sciences, Szent István University, Hungary

³Associate Professor, Director of Climate Change Economics Research Centre, Faculty of Economics and Social Sciences, Szent István University, Hungary

Email address:

czikkely.marton@gtk.szie.hu, tothzsofia1215@gmail.com, fogarassy.csaba@gtk.szie.hu

Abstract

Composting is a long-known and used process to treatment of biodegradable (and thus recyclable) waste containing organic materials. Here we undertake to review and analyse specific compost types, which could be used in multifunctional way due to the nature of mature compost or the composting process.

Keywords

Heating energy production, biogas production, water treatment, microbiological treatment system

1. Introduction

Composting is a microbiological process that depends on the optimum activity of mixed populations of mesophilic and thermophilic bacteria's and ultimately provides a substance that can be used for soil improvement or fertilization [1]. Compost can be considered as an organic fertilizer which is made from solid and liquid organic materials of animal or vegetable origin, in directed degradation processes [2]. To successfully complete the process, mixed "vaccine" with the composted materials containing microorganisms (various bacteria or fungi). The degradation process has the role of anaerobic and aerobic microbe populations. Biodegradation of organic matter of compost is carried out by these microorganisms (Table 1) [2]. At the end of the composting process, mature compost production ended. That means the particles (with a size smaller than 25 mm) contains at least of 90% by weight of the mature compost. [3].

Due to various physical, chemical and microbiological characteristics, the composting process produce mature compost. These indicators are paramount importance for the process. Sometimes these are not most ideal, so regulation required [4]. More parameters could be change easily (such as temperature, water contaminant, diversity of microbiological species) [5]. These physical and chemical parameters have priorities during the composting process [6]:

Table 1. The main bacterial and fungus species of composting processes (Source: De Corato et al., 2018, [3])

Bacterial species	Fungus species
Aerobacter (aerogenes)	Thermomyces lanuginosus
Pseudomonad sp.	Thermoascus aurantiacus
Flavobacterium sp.	Mucor pusillus
Micrococcus sp.	Mucor miehei
Sarcina sp.	Humicola insolens
Cellulomonas folia	Talaromyces duponti
Mycococcus virescens	Chaetomium thermophile
M. fulvus	Sporotrichium thermophilum
Thibacillus thiooxidans	Myriococcum albomyces
Thermomonospora fusca	Saccharomyces sp.

1. Physical parameters:

- Temperature (15-70°C)
- Respiration coefficient (CO₂/O₂ proportion)
- Temperature–oxygen consumption (linear correlation)
- Water contaminant and temperature correlation
- Airways and porosity correlation (inverse correlation)

2. Chemical parameters:

- Proportion of water and degradable dry matter content (10:15)
- Amount of \sum Nitrogen (0,5-2,5 %)
- Amount of \sum Organic matters (10-25 %)
- Proportion of C and N (C/N) (10:30)
- Water soluble organic matter content (0-120 mg/g)
- CO₂ production speed (30-100 ml/kg/h)
- NO₃-N (0-700 ppm), and NH₄-N (0-5000 ppm) contents
- pH value (5,0-8,0)

Maintaining the conditions of composting is the most important key issue. If all the physical, chemical and microbiological parameters are correct, the composting process is shown in the following sematic diagram (Figure 1) [7].

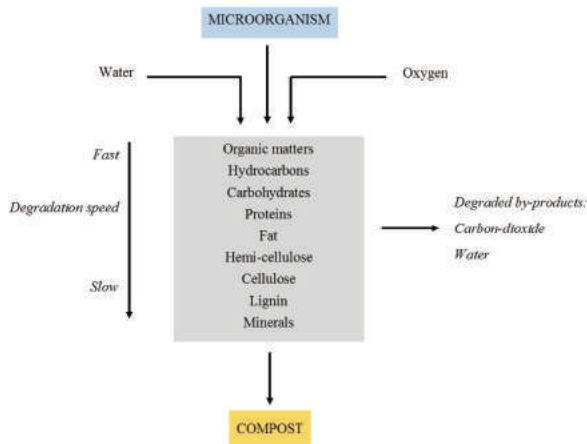


Figure 1. The main biochemical processes during composting phases (Based on Wang et al., 2018, [7]; Authors own edition)

The composting process could be divided into four main phases (initial, thermophilic, transformation and maturation phase). The first stage is introductory-initial phase [8]. In this phase, the mesophilic temperature range is typical. It can be traced to growth of microbes, increasing organic acid content and the consequent decrease in pH value. The second (thermophilic) phase begins with a steady increasing temperature [9]. The most important at this stage the temperature of compost rises above 50°C, and could reach up to 70-75°C value. Another important feature of this thermophilic phase is the partial decomposition of cellulose and hemicellulose matters [10]. The pH value rises and reaches the alkaline range. The thermophilic phase takes 2-5 weeks. As a result of continuous degradation, reduced the amount of nutrient and temperature [10][11]. At this time, the third (transformation) phase begins, which occurs in the mesophilic temperature range at 40-45°C value. At this stage, the lignin compounds are broken down. As a result of a further decrease in temperature, the fourth (maturing) phase begins. This phase is the final composting process. Humic substances formed into humic fractions and humic acids [12].

Most of the compostable substances should be suitable for biodegradations. This can be achieved by mixing different materials (e.g. microbial culture, semi-finished or finished compost). The degradable material must meet the following conditions [12], [13]:

- Humidity (40-60 %)
- Continuously oxygen demand
- Contains soluble salts (pl. FeCl₃, Al) at a lower concentration
- C/N ratio
- Degradable organic matter content
- pH value (optimal: 6,0-7,5)
- Lower concentration of heavy metals

High heavy metal content has negative effect on microorganisms because it stops their physiological processes and changes their metabolic processes. In summary, it can be concluded that the composting raw materials made from several compounds, and all of them are important role during the composting process or at the end of the composting process. The main compounds mentioned are: starch, lignin, fructan, cellulose, chitin, proteins, xylan, pectin and mannan [14].

Proper aeration of compost is one of the most important parameters for the success of composting process. Approximately

about 0,6 m³ to 2,0 m³ of air is needed for about 1 kg of dry matter [15]. The oxygen content in the system is necessary not only for the degradation of organic matter, also for drying because the moisture contents of materials approximately 55-70% [16]. One of the most widespread variants of composting technologies is the 'free-air prismatic method'. The essence of the method is to provide continuous air supply with easily degradable organic material (e.g. straw) or regular rotation. It is a general fact that the continuous flow of air ensured by the difference in temperature between compost and environment [17]. In the order of process phases, aerobic and anaerobic conditions changes. The strong anaerobic conditions and the reduction of the amount of easily degradable organic matter can be deduced from the changes of compost temperature. The ratio of aeration should be changed in the following cases in compost: aeration is essential to regulate moisture removal or to provide aerobic and anaerobic conditions. When monitoring the aeration process, it is important to ensure that oxidative and reductive phases are in composting [18].

When composting, the heat energy released during the oxidation of organic matter ensures the energy demand of the process, in which case the compost temperature may reach 70-75°C [18]. The organic matter content of compost determine by the input material flow in first composting phase. Table 2 shows the values of the input indicators (flows) measured in different compost types [15].

Table 2. The values of nutritional indicators inhabiting of each solid compost types (Source: Pergola et al., 2017, [15])

	Solid compost types		
	Sheep manure	Mixed compost	Average compost
Moisture content %	70	65	60
Dry matter content %	30	35	40
C %	12	15	22
N %	0,66	0,5	0,7
C/N ratio	16,3	22	31
pH	7,8	7,3	6,9
∑ P ₂ O ₅	0,28	1,3	1,8
∑ K ₂ O	0,8	0,9	1,1

The following composting techniques could be differentiate in the way of oxygen input flows [19]:

- Prismatic systems
- Mechanical or air-ventilated systems
- Bunker type composting method
- Reactor type composting method

Based on these, the most applied technologies are the follows [19]:

- Rotating prismatic technique (open prismatic mode, most commonly used in Hungary)
- Air conditioned prismatic version (passive or ventilated type)
- Bunker type composting
- Reactor type method (vertical, rotary or oven version)

During the controlled composting method, the microbiological properties of mature compost are artificially modified [20]. This

has the advantage of providing biologically/biochemically controlled, stable safe composting conditions, obtaining unrestricted marketing and competitive compost with fertilizers, which is competitive with artificial soil improvers in terms of active ingredient content [21].

2. Methodology

The concept of multi-function composting technique

The main importance of our conception is the multi-functional composting method. During the normal composting process, alternative utilizations linked to the system, or a special compost type is produced, which has concrete input and output material flows, with special setting parameters. We would like to present few special (multi-function) compost types and related utilizations in the following.

Analysis of selected compost types and their utilizations

The scope of specific compost type's use described below and the related possibilities were analysed. We did not focus on traditional agricultural utilization for soil improvement, so the focus on composting and utilization of mature compost (wastewater sludge composting - sludge reduction process, biogas production - combined heat energy production and utilization, and special water treatment with compost adsorption).

3. Results and discussions

Special waste management with wastewater sludge composting

The amount of primary and secondary sludge, which generated during wastewater treatment, could be reduced in several possible ways. On each wastewater treatment plant, a part of produced sludge recirculation realized, which means that only excess sludge should remove from the system [22]. However, this should be dewatered for proper storage and further treatments as it has a high water content (~ 98%, which means it is practically liquid sludge). Dewatering is achieved by centrifugation, drying or gravity compression [23]. This is followed by the anaerobic sludge stabilization phase, which is a basic condition for further utilization [24].

Sewage sludge composting is an appropriate method for further treatment and use of excess sludge formed during water purification. Wastewater sludge composting may only take place after dewatering because the high water content of wastewater sludge would blocking the formation of mature compost [23][25]. It is important to note that wastewater sludge composition is special because after the biological phase of wastewater treatment the sludge from the system contains diverse microorganisms with high number and species [3],[25]. This is useful in the composting process so there is no need to microbiological vaccines to produce the mature compost in appropriate quality. Regarding the quality of compost, it is an important requirement that all ingredients should be below the pollution limits (listed by No. CLXXXV/2012. Law about waste management, and No. 50/2001. (IV. 3.) Government decree about the rules of use and placement of wastewater sludge) (the concentration values presented by Table 3.). Untreated or semi-treated wastewater sludge, non-ripe compost or municipal liquid waste can not be used in agriculture production processes [26].

Table 3. Limited concentrations of toxic elements in wastewater sludge composts (in unit of mg/kg dry matter) (Source: No. 50/2001 (IV. 3.) Government decree)

Toxic contaminants	Limited conc. (mg/kg d.m.)
As (<i>arsenic</i>)	25
Cd (<i>cadmium</i>)	5
Co (<i>cobalt</i>)	50
Σ Cr (Σ <i>chromium</i>)	350
Cr VI (<i>chromium – isotope VI</i>)	1
Cu (<i>copper</i>)	750
Hg (<i>mercury</i>)	5
Mo (<i>molybdenum</i>)	10
Ni (<i>nickel</i>)	100
Pb (<i>lead</i>)	400
Se (<i>selenium</i>)	50
Zn (<i>zinc</i>)	2000
Σ PAH (<i>Polycyclic aromatic hydrocarbons</i>)	5
Σ PCB (<i>Polycyclic biphenyls</i>)	0,5
TPH (<i>Total petroleum hydrocarbons</i>)	1000

Sludge composts can be considered as special compost varieties because they could be used for agricultural production to improve soil parameters, better yields and significantly improve the composition and activity of soil microbiological community [20][27]. The compost components of wastewater sludge complies with the active substance content of the fertilizers, while being environmentally friendly and economical as the compost raw material is accessible to any wastewater treatment plant [28].

The wastewater sludge composting process can be studied from a circularly economic point of view also. The fermentation residue can be transformed into suitable materials for agricultural use by appropriate biological procedures, with a cycle time of 60 up to 90 days. This enables the utilization of wastewater sludge, the raw materials can be returned to the biochemical circulation through the soil, and the costs of dumping and storing wastewater sludges as waste could be reduced also [29]. This is the basic condition of biological directed composting technique using. That means we could control the flora of the compost microorganisms of the wastewater sludge and influence its species and numbers [30]. The communities originally present in wastewater sludge, the species associated with lignocelluloses (mushrooms, molds, polyphagous parasites), and the spores in the air blast ventilation. Their proportions should be properly adjusted, as spores (e.g. beetroot) and mold species can also cause damage to compost soil remediation [31].

Biogas and combined heating energy production

The biogas production associated with composting is typically carried out in wastewater treatment plants, but there are also known residential and biogas production. The latter is only tangentially concerned, because the gas thus produced cannot be regarded as biogas in the conventional sense, as it does not meet biogas requirements for supply to the natural gas pipeline system either in terms of composition or in terms of quality. Typically, communal biogas is a small-scale home-use gas that can be used to heat a farm or a garden house [32].

The untreated biogas contains the highest proportion of methane (about 40-45%), which is an energetically usable part of the generated biogas. In addition, large amounts of carbon dioxide (roughly 20%) are generated, which cause problems with the input of biogas into the natural gas pipeline system and energy loss [32].

Figure 2 shows the economic-social and environmental impact of biogas production. The resulting biogas is suitable for many utilizations. Primarily due to methane content, direct energy use can be considered, but indirect use and impact can also be reflected in the socio-economic and natural environment [33]. With regard to the social segment, it can be stated that direct use of untreated biogas can be used directly for communal use, but due to the relative high carbon content the calorific value will be reduced and the risk of accidents will increase. Definitely recommended that whole of the produced biogas must be cleaned before using [32][33].

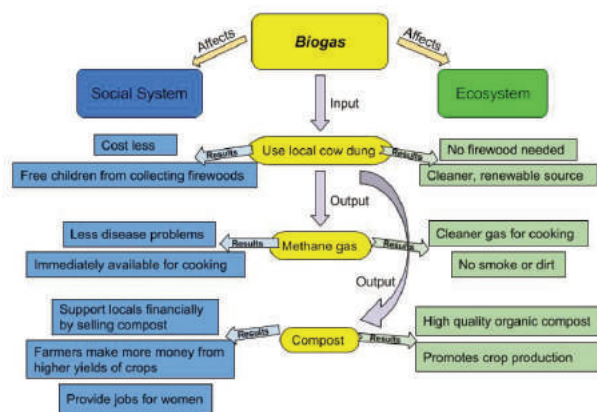


Figure 2. Impacts of biogas production on the social-economic and ecosystem fields
Source: Meng et al., 2018 [33]

In the maturation phase of the composting process, when the compost temperature reaches 70°C, a recoverable amount of heat is generated. For plants with open prism composting technology, composting parameters can be monitored by regular control measurements to determine the maximum temperature value. This can be inferred from the achievement of the mature compost phase, which can be defined by a parameter decrease following the maximum temperature reach [33], [34].

Waste recycling in the form of innovative organic fertilizers and composts - The practical implementation of the circular economic approach

The proportion of bio-chemical recyclable waste in Europe increasing. However, in spite of high organic matter content, the ratio of recycled waste is still below the desired level (at least 65% would be the ideal rate for recycling and a 10% reduction in the amount of waste to be deposited in landfills) [35].

The European Commission declared the "Manure regulation" in 2016, which will increase the proportion of recycled waste amount (No. 2016/157. COM decree) [15]. The Regulation will apply to organic fertilizers, so composts and various fermentation residues (e.g. biogas for plant residues). The organic fertilizer using could increase by re-utilizing (composting) bio-waste [35].

Under the Regulation, it has made it possible to utilize secondary raw materials in order to realize more efficient raw material use, and the regulation increases resource efficiency and reduces import dependence on organic (organic matter-bound) phosphorus.

The indirect effect of the Regulation is that contributes to the classification of organic fertilizers (composts) under a single system of limit values since uniformity of phosphorus, nitrogen and cadmium limits can be effectively influenced by soil composition and the mobility factor for each element [15][26][34][35].

The transition from fertilizer production to the production of organic manures provides a conceptual framework for understanding the parts of bio-waste management in the circular economic concept. This economic strategy can be reconciled with the idea that a product with added value after the biological treatment of wastes can be produced, and thus some degree of modification of waste streams is possible [35].

4. Conclusions

Multifunctional composting has become a common practice today. During the composting process, or after the phase of the mature compost, alternative utilization options seems to be available based on the quality properties of the compost. Combined thermal energy production and biogas production are the most commonly used multifunctional utilizations today. Sludge, as special liquid medium, are suitable for producing compost so that biochemical materials can be returned to the material flow, reducing the volume of waste production. The circular economic concept also appears in composting. The modification of the waste flow with a quantitative reduction has become available with the realization of the economic competitive advantage based on the biodegradation of waste.

References

- [1] Arrigoni, J. P., Paladino, G., Garibaldi, L. A., Laos, F.: 2018. Inside the small-scale composting of kitchen and garden wastes: Thermal performance and stratification effect in vertical compost bins. *Waste Management*, Vol. 76, pp. 284–293. <http://dx.doi.org/10.1016/j.wasman.2018.03.010>.
- [2] Asses, N., Farhat, A., Cherif, S., Hamdi, M., Bouallagui, H.: 2018. Comparative study of sewage sludge co-composting with olive mill wastes or green residues: Process monitoring and agriculture value of the resulting composts. *Process Safety and Environmental Protection*, Vol. 114, pp. 25–35. <http://dx.doi.org/10.1016/j.psep.2017.12.006>.
- [3] Cáceres, R., Malińska, K., Marfà, O.: 2018. Nitrification within composting: A review. *Waste Management*, Vol. 72, pp. 119–137. <http://dx.doi.org/10.1016/j.wasman.2017.10.049>.
- [4] Cerda, A., Artola, A., Font, X., Barrena, R., Gea, T., Sánchez, A.: 2018. Composting of food wastes: Status and challenges. *Bioconversion of Food Wastes*, Vol. 248, pp. 57–67. <http://dx.doi.org/10.1016/j.biortech.2017.06.133>.
- [5] Chew, K. W., Chia, S. R., Yap, Y. J., Ling, T. C., Tao, Y., Show, P. L.: 2018. Densification of food waste compost: Effects of moisture content and dairy powder waste additives on pellet quality. *Process Safety and Environmental Protection*, Vol. 116, pp. 780–786. <http://dx.doi.org/10.1016/j.psep.2018.03.016>.

- [6] Czekala, W., Dach, J., Dong, R., Janczak, D., Malińska, K., Józwiakowski, K., Smurzyńska, A., Cieślík, M.: 2017. Composting potential of the solid fraction of digested pulp produced by a biogas plant. *Biosystems Engineering*, Vol. 160, pp. 25–29. <http://dx.doi.org/10.1016/j.biosystemseng.2017.05.003>.
- [7] De Corato, U., Salimbeni, R., De Pretis, A., Patruno, L., Avella, N., Lacolla, G., Cucci, G.: 2018. Microbiota from 'next-generation green compost' improves suppressiveness of composted Municipal-Solid-Waste to soil-borne plant pathogens. *Biological Control*, Vol. 124, pp. 1–17. <http://dx.doi.org/10.1016/j.biocontrol.2018.05.020>.
- [8] Eslami, H., Hashemi, H., Fallahzadeh, R. A., Khosravi, R., Fard, R. F., Ebrahimi, A. A.: 2018. Effect of organic loading rates on biogas production and anaerobic biodegradation of composting leachate in the anaerobic series bioreactors. *Ecological Engineering*, Vol. 110, pp. 165–171. <http://dx.doi.org/10.1016/j.ecoleng.2017.11.007>.
- [9] Fan, Y. V., Lee, C. T., Klemeš, J. J., Chua, L. S., Sarmidi, M. R., Leow, C. W.: 2018. Evaluation of Effective Microorganisms on home scale organic waste composting. *Sustainable waste and wastewater management*, Vol. 216, pp. 41–48. <http://dx.doi.org/10.1016/j.jenvman.2017.04.019>.
- [10] Fernández-Delgado Juárez, M., Mostbauer, P., Knapp, A., Müller, W., Tertsch, S., Bockreis, A., Insam, H.: 2018. Biogas purification with biomass ash. *Waste Management*, Vol. 71, pp. 224–232. <http://dx.doi.org/10.1016/j.wasman.2017.09.043>.
- [11] Idrovo-Novillo, J., Gavilanes-Terán, I., Angeles Bustamante, M., Paredes, C.: 2018. Composting as a method to recycle renewable plant resources back to the ornamental plant industry: Agronomic and economic assessment of composts. *Process Safety and Environmental Protection*, Vol. 116, pp. 388–395. <http://dx.doi.org/10.1016/j.psep.2018.03.012>.
- [12] Jain, M. S., Jambhulkar, R., Kalamdhad, A. S.: 2018. Biochar amendment for batch composting of nitrogen rich organic waste: Effect on degradation kinetics, composting physics and nutritional properties. *Bioresource Technology*, Vol. 253, pp. 204–213. <http://dx.doi.org/10.1016/j.biortech.2018.01.038>.
- [13] Jain, M. S., Daga, M., Kalamdhad, A. S.: 2018. Composting physics: A degradation process-determining tool for industrial sludge. *Ecological Engineering*, Vol. 116, pp. 14–20. <http://dx.doi.org/10.1016/j.ecoleng.2018.02.015>.
- [14] Luo, Y., Liang, J., Zeng, G., Chen, M., Mo, D., Li, G., Zhang, D.: 2018. Seed germination test for toxicity evaluation of compost: Its roles, problems and prospects. *Waste Management*, Vol. 71, pp. 109–114. <http://dx.doi.org/10.1016/j.wasman.2017.09.023>.
- [15] Margaritis, M., Psarras, K., Panaretou, V., Thanos, A. G., Malamis, D., Sotiropoulos, A.: 2018. Improvement of home composting process of food waste using different minerals. *Waste Management*, Vol. 73, pp. 87–100. <http://dx.doi.org/10.1016/j.wasman.2017.12.009>.
- [16] Meng, L., Li, W., Zhang, S., Wu, C., Lv, L.: 2017. Feasibility of co-composting of sewage sludge, spent mushroom substrate and wheat straw. *Bioresource Technology*, Vol. 226, pp. 39–45. <http://dx.doi.org/10.1016/j.biortech.2016.11.054>.
- [17] Meng, L., Zhang, S., Gong, H., Zhang, X., Wu, C., Li, W.: 2018. Improving sewage sludge composting by addition of spent mushroom substrate and sucrose. *Bioresource Technology*, Vol. 253, pp. 197–203. <http://dx.doi.org/10.1016/j.biortech.2018.01.015>.
- [18] Meng, X., Dai, J., Zhang, Y., Wang, X., Zhu, W., Yuan, X., Yuan, H., Cui, Z.: 2018. Composted biogas residue and spent mushroom substrate as a growth medium for tomato and pepper seedlings. *Sustainable waste and wastewater management*, Vol. 216, pp. 62–69. <http://dx.doi.org/10.1016/j.jenvman.2017.09.056>.
- [19] Muscolo, A., Papalia, T., Settineri, G., Mallamaci, C., Jeske-Kaczanowska, A.: 2018. Are raw materials or composting conditions and time that most influence the maturity and/or quality of composts? Comparison of obtained composts on soil properties. *Journal of Cleaner Production*, Vol. 195, pp. 93–101. <http://dx.doi.org/10.1016/j.jclepro.2018.05.204>.
- [20] Pergola, M., Persiani, A., Palese, A. M., Di Meo, V., Pastore, V., D'Adamo, C., Celano, G.: 2017. Composting: The way for a sustainable agriculture. *Applied Soil Ecology*. <http://dx.doi.org/10.1016/j.apsoil.2017.10.016>.
- [21] Proietti, P., Calisti, R., Gigliotti, G., Nasini, L., Regni, L., Marchini, A.: 2016. Composting optimization: Integrating cost analysis with the physical-chemical properties of materials to be composted. *Journal of Cleaner Production*, Vol. 137, pp. 1086–1099. <http://dx.doi.org/10.1016/j.jclepro.2016.07.158>.
- [22] Reyes-Torres, M., Oviedo-Ocaña, E. R., Dominguez, I., Komilis, D., Sánchez, A.: 2018. A systematic review on the composting of green waste: Feedstock quality and optimization strategies. *Waste Management*. <http://dx.doi.org/10.1016/j.wasman.2018.04.037>.
- [23] Sánchez, Ó. J., Ospina, D. A., Montoya, S.: 2017. Compost supplementation with nutrients and microorganisms in composting process. *Waste Management*, Vol. 69, pp. 136–153. <http://dx.doi.org/10.1016/j.wasman.2017.08.012>.
- [24] Sedničková, M., Pekařová, S., Kucharczyk, P., Bočak, J., Janigová, I., Kleinová, A., Johec-Mošková, D., Omaníková, L., Perd'ochová, D., Koutný, M., Sedlářík, V., Alexy, P., Chodák, I.: 2018. Changes of physical properties of PLA-based blends during early stage of biodegradation in compost. *International Journal of Biological Macromolecules*, Vol. 113, pp. 434–442. <http://dx.doi.org/10.1016/j.ijbiomac.2018.02.078>.
- [25] Shi, M., Wei, Z., Wang, L., Wu, J., Zhang, D., Wei, D., Tang, Y., Zhao, Y.: 2018. Response of humic acid formation to elevated nitrate during chicken manure composting. *Bioresource Technology*, Vol. 258, pp. 390–394. <http://dx.doi.org/10.1016/j.biortech.2018.03.056>.
- [26] Smith, M. M., Aber, J. D.: 2018. Energy recovery from commercial-scale composting as a novel waste management strategy. *Applied Energy*, Vol. 211, pp. 194–199. <http://dx.doi.org/10.1016/j.apenergy.2017.11.006>.
- [27] Vázquez, M. A., Soto, M.: 2017. The efficiency of home composting programmes and compost quality. *Waste Management*, Vol. 64, pp. 39–50. <http://dx.doi.org/10.1016/j.wasman.2017.03.022>.
- [28] Wang, H., Zhao, Yue, Wei, Y., Zhao, Yi, Lu, Q., Liu, L., Jiang, N., Wei, Z.: 2018. Biostimulation of nutrient additions on indigenous microbial community at the stage of nitrogen limitations during composting. *Waste Management*, Vol. 74, pp. 194–202. <http://dx.doi.org/10.1016/j.wasman.2017.12.004>.
- [29] Wang, K., Yin, X., Mao, H., Chu, C., Tian, Y.: 2018. Changes in structure and function of fungal community in cow manure composting. *Bioresource Technology*, Vol. 255, pp. 123–130. <http://dx.doi.org/10.1016/j.biortech.2018.01.064>.
- [30] Wang, X., Bai, Z., Yao, Y., Gao, B., Chadwick, D., Chen, Q., Hu, C., Ma, L.: 2018. Composting with negative pressure aeration for the mitigation of ammonia emissions and global warming potential. *Journal of Cleaner Production*, Vol. 195, pp. 448–457. <http://dx.doi.org/10.1016/j.jclepro.2018.05.146>.
- [31] Waqas, M., Nizami, A. S., Aburizaiza, A. S., Barakat, M. A., Ismail, I. M. I., Rashid, M. I.: 2018. Optimization of food waste compost with the use of biochar. *Sustainable waste and wastewater management*, Vol. 216, pp. 70–81. <http://dx.doi.org/10.1016/j.jenvman.2017.06.015>.
- [32] Yu, Z., Tang, J., Liao, H., Liu, X., Zhou, P., Chen, Z., Rensing, C., Zhou, S.: 2018. The distinctive microbial

community improves composting efficiency in a full-scale hyperthermophilic composting plant. *Bioresource Technology*, Vol. 265, pp. 146–154.

<http://dx.doi.org/10.1016/j.biortech.2018.06.011>.

[33] Zhang, D., Luo, W., Li, Y., Wang, G., Li, G.: 2018. Performance of co-composting sewage sludge and organic fraction of municipal solid waste at different proportions. *Bioresource Technology*, Vol. 250, pp. 853–859. <http://dx.doi.org/10.1016/j.biortech.2017.08.136>.

[34] Zhang, L., Sun, X.: 2018. Effects of bean dregs and crab shell powder additives on the composting of green waste.

Bioresource Technology, Vol. 260, pp. 283–293. <http://dx.doi.org/10.1016/j.biortech.2018.03.126>.

[35] Zheng, G., Wang, T., Niu, M., Chen, X., Liu, C., Wang, Y., Chen, T.: 2018. Biodegradation of nonylphenol during aerobic composting of sewage sludge under two intermittent aeration treatments in a full-scale plant. *Environmental Pollution*, Vol. 238, pp. 783–791.

<http://dx.doi.org/10.1016/j.envpol.2018.03.112>.



DEVELOPMENT OF BIOMASS-BASED PYROLYSIS CHP (R + D)

Author(s):

V. Madár¹ – I. Bácskai² – A. Dhaundiyal³ – L. Tóth³

Affiliation:

¹ Szent István University, Faculty of Mechanical Engineering, Cső-Montage Ltd. and Pyrowatt Ltd.

²National Agricultural Research and Innovation Centre, Institute of Mechanical Engineering

³Szent István University, Faculty of Mechanical Engineering

Email address:

madar.viktor@pyrowatt.hu, bacsikai.istvan@mgi.naik.hu, alok.dext@hotmail.com, toth.laszlo@gek.szie.hu

Abstract

In our study, we dealt with the agricultural materials and waste to which the pyrolysis process is applicable, as part of a CHP pyrolysis power plant. We introduce the processes of planning, actualisation, and preceding experiments. We finish the study with introducing the experiences gathered from analysing the designed and manufactured prototype machinery. We hope that the solution will be in good service to the decentralised energy supply of rural and agricultural areas, and its usage will offer jobs and a source of income for both entrepreneurs and civilian population.

Keywords

pyrolysis, CHP power plant, heat disintegration, fixed bed generator, efficiency of pyrolysis

1. Introduction

Usability of biomass

In Hungary, plant production binds three times as much atomic carbon and energy as the total amount of energy resources produced in the country. However, this plant product is only partially exploited as foodstuffs, fodder, or industrial materials. The part we do not use (energy plants, by-products, waste) are used either for soil resupplying or energy production. The amount theoretically usable for energetics is about 9-10 million tonnes annually. We could use this to produce an annual 60-70 PJ heat energy from this amount, even if we consider a 50% efficiency, dried to 12-15% moisture.

The possible uses for agricultural main and by-products are as follows:

- heating technology,
- pyrolytic gasification,
- fermentation using methane (biogas),
- plant oil and spirit manufacturing as engine fuel (ethanol, methyl ester)

Of the four possibilities, agricultural production is served best by methane fermentation. This is due to getting quality bio-fertiliser, apart from the produced gas with 23-25 MJ/m³ heat energy. This helps us with an environmentally friendly realisation of soil resupplying [1-5].

Biomass can be categorised from the perspective of energy technology into the following three groups [6]:

- PRIMARY (wood, woody and herbaceous plants, produce, nuts, buds, etc.)
- SECONDARY (animal by-products, fertiliser, other wastes, etc.)
- TERTIARY (foodstuffs waste, animal carcasses, waste from the abattoir, wastewater from water treating plants, etc. often categorised into secondary).

Biomass can be transformed into heat energy with a high efficiency, and although with a lower efficiency, may become electricity as well. The joint production of heat and electric energy (CHP) is the most advantageous. In larger power plants, this can produce good efficiency, however, the heat produced is rarely used. When the travel distance to large power plants increase (transportation energy), efficiency is further worsened [7].

Energy used for production is especially high for so-called energy plants' (plantations) materials produced for energetics usage (f. e. manufacturing hard combustion pellet from herbaceous plant biomass - hay). This efficiency is usually marked with the OUTPUT / INPUT (O/I) ratio. This means that they compare the chemically bound energy content to the total energy requirement of production and preparation before usage. In the case of traditional firewood, this ratio can be considered an advantageous 8-10:1 when naturally dried and processed into logs, however, even this can be worsened by up to 2-3 if transport distance is large. In cases where both production and pellet manufacturing are done, this decreases until less than 2:1 [4].

The CHP power plant usage seems to be a promising new technological solution, as the machinery can be installed directly next to the area of production, and there are a multitude of options for heat usage as well [8].

The pyrolysis power plant, which is the focus of the study, decentralises energy production in reality. This offers a good opportunity for local employment (keeping the local neighbourhood intact), and monetary resources coming from this also serve the town [9].

The wooden gas power plant designed by SZIE GEK and CSŐ-MONTAGE Co. Ltd. abides by all the aforementioned requirements. The electric performance (100 kW) can be used for satisfying local (small enterprise) demands, but may be used by linking to the power grid (cooperation) as well.

2. Description of the pyrolysis process

Gasification process

During gasification, the heating material goes through various physical and chemical changes. The fuel placed into the gas

generator starts to dry at first using the heat from burning gases, then further heating causes the pyrolysis. This process releases water vapour, carbon-dioxide, hydrogen, heavy carbon-hydrogen variants, mainly ethylene, methane, carbon-monoxide, tar vapours, vinegar acid, methyl alcohol, nitrogen, ammonia, and sulphur-hydrogen variants [1, 7]. During the gasification of wooden heating materials, a significant amount of vinegar acid, methyl alcohol and carbon-dioxide are produced. After the process of gasification, the remaining coke and oxygen produce the so-called illuminating gas [9-11]. Gases in this category mix and result in generator gas. Many processes are used, of which the one that fits our purposes the most, the so-called top-fill bottom-airflow countercurrent system was chosen [12, 13].

Within the system, processes concluding in the gasification tank can be separated into zones (Figure 1):

- Drying zone (60- 180 °C)
- Carbonisation (pyrolysis) zone (180- 600 °C)
- Oxidation (combustion) zone (1000- 1250 °C)
- Reduction zone (1000-800 °C)
- Ash zone

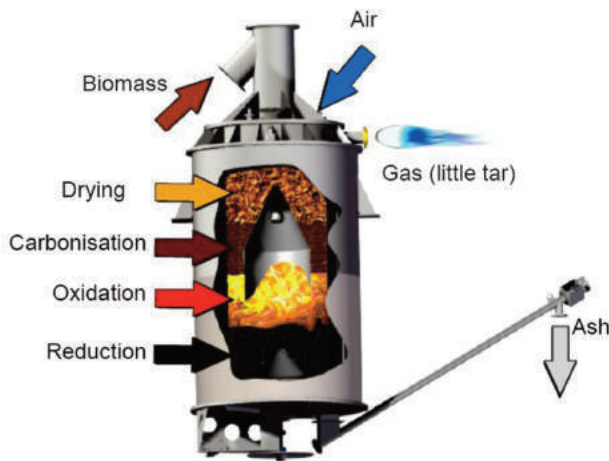


Figure 1. Schematics for the so-called top-fill bottom-airflow countercurrent system

In the reduction zone important for gas quality, the non-combustible pyrolysis gases and non-combustible carbon-dioxide and water is guided through the sizzling coal found in the lower layer [14]. At this place, coal causes further chemical reactions to reduce them.

- $C+CO_2=2CO$ (-164,9 MJ/kg mol)
- $C+H_2O=CO+H_2$ (-122,6 MJ/kg mol)
- $CO+H_2O=CO_2+H_2$ (+42 MJ/kg mol)
- $C+2H_2=CH_4$ (+75 MJ/kg mol)
- $CO_2+H_2=CO+H_2O$ (-42,3 MJ/kg mol)

In this zone, endothermal processes drain heat from the environment, and if the ideal temperature of 800-1000 °C is not met, the quality of produced gas will be lowered [15]. Carbon-hydrogen variants are released at an average of 800 °C, and gases combust visibly with the entrance of the secondary airflow into the combustion bed.

Notable requirements for pyrolysis

- Produced generator gas needs to have a high heating coefficient, meaning it needs to have a high content of combustible gases - in the case of H_2 and CO . contents of 25% moisture content heating material, acceptable heating coefficient if around 3500-5000 kJ/Nm³

- In order to protect the durability of engines, the tar content of the produced gas cannot exceed 0,05g/Nm³
- The coal input that accompanied the fuel (>95%) has to fully combust, which assures the advantageous efficiency of the whole process (70-80%)
- The fuel has to flow downwards without inhibition
- The system needs a low pressure drop (in the gas generator and attached parts as well)
- The system has to react to changing the loads according to the network's requirements.

Notable requirements for fuel

- High energy contents
- Low moisture content
- High volatile matter content
- Low amount of ash
- Good reaction capability
- High density
- Good carbonisation attributes
- The grain size of input material (fragmentation, etc.).

Energy contents is basically the same as heating efficiency / coefficient. Moisture content is important for gasification, as it results in combustible gases. However, when beyond a certain level, it will decrease the efficiency of the gas generator. This is caused by water being in a bound form inside it, which can only be removed by either drying or evaporation. Drying removes heat from the process, which also means energy loss [16]. The moisture content of freshly harvested wood is ~50-60%, which needs about a year to decrease to 25-30%, even with advantageous log size, and drying under roof in open air. A moisture content of 14-30% for wood materials and other biomass usable in gas generators is advantageous.

3. Analyses before planning and actualisation

We analysed the attributes of material pelletised and chopped to various sizes. If the group has no significant - disadvantageous for the process - impurities within it (such as sawdust, soil, bark waste, etc.), the flow resistance is decreased with increasing fraction size to f. e. 25-100 mm, which hastens the process.

The various materials were carbonised in an inert (nitrogen) context, to obtain information on the estimated gas yield. The heating efficiency of these gases was also determined, and our resulting values are summarised in Table 1.

Table 1. Energy content of gases from carbonisation

Material	Heating value of gas (MJ/m ³)
Willow waste	5,53
Hemp	4,78
Energy grass waste	4,43
Acacia waste	4,14
Corn stem	4,01
Sunflower stem	3,91
Poplar waste	3,89
Rapeseed hay	3,86
Chinese bamboo	3,51
Wheat hay	3,24

The base moisture content for all materials was between 14-15%, and their heating efficiency for dry material was between

11-19 MJ/kg. The highest heating efficiency was produced by poplar waste.

During carbonisation in inert gases, mass changes were also measured among different temperatures using a precision scale. We introduce such changes on Figure 2.

Usually, lower temperatures yielded more remaining materials (carbon, and other materials that cannot be subject to pyrolysis). Therefore, by increasing the temperature of pyrolysis, remaining materials lessen, meaning the samples "burn out" more [17].

On low temperature, the highest amount of remaining material resulted for soil-contaminated wooden waste, which may be due to how this sample also had much more, harder to combust materials as well, which can't be combusted on 400°C. A similar case happened for cut roots, which had significant amounts of soil.

Between hay, agri- and corn stem pellets, there was no significant difference of carbonisation speed on 400 and 600°C.

However, in cases of lower temperatures, there was always a higher difference. If latter materials are compared to pine waste and pellet made out of it, we will always result in faster carbonisation.

For hay and cane variants, there was difference in intensity of carbonisation, but the decomposition of remaining materials is also faster on lower temperatures.

This phenomenon may be due to the ligno-cellulose content (according to literature sources as well), and the temperature interval of their decomposition, which is intensive between 400 – 500°C.

After multiple analyses conducted with materials not listed here, and trials of ash decomposition, we conducted the designing phase of the machinery.

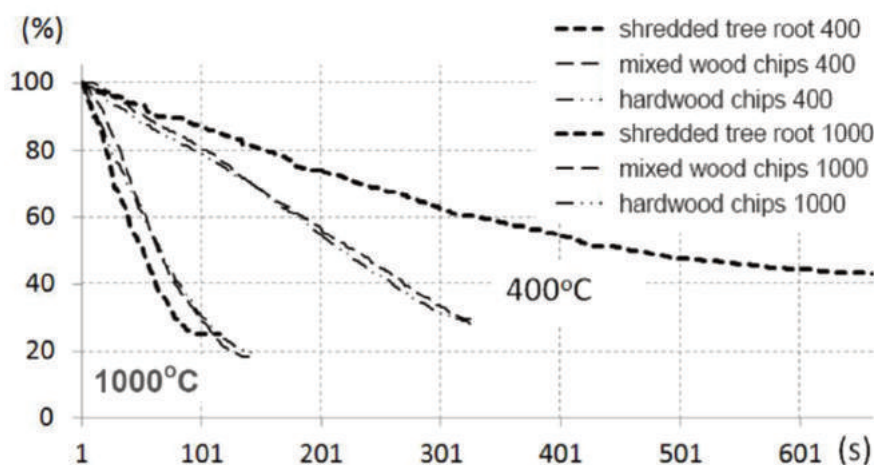


Figure 2. Mass change intensity of materials in inert gas between 400 and 1000°C

4. The planned system

(GG-100 wooden gas generator example's characteristics)

The system is a so-called multiphase fixed bed solution, which separates the thermo-chemical transformation process into multiple parts using separate reaction zones into partial processes (drying, pyrolysis, oxidation, reduction). This makes the whole process easier to regulate (Figure 3). Therefore, the system can produce quality generator gas.

The freed energy is used to sustain the endothermal reduction process of the pyrolysis that happens with coke, thus reducing said coke (or coal) into generator gas, via the partial oxidation's resulting gaseous by-products.

Most of the energy of the high heat-content gas exiting the gas generator can be reclaimed by drying the fuel. The oxidation airflow is fed into the reactor after pre-heating it to 250°C in the heat exchanger next to the input area, which also increases the efficiency of the system.

The system consists of five main parts

I. Fuel system

- fuel (biomass waste) container,
- fuel dredging system,
- fuel drier,
- collector, elevator system.

II. Gas generator

- fuel input floodgates,
- combustion airflow system,
- hot air ignition grate,
- ash disperser.

III. Gas preparation area

- gas cooling,
- gas filtering,
- gas purifying,
- pressurisation.

IV. Gas engine and electricity generator

- engine,
- electric generator,
- hydraulics system,
- heat usage system (smoke gas- and engine - water. oil – heat exchangers)

V. Electronic operation system

- material input, temperature control of gas generator, gas quality (purifiers), gas temperature and pressure control
- gas generator, gas engine and electric generator controls
- management of aforementioned systems, cooperation with the electric grid.
- The entire control system is placed in the control technology container (with the visualisation of data, and the option of local intervention).

Structure of the system

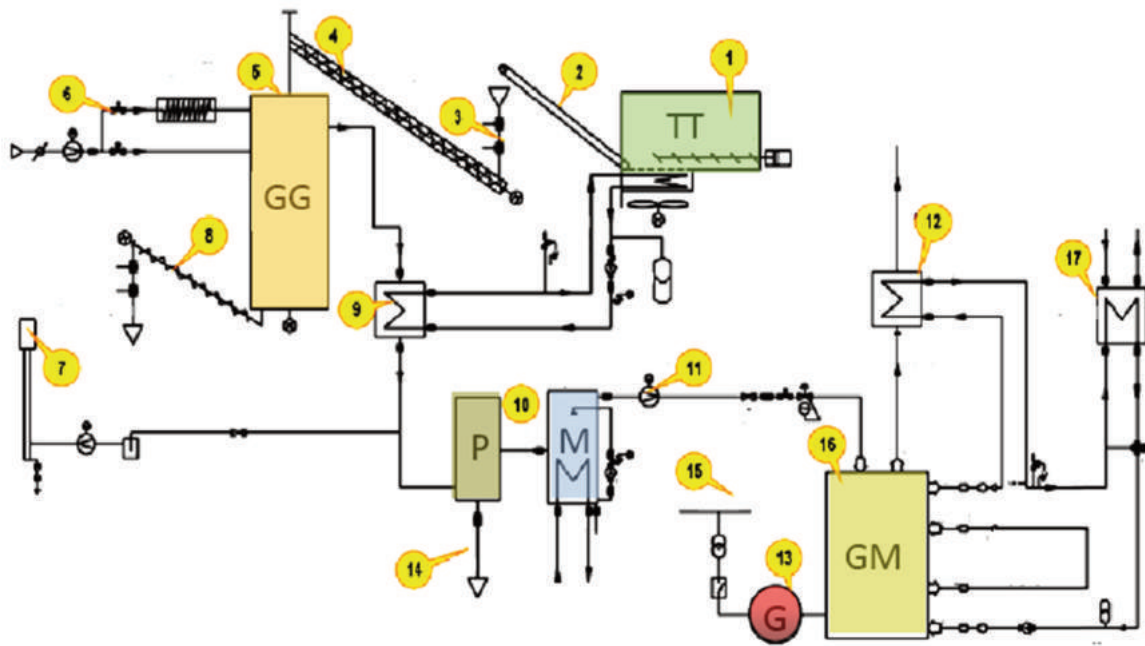


Figure 3. Schematics of the system, name of components

- (1) fuel container and drier machine, expulsion machine (TT),
- (2) transport lane,
- (3) feeder (floodgates), (4) fuel pulley, (5) wood gasification generator (GG), (6) airflow, electric ignition,
- (7) gas torch, (8) ash separator, ash disperser, (9) heat exchanger, (10) gas purification filter, gas purifier (P and M),
- (11) pressuriser, (12) gas engine's expulsor heat exchanger (gas / water, heating and / or HMV),
- (13) electric generator (G), (14) ash separated in the purifier, (15) electric grid connection,
- (16) gas engine (GM), (17) engine heat waste heat exchanger (heating and / or HMV)

The reactor-side part of the system's example can be seen on Figure 4.

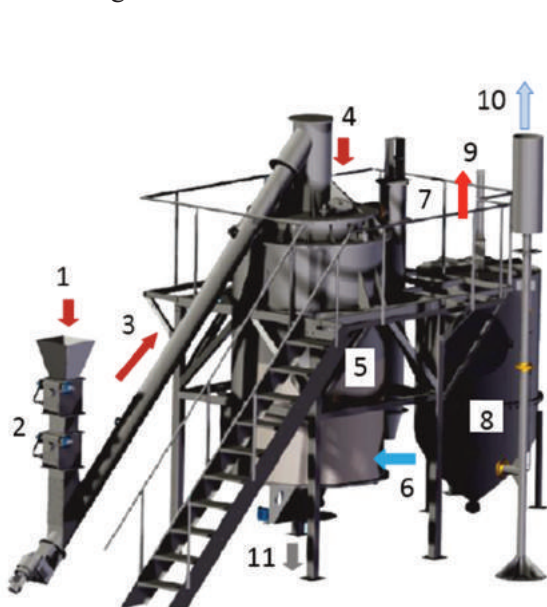


Figure 4. Fuel (1), input floodgates (2), pulley (3), input into reactor space (4), dual-layer reactor (5), floating input (6), gas / air heat exchanger (7), dry dust filter (8), gas feed into gas engine (9), gas torch (10).

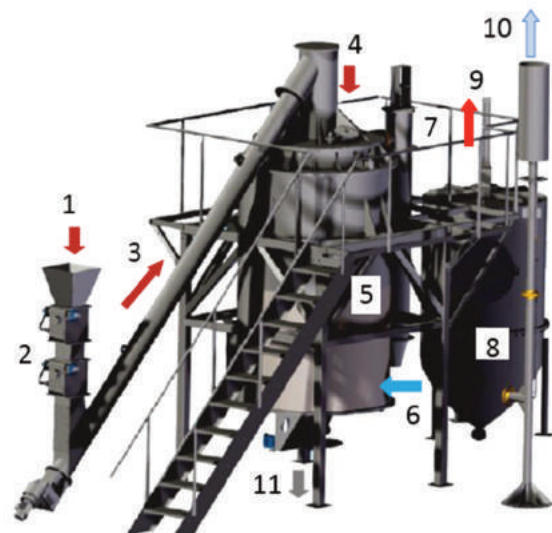


Figure 5. Turbo load gas engine (1), turbo injector (2) electric generator (3), pressure valve (4) heat exchangers of engine waste (5)

The generator gas has to be filtered to 0,5 micron softness before it goes into the gas engine. The

maximum permissible dust content is 50 mg/Nm³. The generator gas is 90-150°C when going from the heat exchanger to the gas filter, where it collides into a Nomex filtering bag with the dimensions of 1000 and 1200 mm. Following this, we also need to remove the volatile components, and those that dilute in water as well, which happens in a water purifier. The purified gas is fed to the turbo load gas engine via a pressuriser.

(Made by LIEBHERR) This is integrated into the electric generator (Figure 5).

The GAS ENGINE is four-cycle, six-cylinder, watercooled, sequential. The turbo loader operating with exhaust gas inputs the mixture under pressure.

System operation, communication

Within the operation and communication system, there are two sub-PLC systems and a main PLC system (made by UNITRONICS), connected to each other on a CAN bus, using a UNICAN protocol. The master PLC system has RS232, RS485, CAN and ETHERNET communication protocols installed. Local and internet overseeing connects to the control centre via the ETHERNET port, but its operations are unrelated to that of communications necessary for the system.

The roles of the three-sided PLC group:

PLC1 tasks:

- visual representation of the system (Figure 6),
- regulation, controlling,
- generating and managing technical and electric protection protocols,
- error management, logging,
- communication with PLC2 and PLC3,
- local and web overseeing,
- network connection with EID-EP.

PLC2 tasks:

- normal operation of gas engine,
- rev and performance regulation,
- performance factor regulation,
- watercooling system regulation,
- mixture regulation,
- technical and electric protection protocols of gas engine,
- gas fuel system regulation.

PLC3 management and overseeing tasks:

- pre-drier,
- fuel input floodgates,
- temperature processes in gas generator,
- gas constitution,
- airflow intake,
- movement of floodgates,
- ash dispersion,
- units of dry filter and wet purifier, etc.

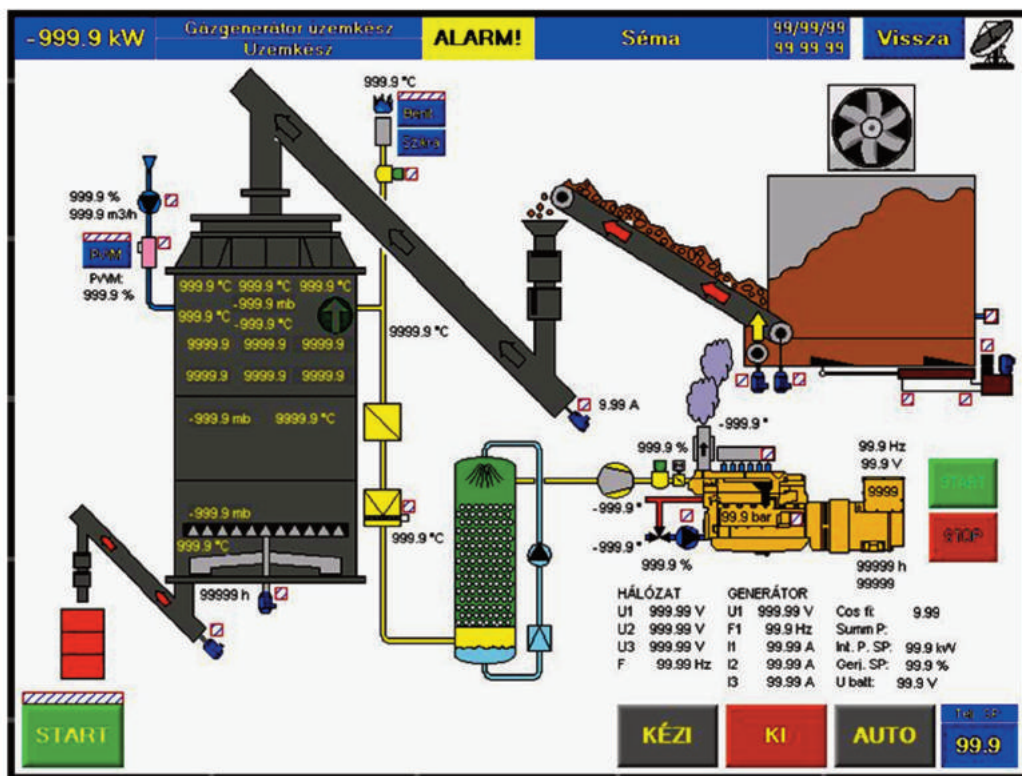


Figure 6. Information manual management interface shown in PLC1 (fuel system, gas generator, gas engine operation parameters and necessary management appliances included)

5. System analysis, results

We measured the energetic parameters of the system after the complete "heating". We precisely described the grain constitution of the input material (in accordance with relevant standards), similarly to its moisture content, heating coefficient, the

temperature values within the gas generator, the gas temperature, gas composition, etc.

Due to the pre-heated air in the system, the oxidation zone has a higher temperature, and cracking the long carbon chain of tar also happens (Figure 7).

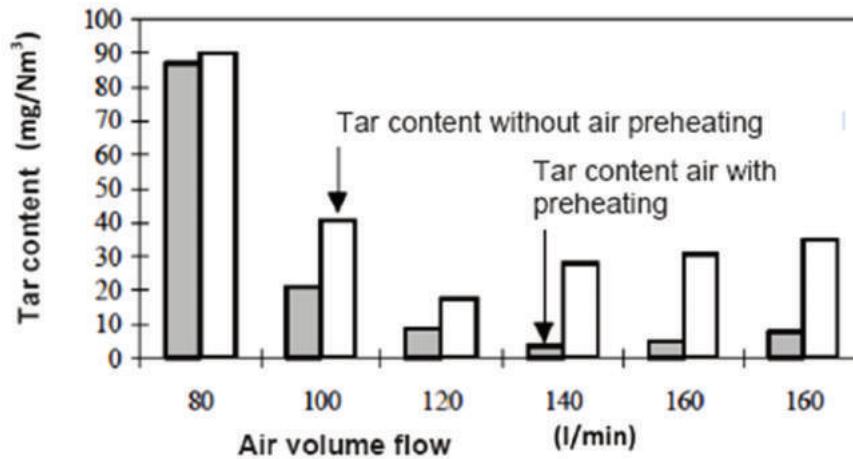


Figure 7. Tar content in light of preheated airflow effects

Table 2. Temperatures of the experimental

Temperature values	[°C]
Gas on generator output side	550
After the drier's heat exchanger	130
Before / after drier calorifer	90/80
After gas filter	110
Exhaust smoke gas	550
After exhaust heat exchanger (into the outside)	120-140

Table 3. Performance measurements of the experimental device

Performance	Sign	[kW]
Fuel drier	Q_{sz}	30
Wet purifier	Q_m	5
Heat usage (H MV, heating) stb.)	Q_{hh}	160
Electric	P_v	100
Loss*	Q_v	51
Total	E_{δ}	346

*Calculated

The fuel consumption of the system is 13 MJ/kg heat performance, 25% moisture content biomass waste, with at most 1,5% ash content. The fuel requirement for an hour if moisture content of the waste is 25% (for dry material) is 108 kg.

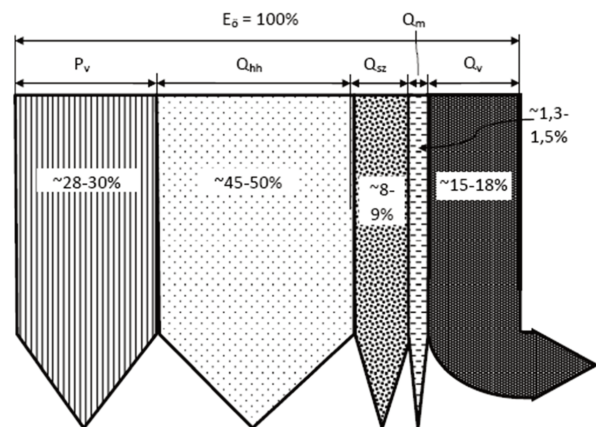


Figure 8. Percentage of performance values for experimental device

In our experimental device, we used 1kg of biomass to produce 2,5 m³ wood gas, which had an average of 5,35 MJ/m³ heating efficiency (when the heat efficiency of the dry wood used for the experiments was 18 MJ/kg). Cold efficiency of the gas generator:

$$\eta_{HG} = \frac{H_{agas} * q_{gas}}{H_{ah} * q_{fm}} = 0,75 \rightarrow 80\%$$

Where:

- H_{agas} : Heating coefficient of generator gas [kJ/mn3]
- q_{gas} : Volume flow of generator gas [mn3/h]
- H_{ah} : Heating coefficient of average fuel [kJ/kg]
- q_{fm} : Fuel mass flow [kg/h]

Finally, by using the pyrolysis generator, we were able to make an efficient CHP power plant system, where in the case of 18-19% moisture content hardwood waste (12-45cm):

- Total efficiency for electricity is: 28,4-28,9% (~29%).
- CHP efficiency is: ~75%,
- $\sigma = 0,63$ after "lab measurements".

6. Operation conditions

The system links into a mid-voltage grid, and cooperates with it, but the transportation of electricity at the point of intersection is one-way, it can only draw.

The machinery is placed in a facility processing woodwork waste, where top electricity consumption is around 124 kW. The main machines responsible for consumption are the shredder, pellet maker and bricket maker machines that describe the facility's profile.

On the electric intersection point, there's an EID-EP unit from the EuroProt+ Smart series, made by PROTECTA Co. Ltd. This offers a solution for protecting free cable and cable systems on the grid, for both civilian and industrial use. This means that (in its current place) the facility draws 24 kW performance from the grid for TDP, however, when the demand is lower, the operation of the power plant cooperating with the EID-EP stops the drawing, and feeds demand back to the gas generator. The highest rate of this process - without significantly debilitating efficiency - is ~50%. Demand below this only happens during 20% of the facility's time in operation. Currently, the machinery don't operate on Saturdays and Sundays.

We wish to make the machinery operate around the clock. This requires that we construct a two-part fuel container unit that's larger in size. One part contains the dry fuel, another the wet fuel. On weekends, the gas generator of the machinery can keep operating, if the gas produced is combusted, and its heat energy is used in the larger thermo-ventilator installed at the pre-drier (meaning it's used for pre-drying its own fuel).

Conclusions

According to our goals, we were able to create a pyrolysis power plant of CHP 100kWpe, which can be used to process woodwork waste and agricultural solid biomass (f. e. by-products) for energetics purposes. The solution is exceptionally good for sustaining rural SMEs as an energy supply. They can employ part-timers for the system's heat production, but it can also be used well as an energy supply unit for small factories needing electricity and heat energy. Using this machinery, materials produced in the direct neighbourhood of rural areas can be used. The collection and processing of said materials can also mean more workplaces. We can exploit areas only usable for producing energy plants, the environment becomes more refined, and the gains also serve the locals, increasing the capability of rural areas to keep inhabitants.

References

- [1] **Birkás M.:** 2015. Környezetkímélő alkalmazkodó talajművelés. Szent István Egyetemi Kiadó, Gödöllő, pp. 368.
- [2] **D'Antonio C. M.:** 1993 Mechanisms controlling invasion of coastal plant communities by the alien succulent *Carpobrotus edulis*. Ecology, Vol. 74. No. 1. pp. 83–95. <http://dx.doi.org/10.2307/1939503>
- [3] **Dassonville N., Vanderhoeven S., Vanparys V., Hayez M., Gruber W., Meerts P.:** 2008. Impacts of alien invasive plants on soil nutrients are correlated with initial site conditions in NW Europe. Oecologia, Vol. 157. pp. 131–140. <http://dx.doi.org/10.1007/s00442-008-1054-6>
- [4] **Ehrenfeld J. G.:** 2003. Effects of exotic plant invasions on soil nutrient cycling processes. Ecosystems, Vol. 6. pp. 503–523. <http://dx.doi.org/10.1007/s10021-002-0151-3>
- [5] **Evans H. C.:** 1997. *Parthenium hysterophorus*, a review of its weed status and the possibilities for biological control. Biocontrol News and Information, Vol. 18. No. 3. pp. 89–98.
- [6] **Tóth L.:** 2012 Alternatív energiaellátási rendszerek az agrárgazdaságban, Szaktudás Kiadó, Budapest, pp. 320.
- [7] **Lettnner, F., Haselbacher, P., Timmerer, H., Leitner P.:** 2007. Latest results of "CleanStGas" - Staged biomass gasification CHP, Proceedings of the 15th European Biomass Conference & Exhibition, Berlin
- [8] **Madár V., Tóth L.:** 2012. Fagázgenerátor üzemű bio-kiserőmű és öntözőberendezés, Mezőgazdasági Technika, Vol. 52. No. 9. pp. 3-8.
- [9] **Di Blasi C.:** 2009. Combustion and gasification rates of lignocellulosic chars. Progress in Energy and Combustion Science, Vol. 35. No. 2. pp. 121–140. <http://dx.doi.org/10.1016/j.pecs.2008.08.001>
- [10] **Raman P., Ram N.K., Gupta R.:** 2013. A dual fired downdraft gasifier system to produce cleaner gas for power generation, Design, development and performance analysis. Energy Vol. 54. pp. 302-314. <http://dx.doi.org/10.1016/j.energy.2013.03.019>
- [11] **Bhattacharya S.C., Siddique A.H.M.R., Pham H.L.:** 1999. A study on wood gasification for low-tar gas production. Energy Vol. 24. No. 4. pp. 285-296. [http://dx.doi.org/10.1016/S0360-5442\(98\)00091-7](http://dx.doi.org/10.1016/S0360-5442(98)00091-7)
- [12] **Madár V., Tóth L., Madár Gy., Schrempf N.:** 2014. Kísérleti fagázgenerátor Mezőgazdasági Technika, Vol. 55. No. 4. pp. 2-5.
- [13] **Barman N.S., Ghosh S., Sudipta D.:** 2012. Gasification of biomass in a fixed bed downdraft gasifier – A realistic model including tar. Bioresource Technology, Vol. 107. pp. 505-511. <http://dx.doi.org/10.1016/j.biortech.2011.12.124>
- [14] **Antonopoulos I.S., Karagiannidis A., Elfsionitis L., Perkoulidis G., Gkouletsos A.:** 2011. Development of an innovative 3-stage steady-bed gasifier for municipal solid waste and biomass. Fuel Processing Technology, Vol. 92. No. 12. pp. 2389-2396. <http://dx.doi.org/10.1016/j.fuproc.2011.08.016>
- [15] **Dhaundiyal A., Gupta V. K.:** 2014. The analysis of pine needles as a substrate for gasification. J. Water, Energy Environ. Vol. 15. pp. 73–81. <http://dx.doi.org/10.3126/hn.v15i0.11299>
- [16] **Martínez J. D., Lora E. E. S., Andrade R. V., Jaén R. L.:** 2011. Experimental study on biomass gasification in a double air stage downdraft reactor. Biomass and Bioenergy, Vol. 35. No. 8. pp. 3465-3480. <http://dx.doi.org/10.1016/j.biombioe.2011.04.049>
- [17] **Borocz M., Herczeg B., Horvath B., Fogarassy Cs.:** Evaluation of biochar lifecycle processes and related lifecycle assessments. Hungarian Agricultural Engineering, Vol. 29. pp. 60-64. <http://dx.doi.org/10.17676/HAE.2016.29.60>



INFLUENCE OF MOISTURE AND CURRENT FREQUENCY ON ELECTRICAL POTENTIAL OF SORGHUM GRAINS (SORGHUM BICOLOUR (L.) MOENCH)

Author(s):

J. Audu – O. J. Ijabo – J. O. Awulu

Affiliation:

Dept. of Agric. & Environmental Engineering, College of Engineering,
University of Agriculture, Makurdi, Nigeria

Email address:

audujoh@gmail.com, ojjabo@gmail.com, jawulu@yahoo.com

Abstract

Non-destructive quality parameter determination of agricultural produce is the latest technological trend in agricultural metrology. This study tends to establish the use of electrical potential values to determine moisture content of sorghum grains at certain current frequency range. Electrical potential values of sorghum grains at 10, 13, 16, 19 and 22% db were measured using a circuit arrangement consisting of functional generator, grain sample holder and oscilloscope. These measure grains were carried out at current frequencies of 1, 500, 1000, 1500 and 2000 kHz using three (white, red and yellow) varieties of sorghum. Measured values obtained across all varieties ranges from – 0.2 to -14.36 volts. Statistic analysis carried out on these data shows that moisture, current frequency and variety with their interactions has significant effect at $p \leq 0.05$ on electrical potential. The study also shows that Behavioral trend between moisture and electrical potential are more visible at current frequency range of 1000 to 1500 kHz in all varieties. Regression equations were developed to predict moisture using electrical potential values.

Keywords

moisture, current frequency, sorghum, variety, electrical potentials

1. Introduction

Sorghum (*Sorghum bicolour* (L.) Moench) is an indigenous crop to Africa, and though commercial needs and uses may change over time, sorghum will remain a basic staple food for many rural communities. Sorghum belongs to the grass family Gramineae [1]. According to Kimber [2] Sorghum is a cultivated tropical cereal grass. It is generally, although not universally, considered to have first been domesticated in North Africa, possibly in the Nile or Ethiopian regions as recently as 1000 BC. Today, sorghum is cultivated across the world in the warmer climatic areas. It is quantitatively the world's fifth largest most important cereal grain, after wheat, maize, rice and barley. World annual sorghum production is over 60 million tonnes, of which Africa produces about 20 million tonnes. Oluwakemi and Omodele [3] reported that the highest producer of sorghum USA produces 10,400,000 metric tonnes alone while Nigeria produces 6,300,000 metric

tonnes making it the highest in Africa and the third highest in the world.

Electrical properties of agricultural products are very important attributes of the products to be noted by Engineers, scientists and farmers in order to understand the behaviour of these products around electrical field [4]. These properties include: Electrical potential (Voltage), resistance, resistivity, conductance, conductivity, capacitance, dielectric constant, Permittivity, impedance, capacitance reactant etc. These properties can also be used to predict, determine, measure and preserve the quality of agricultural products and its environments. Other importance of electrical properties to agricultural products includes: drying, ohmic heating, bio-sensing (in instrumentation, processing, harvesting, grading, storage and environmental control), automation and robotization of agricultural operations [5-8].

Electrical potential (Voltage) is measures in Joules/Coulomb, or Volts. It is the energy per unit charge required to transport any electric charge in the electric field from one sport to another. It is a scalar quantity with no direction and said to be a property of the source charges. Knowledge of electrical potentials is used in batteries and capacitors. Electrical potential can also be called electrical potential difference [9]. Electrical potential can also be related theoretically with electrical potential energy, electrical work done and electrical field (see equation 1-4).

$$\Delta V = V_2 - V_1 \quad (1)$$

$$\Delta V = \frac{\Delta U}{q} \quad (2)$$

$$\Delta V = -\frac{W}{q} \quad (3)$$

$$\Delta V = -\int_1^2 E ds \quad (4)$$

Where ΔV is electrical potential in volts, V_2 is voltage at point 2, V_1 is voltage at point 1, ΔU is electrical potential energy in Joules, q is electric charge in coulomb, W is electrical work done in joules, E is the electric field in Newton/ coulomb and S is distance in meters.

Most researches that pass electrical current through agricultural seeds and measure the voltage used it to correlate with the seeds germinating power and plant growth [9-13]. This research wants to look at electrical voltage through sorghum in order to develop

moisture content measuring equipment using electrical potential. Although other researchers have developed moisture meters using other electrical properties like resistance, conductance and dielectric properties. It is always cheaper to use direct voltage measurement.

The objective of this research is to study the effect of moisture and current frequency on electrical potential of some sorghum varieties, with and intend of using these information to develop a grain moisture meter. To also generate regression equations relating moisture content to electrical potential.

2. Material and Methods

Sample

Sorghum (*Sorghum bicolor* (L.) Moench varieties that were considered in this study are; NGB 01907 (red sorghum), NGB 01589 (White sorghum), NGB 01227(yellow sorghum). Samples were acquired at the National Center for Genetic Resources and Biotechnology (NACGRAB), Ibadan, Nigeria. The samples were divided into their respective varieties and their moisture content determined according to ASAE standard [14]. The samples were then conditioned as described by Sangamithra et al [15] to 10, 13, 16, 19 and 22% db.

Determination of Electrical potential

Grain samples were poured into constructed grain sample holder shown in Figure 1. Sample holder was connected to the complete circuit for the measurement as shown in Figure 2. The circuit is made up of a functional generator, Digital Oscilloscope, sample holder and connecting wires. Input and output voltage readings from the oscilloscope were used to calculate the electrical potential using equation 5. Current frequency ranges used in this research were 1, 500, 1000, 1500 and 2000 kHz. All readings were replicated three times.

$$\Delta V = V_{input} - V_{output} \quad (5)$$

Statistic Analysis

A univariate analysis of variance (ANOVA) was done on the data collected from the experiment using SPSS software version 21. Means separation was carried out using Turkey HSD test. Regression equations were generated using Microsoft excel software.

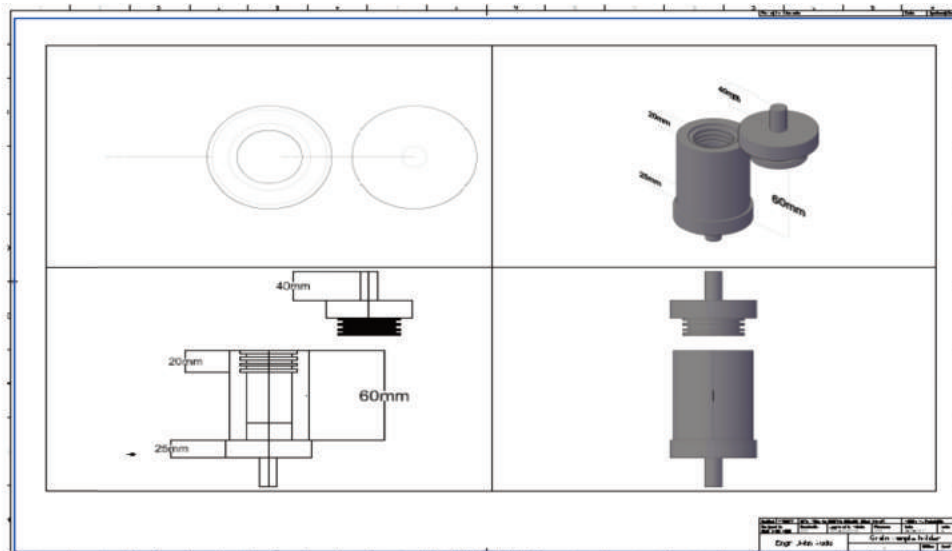


Figure 1. Grain Sample holder

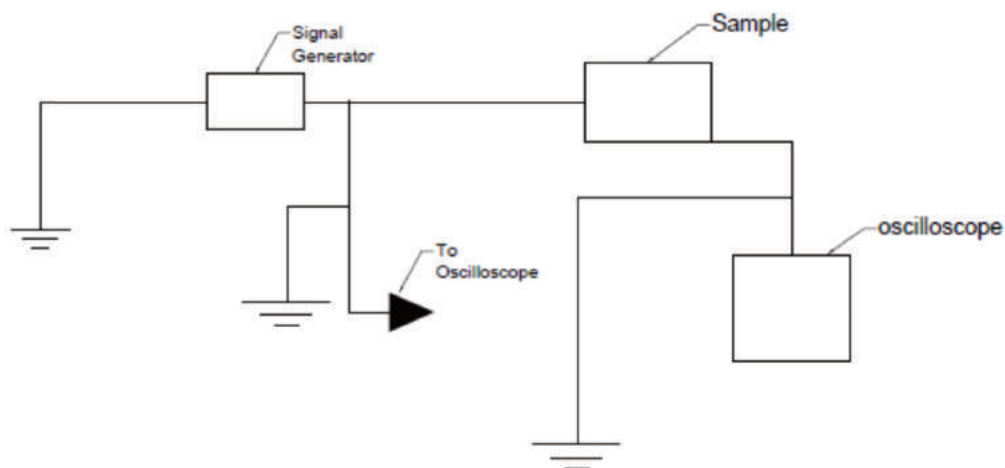


Figure 2. Circuit diagram for measuring Electrical potential

Table 1. Mean Results showing the effect of Moisture, current frequency and Variety on electrical potential (Δv)

*Different alphabets along row or column are statistically different from each other according to Tukey HSD ($P \leq 0.05$, Harmonic Mean Sample Size = 45,000, Mean Square (Error) = 0.072)

Varieties	Moisture	1 kHz	500 kHz	1000 kHz	1500 kHz	2000 kHz	Total
NGB 01589a	10%	-11.437	-13.187	-12.750	-12.613	-10.213	-12.040
	Std. Dev.	2.284	0.012	0.052	0.115	0.115	1.415
	13%	-10.300	-11.480	-11.540	-11.560	-11.560	-11.288
	Std. Dev.	0.000	0.000	0.000	0.000	0.000	0.512
	16%	-10.000	-11.520	-11.560	-11.600	-11.440	-11.224
	Std. Dev.	0.000	0.000	0.000	0.000	0.000	0.636
	19%	-0.200	-4.400	-5.800	-6.600	-6.800	-4.760
	Std. Dev.	0.000	0.000	0.000	0.000	0.000	2.516
	22%	-14.240	-14.767	-3.200	-4.800	-12.400	-9.881
	Std. Dev.	0.000	0.058	0.000	0.000	0.000	5.064
Total	-9.235	-11.071	-8.970	-9.435	-10.483	-9.839	
Std. Dev.	5.001	3.674	3.899	3.235	2.039	3.685	
NGB01907b	10%	-10.840	-11.317	-11.280	-11.720	-12.080	-11.447
	Std. Dev.	0.010	0.006	0.000	0.000	0.000	0.436
	13%	-3.800	-9.280	-9.160	-9.120	-9.280	-8.128
	Std. Dev.	0.000	0.000	0.000	0.000	0.000	2.241
	16%	-9.700	-11.200	-11.600	-11.760	-11.560	-11.164
	Std. Dev.	0.000	0.000	0.000	0.000	0.000	0.781
	19%	-9.120	-10.400	-10.480	-10.680	-10.520	-10.240
	Std. Dev.	0.000	0.000	0.000	0.000	0.000	0.587
	22%	-14.360	-13.160	-13.240	-13.520	-13.400	-13.536
	Std. Dev.	0.000	0.000	0.000	0.000	0.000	0.446
Total	-9.564	-11.071	-11.152	-11.360	-11.368	-10.903	
Std. Dev.	3.528	1.317	1.388	1.495	1.446	2.082	
NGB 01227c	10%	-11.390	-11.953	-12.920	-12.600	-12.997	-12.372
	Std. Dev.	0.010	0.011	0.001	0.000	0.006	0.635
	13%	-10.160	-10.980	-11.000	-11.000	-11.000	-10.828
	Std. Dev.	0.000	0.000	0.000	0.000	0.000	0.346
	16%	-12.000	-11.760	-11.480	-11.720	-11.760	-11.744
	Std. Dev.	0.000	0.139	0.346	0.000	0.000	0.222
	19%	-8.360	-9.880	-10.240	-10.480	-10.360	-9.864
	Std. Dev.	0.000	0.000	0.000	0.000	0.000	0.806
	22%	-11.280	-13.120	-13.080	-13.640	-13.440	-12.912
	Std. Dev.	0.000	0.000	0.000	0.000	0.000	0.871
Total	-10.638	-11.539	-11.744	-11.888	-11.911	-11.544	
Std. Dev.	1.330	1.115	1.146	1.169	1.205	1.256	
Overall Total	10%	-11.222	-12.152	-12.317	-12.311	-11.763	-11.953b
	Std. Dev.	1.178	0.823	0.781	0.447	1.230	0.988
	13%	-8.087	-10.580	-10.567	-10.560	-10.613	-10.081d
	Std. Dev.	3.216	0.999	1.081	1.107	1.029	1.925
	16%	-10.567	-11.493	-11.547	-11.693	-11.587	-11.377c
	Std. Dev.	1.083	0.253	0.181	0.072	0.140	0.639
	19%	-5.893	-8.227	-8.840	-9.253	-9.227	-8.288e
	Std. Dev.	4.283	2.879	2.282	1.992	1.821	2.953
	22%	-13.293	-13.682	-9.840	-10.653	-13.080	-12.11a
	Std. Dev.	1.511	0.814	4.980	4.390	0.510	3.327
Total	-9.813d	-11.227a	-10.622c	-10.894b	-11.254a	-10.762	
Std. Dev.	3.584	2.301	2.706	2.369	1.674	2.634	

3. Results and Discussion

Mean values obtained for electrical potentials after experimentation are shown in table 1. These values are obtained at a current frequency range of 1 – 2000 kHz. All electrical potential values obtained in this study had a negative sign. This shows that sorghum like other agricultural grains offer resistance to electrical currents. Similar observation had been reported by Oluwakemi and Omodele [3], Burubai [16], Kardjilova et al. [17] Shyam et al. [18], Moisés and Marcos [19] and Hlaváčová Z. [20],

For NGB 01589 variety electrical potential values obtained ranges from - 0.2 to - 14.767 volts. The electrical potential trend in this variety show, that it had low values at higher moisture content and high values at lower moisture content across all current frequencies. This occurrence may be due to the fact that water molecules form ions when electric current pass through it therefore carrying electric current faster between sorghum grain

surfaces. The faster the electric current moves through the grains, the lower the electrical potentials. Also Physical examination of data from this variety show, that increasing current frequency within the frequency range of study does not increase or reduce the electrical potential. The trend has a sinusoidal behaviour. It shows that increasing the current frequency from 1 – 500 kHz, produces almost the same electrical potential as increasing it from 1000 – 2000 kHz. This Phenomenon could be because at certain current frequency the molecular ions carrying electrical charges had reached their excitement peak and then it begins to lose this excitement caused by current frequency. Among individual current frequency used in this study, only 1000 and 1500 kHz shows a steady pattern. This pattern shows that increase in moisture content produces decrease in electrical potential values. These two current frequencies range are the recommended frequencies range to be used to measure moisture content when using electrical potential values for this variety.

The values obtained for NGB 01907 variety ranges from -3 to -14.36 volts. The electrical potential trends for increase in moisture show a wave like fluctuations along their paths. This behaviour could be because of the cellular structural arrangement or the present of colour pigment found in this variety. Low potential values are found within 13% moisture content. Below or above this moisture level the electrical potential value increases. This could be due to the fact that, this is the point where tightly held water molecule in the grains cells can be allowed to flow. Increase in current frequency increase the electrical potential of this variety. This occur because increase in current frequency the increases the excitements of water molecules causing to collusion among molecules therefore hinder current flow and reduce electrical potentials. For this variety any current frequency used produced similar behavioral trend on moisture.

Electrical potential values obtained in this study for NGB 01227 variety ranges from - 8.36 to - 13.64 volts. Data trend

shows that increase in moisture show a wave like fluctuations along their paths. This behaviour could be because of the present of colour pigment found in this variety. Also increase in current frequency shows similar behaviour to that of NGB 01907. Low potential values are found within 19% moisture content. This occurs due to the same reason as that of NGB 01907 too.

Analysis of variance done for data of electrical potential displayed in table 2 shows that the choice of analysis (corrected model) is significant at $p \leq 0.05$. This analysis also shows that all factors considered in this study and all its interactions were all significant at $p \leq 0.05$. Tukey HSD mean separation done shows that all levels of the three factors considered (Moisture, current frequency and variety) were statistical different from each others. This is an important factor to be considered when developing instrument that will be used to measure moisture level of sorghum grains use electrical potential values.

Table 2. Analysis of variance (ANOVA) for electrical potential of sorghum

Source	Type III Sum of Squares	Df	Mean Square	F	Sig.
Corrected Model	1542.845 ^a	74	20.849	290.159	1.835 x 10 ^{-133*}
Intercept	26059.214	1	26059.214	362666.344	1.106 x 10 ^{-255*}
Variety	111.291	2	55.645	774.418	8.821 x 10 ^{-80*}
Moisture	458.904	4	114.726	1596.643	8.442 x 10 ^{-122*}
Current frequency	62.857	4	15.714	218.696	1.669 x 10 ^{-61*}
Variety vs. Moisture	381.546	8	47.693	663.747	5.794 x 10 ^{-113*}
Variety vs. Current frequency	36.693	8	4.587	63.831	1.818 x 10 ^{-44*}
Moisture vs. Current frequency	176.826	16	11.052	153.806	2.239 x 10 ^{-84*}
Variety vs. Moisture vs. Current frequency	314.728	32	9.835	136.877	2.776 x 10 ^{-95*}
Error	10.778	150	0.072		
Total	27612.838	225			
Corrected Total	1553.623	224			

Alphabet (a) signify that R Squared = .993 (Adjusted R Squared = .990)

*Significant at $p \leq 0.05$

Regression analyses done for the three varieties are shown in Figure 3/A/B/C. The regression equations developed are:

NGB 01589

$$M = 82.866 - 36.329(\Delta V) - 3.6326(\Delta V)^2 - 0.1043(\Delta V)^3 \quad [R^2 = 0.9616] \quad (6)$$

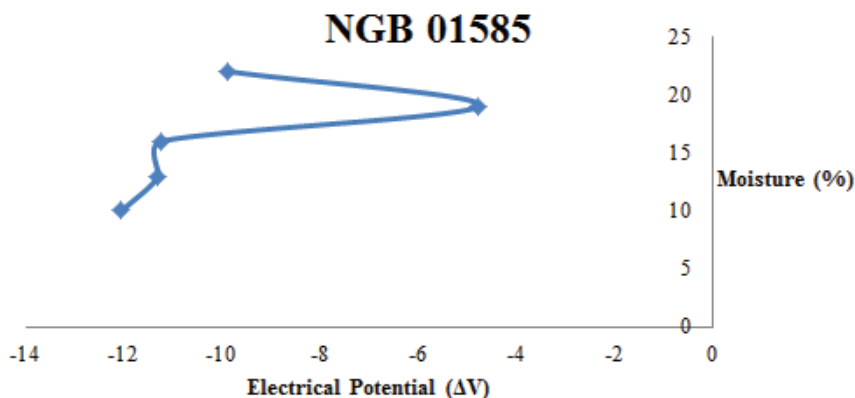


Figure 3/A. Graph of regression of moisture content on electrical potential

NGB 01907

$$M = -1348.6 - 393.93(\Delta V) - 37.226(\Delta V)^2 - 1.1527(\Delta V)^3 \quad [R^2 = 0.8885] \quad (7)$$

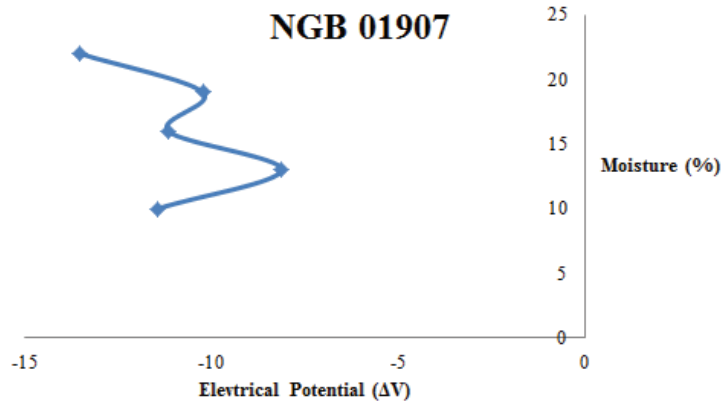


Figure 3/B. Graph of regression of moisture content on electrical potential

NGB 01227

$$M = -1910.4 - 547.9(\Delta V) - 51.477(\Delta V)^2 - 1.5975(\Delta V)^3 \quad [R^2 = 0.572] \quad (8)$$

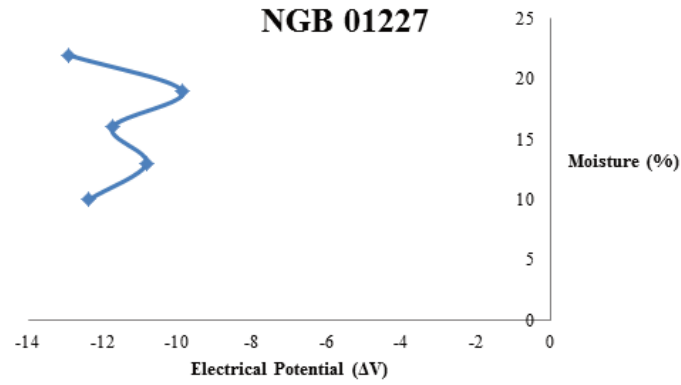


Figure 3/C. Graph of regression of moisture content on electrical potential

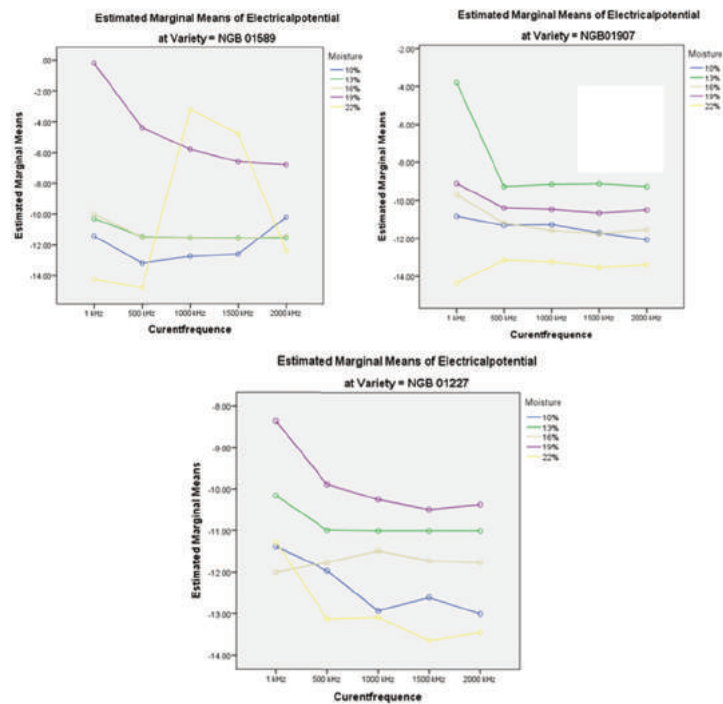


Figure 4. Graphical representation of all three factors (Moisture, current frequencies and variety) and electrical potential

An interaction graph between all factors and their interaction with the values of electrical potential are displayed in Figure 4. It shows that for NGB 01589 variety interactions occur between almost all moisture levels except 19% which has interaction only between 22%. For NGB 01907 variety interaction took place only between 16 and 10%. Interactions in NGB 01227 variety take place only between 10, 16 and 22%.

4. Conclusion

The following conclusion were drawn from this study

- Moisture, current frequency and variety with their interactions has significant effect at $p \leq 0.05$ on electrical potential of sorghum grains
- Behavioral trend between moisture and electrical potential are more visible at current frequency range of 1000 to 1500 kHz in all varieties
- Regressions equations developed shows that electrical potential values can be used to predict moisture of sorghum grains.

References

- [1] **du Plessis J.:** 2008. Sorghum production. ARC-Grain Crops Institute & South Africa Department of Agriculture. Revised edition.
- [2] **Kimber C.T.:** 2000. Origins of domesticated sorghum and its early diffusion into India and China. In 'Sorghum: Origin, History, Technology, and Production', (C. Wayne Smith and R.A. Frederiksen, eds), John Wiley & Sons, New York pp. 3-98.
- [3] **Oluwakemi A. O., Omodele I.:** 2015. The current status of cereals (maize, rice and sorghum) crops cultivation in Africa: Need for integration of advances in transgenic for sustainable crop production. *Int. J. Agric. Pol. Res.*, Vol. 3. No. 3. pp. 233-245. <http://dx.doi.org/10.15739/IJAPR035>
- [4] **Fogarassy Cs., Kovacs A.:** 2016. The Cost-Benefit Relations of the Future Environmental Related Developments Strategies in the Hungarian Energy Sector. *YBL Journal of Built Environment*, Vol. 4. No. 1. pp. 33-48. <http://dx.doi.org/10.1515/jbe-2016-0004>
- [5] **Kardjilova K., Bekov E., Hlavacova Z., Kertezs A.:** 2012. Measurement of Electrical Properties of Rapeseed Seeds with LCR Meter Good Will 8211. *International Journal of Applied Science and Technology*. Vol. 2. No. 8. pp. 35-44.
- [6] **Kondo, N. and Ogawa, Y.:** 2012. Bio-Sensing Engineering for Food Production and Product Utilization. Division of Environmental Science and Technology, Graduate School of Agriculture, Kyoto University.
- [7] **Kondo N., Mitsuji M., Noboru N.:** 2011. *Agricultural Robots: Mechanisms and Practice*, Kyoto University Press.
- [8] **Hlaváčová Z., Kertész Á., Staroňová L., Regrut T., Valach M., Hřeš L., Petrović A., Wollner A.:** 2015. Connection between Biological Material Drying Characteristics and Electrical Properties. *Journal on Processing and Energy in Agriculture*. Vol. 19. No. 1. pp. 1-6.
- [9] **Sedighi N. T., Abedi M., Hosseini S. E.:** 2013. Effect of electric field intensity and exposing time on some physiological properties of maize seed. *Euro. J. Exp. Bio.*, Vol. 3. No. 3. pp. 126-134.
- [10] **Nelson O. E., H. S. Burr.:** 1946. Growth Correlates of Electromotive Forces in Maize Seeds. *Proceedings of The National Academy of Sciences*. Vol. 32. No. 4. pp. 73-84.
- [11] **Wheaton F. W.:** 1968. Effects of various electrical fields on seed germination. Published Retrospective Theses and Dissertations. 3521. Iowa State University. <http://dx.doi.org/10.31274/rtd-180813-928>
- [12] **Demir K. M.:** 2014. Conformity of vigor tests to determine the seed quality of safflower (*Carthamus tinctorius L.*) cultivars. *Australian Journal of Crop Science*, Vol. 8. No. 3. pp. 455-459.
- [13] **ASAE.:** 1998. ASAE S352.2 Standards, 45th Ed. DEC. 97. Moisture Measurement. Unground grain and seeds. 551. St. Joseph, Mich: ASAE
- [14] **Porsev E. G., Malozyomov B. V., Rozhkova M. V.:** 2017. Application of electric corona discharge for grain seeds treatment before sowing. IOP Conf. Series: Earth and Environmental Science Vol. 87. 042013. IPDME 2017. <http://dx.doi.org/10.1088/1755-1315/87/4/042013>
- [15] **Sangamithra A., Swamy G. J., Sorna P. R., Nandini K., Kannan K., Sasikala S., Suganya P.:** 2016. Moisture dependent physical properties of maize kernels. *International Food Research Journal* Vol. 23. No. 1. pp. 109-115.
- [16] **Burubai W.:** 2014. Some Electrical Properties of Melon (*Citrullus colosynthis L.*) Seeds. *J Food Process Technol*, Vol. 5. No. 1. <http://dx.doi.org/10.4172/2157-7110.1000290>
- [17] **Kardjilova K., Yulian R., Zuzana H.:** 2013. Measurement of the Electrical Properties of Spelled Grains – T. Diccocum. *International Journal of Applied Science and Technology*, Vol. 3. No. 7. pp. 118-126.
- [18] **Shyam N. J., Narsaiah K., Basediya A. L., Sharma R., Jaiswal P., Kumar R., Bhardwaj R.:** 2011. Measurement techniques and application of electrical properties for nondestructive quality evaluation of foods—a review. *J Food Sci Technol*, Vol. 48. No. 4. pp. 387–411. <http://dx.doi.org/10.1007/s13197-011-0263-x>
- [19] **Lagares M. L., Morais de Sousa M.:** 2008. Design of a Low-Cost Capacitive-Type Moisture Measurement System Embedded in Combine: Construction and Electrical Characteristics. *ABCM Symposium Series in Mechatronics*, Vol. 3. pp.493-500.
- [20] **Hlaváčová Z.:** 2003. Low frequency electric properties utilization in agriculture and food treatment. *Res. Agr. Eng.*, Vol. 49. No. 4. pp. 125–136.



THE CHANGE ON OPERATOR'S FOCUSING SCHEME INSIDE A MULTI-TASKING OFF-ROAD VEHICLE ALONG WORKING HOURS

Author(s):

I. Szabó – M. Hushki – Z. Bártfai – L. Kátai

Affiliation:

Faculty of Mechanical Engineering, Institute of Mechanics and Machinery, Szent István University, Páter K. u. 1., Gödöllő, H-2103, Hungary

Email address:

szabo.istvan@gek.szie.hu, bartfai.zoltan@gek.szie.hu, mohamma.hushki@hallgato.szie.hu, katali.laszlo@gek.szie.hu

Abstract

Operator's workplace design takes a priority to be developed to increase the level of Quality, Safety and productivity. The multi-tasking vehicles industry design and development process requires dependable and deterministic measures to decide about the tools and equipment in which the new enhancement is ensured to be valuable and reliable using the state-of-the-art engineering solutions. This research is made based on literature of the accumulated knowledge from different studies and analysis are made to provide the necessary input for Human Centred Design process. The results of this research are demonstrating the change on operator's focusing scheme inside a multi-tasking off-road vehicle along working hours for the attached tool for the multi-tasking vehicle.

Keywords

off-road vehicle, measuring operator's focusing scheme, eye tracking, lining operation.

1. Introduction

Human-centred-design approach is considered one of the most effective factors enhancing the productivity of vehicles used in the industrial and agricultural fields. The development of operator's workstation needs to be based on deterministic data which is validated, verified and dependable.

Due to the operational nature of multi-tasking off-road vehicles, operators need to spend long working hours; which increases the level of mental workload leading to human error. 'Li and Haslegrave [1] introduced similar conclusion of which the vehicle design should be human oriented in order to maximize comfort and ability to perform the driving task perfectly and safely by reducing the human error possibilities'. Nowadays more and more agricultural machines are equipped with continuous measurement sensors e.g. measurement of soil resistance [2] to have more exact information on energy demand. This means that the driver attention is split by many signals.

Operating an off-road vehicle is a complex task, requiring a concurrent execution of various cognitive, physical, sensory and psychomotor skills [3], additionally to control attached tools to perform in-field productive tasks such as agricultural and industrial operations. Ensuring the comfortable ride is considered

essential for any vehicle, as well as executing happily and safely requested operational tasks, to that end; the driver ergonomics comes to play as considered as an important parameter that can't be neglected in the design phase of the vehicle [4].

Tractors are companions for many agriculture workers. Well-designed human – tractor interfaces, such as well-accommodated tractor operator enclosures can enhance operations productivity, comfort and safety [4-7].

Many studies have been carried on finding preferred locations of in certain types of tractor controls [8], moreover; emphasizing how critical is the placement of controls in some tractors stating that; it actually creates an impediment to body movement [4].

When we are talking about automation, it is a general aim to improve comfort and safety [9-13], additionally, it is stated that, in the automated driving condition, driver responses to the safety critical events were slower, especially when engaged in a non-driving task. At the same time in their paper – dealing with driver visual attention 'Louw & Merat [14] reached a conclusion shows that the drivers' understanding of the automated system increases as time progressed, and that scenarios which encourage driver gaze towards the road centre are more likely to increase situation awareness during high levels of automation'.

Generating dependable and deterministic data representing human behaviours inside the workplace using validated method will be beneficial for enhancing current cabin designs as well as the future cabin designs.

This research scope is studying operator's focusing scheme, which is one of the most beneficial behaviours to be recognized inside the tractor's cabin using the state of the art engineering solutions to obtain useful results to be considered in the improvement of tractor's cabin design (i.e. upgrading notification system inside the tractor's cabin and allocating new equipment or components inside the tractor's cabin). In addition to enhancing the operation's work procedures design to increase the productivity of a specific agricultural operation (i.e. break time scheduling).

Driving is not only a physical task but also visual and mental tasks [15]. The eyes of a driver are indispensable in performing visual tasks such as scanning the road, and monitoring in-vehicle devices. Mental tasks are important during driving, and include such factors as understanding vehicle dynamics, making situation-dependent decisions, and judging time/space relationships [16-19] were examined the eye-related measures of drivers' mental workload. The mental workload could be defined



Figure 3. CLAAS tractor (Model: ARES 567 ATZ)

Selection of experimental field

Experimental trials are conducted under the supervision of Szent István University management in a field called by Babat-völgy to the north west of Godollo city (Figure 4).



Figure 4. Babat-völgy field



Figure 5. CLAAS LINER 450T used for hay lining

Selection of operation and attached tool

Lining agricultural operation is selected to be the studied operation in this research. After hay cutting in the agricultural field, lining operations are conducted to sort hay into lines in the field. The operation is conducted by specific tools attached to tractors generating hay lines in order to prepare for the hay baling operation. To the purpose of this research, the used attached tool to the CLAAS tractor (Model: ARES 567 ATZ) is CLAAS LINER 450T (Figure 5).

Tobii Glasses 2 equipment

Tobii Glasses 2 (Figure 6) is used to the purpose of obtaining the operator's focusing scheme from his real-time gaze analysis to predefined areas of interest. Which is feeding the research results with the main source of data regarding the target behaviour to be studied.

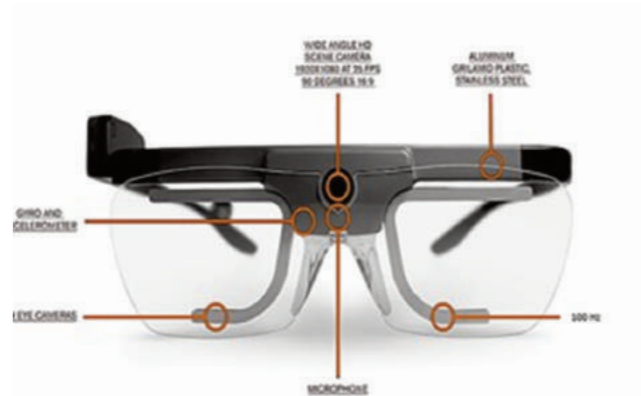


Figure 6. Tobii glasses 2

Controller software

To record eye tracking data, the Tobii Glasses head unit must be fitted onto the test operator's head (similar to a standard pair of glasses). The system must then be calibrated separately for each participant. In the calibration process the test participant is asked to look at a Calibration Card held in-front of the participant for a few seconds. The researcher then starts the recording from Tobii Glasses Controller Software running on a Windows 8/8.1 Pro tablet or any Windows 8/8.1 or 7 computer. After the session, the researcher stops the recording and removes the head unit from the test participant. All interactions with the eye tracker (adding participants to test, initiating calibration, starting/stopping recordings etc.) are done through Tobii Glasses Controller Software.

The controller software also enables the researcher to view/hear the eye tracking session both in real-time (streamed through a wireless or wired connection) and after the recording. When viewing a recording, you can hear what was recorded on the integrated microphone of the Tobii Glasses 2 Head unit, the participant's gaze point also appears as a coloured dot on the scene camera video from the HD camera integrated in the Tobii Glasses 2 Head Unit.

Processing of raw data

The main processing tool of the operators' gazes is the Tobii Pro Lab (Figure 7) which has a powerful post-analysis and visualization tools provide a full spectrum of qualitative and quantitative gaze data analysis and visualizations. Tobii Pro Lab logs events, defines areas of interest, calculates statistics, creates heat maps, and exports data for further analysis in other software.

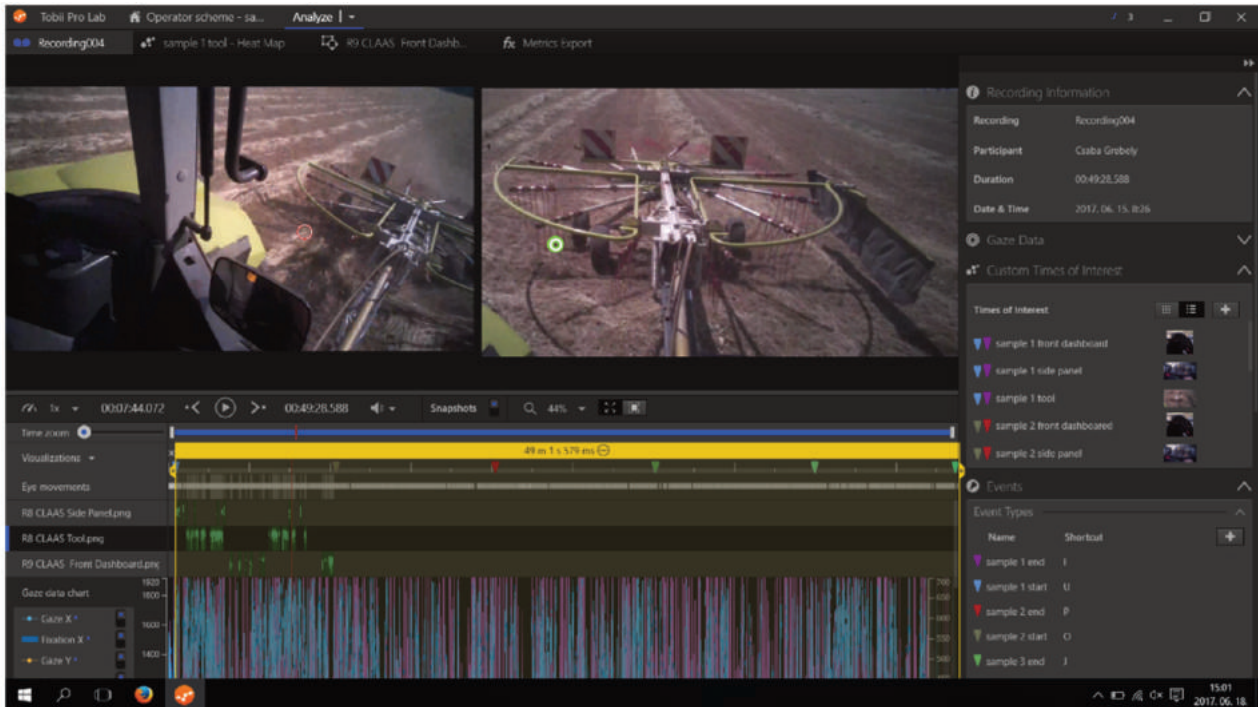


Figure 7. Tobii pro lab – analyser software

Tobii Pro Studio has three different types of fixation filters to group the raw data into fixations and Tobii Pro Lab uses one type of fixation filter to process the data. These filters are composed of algorithms that calculate whether raw data points belong to the same fixation or not. The basic idea behind these algorithms is that if two gaze points are within a pre-defined minimum distance from each other (Tobii Fixation and ClearView Fixation Filter), or possess a speed below a certain threshold (Tobii I-VT Filter), then they should be allocated to the same fixation. In other words, the user has kept the eyes relatively still between the two sampling points.

MATLAB curve fitting toolbox

Curve Fitting Toolbox™ provides an app and functions for fitting curves and surfaces to data. The toolbox lets you perform exploratory data analysis, preprocess and post-process data, compare candidate models, and remove outliers. The application can be used to conduct regression analysis using the library of linear and nonlinear models provided or specify custom equations. The library provides optimized solver parameters and starting conditions to improve the quality of your fits. The toolbox also supports nonparametric modeling techniques, such as splines, interpolation, and smoothing.

To the purpose of this research, the Curve Fitting Toolbox™ is used to generate the formula represents the change on operator's focusing scheme inside a multi-tasking off-road vehicle along working hours from the normalized collected data of the operator's focusing scheme on the attached lining tool CLAAS LINER 450T.

Areas of interest (AOIs) and reference snapshot

The area of interest is a concept and a Pro Lab tool that allows the eye tracking researcher or analyst to calculate quantitative eye movement measures. These include fixation counts and durations. Using this tool, the researcher simply draws a boundary around a feature or element of the eye tracking stimulus whether it's a button on a web page or actor walking across a scene in a video clip. Pro Lab then calculates the desired metrics within the boundary over the time interval of interest.

To the purpose of this research, the selected area of interest is the attached tool CLAAS LINER 450T. Reference snapshot is taken for the item in the area of interest from the video recorded by the Tobii Glasses 2 equipment (Figure 8).



Figure 8. Reference snapshot

Sampling

To measure the operator's focusing on the AOI during the experimental samples of execution times 11 recording samples are used. Each recording sample (X) represents 600 seconds of the real-time recording of the operator's gaze during the lining operation.

Due to the differences between the planned and actual recording time, each sample is normalized to represent the 600 seconds of recording with a factor (N) not exceeding the 17% of the planned recording time. However, collected snap times on the attached tool is multiplied by the Normalization factor (N) according to the formula:

$$\text{Normalized snap time of (X) sample} = \text{Normalization factor (N)} * \text{Actual snap time of (X) sample.}$$

Real world mapping and time of interest

Wearable eye tracking devices; such as Tobii Pro Glasses 2; produce eye gaze data mapped to a coordinate system relative to the wearable eye tracker and the recorded video, not to static objects of interest in the environment around the participant wearing the eye tracker. For most statistical/numerical analysis to be meaningful, the collected eye tracking data needs to be mapped on to items of interest and into a new coordinate system with its origin fixed in the environment around the participant.

To the purpose of this research, automatic real-world mapping tool is used along the time of interest (about 6600 seconds) to measure the operator's gaze on the selected area of interest in the reference snapshot.

3. Results and Discussion

Experimental procedure

An operator is selected to wear the Tobii Glasses 2 equipment which is connected to the central device running Tobii controller software by which the calibration process of operator focusing is conducted and recording process is controlled.

The used tractor (CLAAS Model: ARES 567 ATZ) is located to the operational field (Babat-völgy) attached to the lining tool (CLAAS LINER 450T) conducting the hay lining agricultural operation. The selected area of interested (AOI) is defined to be the attached lining tool.

The operator is mandated to go through the calibration process, start the recording process and get in the tractor cabin for conducting the hay lining operation along 6600 working seconds.

Thereafter; the recording process is stopped. And the recorded video is processed by the Tobii Lab pro software using the automatic real-world mapping tool, which took about 86 working hours. Heat maps representing operator's focusing scheme during

the recording time are generated by the software, which leads to generate the statistic readings using MS Excel software.

The obtained data is Normalized in accordance to the formula: Normalized snap time of (X) sample = Normalization factor (N) * Actual snap time of (X) sample. And resulted data is processed using the MATLAB Curve Fitting Toolbox™ to obtain the representing formula for the change on Operator's focusing scheme inside a multi-tasking off-road vehicle along working hours.

Results

In prior to start recording, the calibration process is done successfully and confirmed automatically by the Tobii controller software and the special calibration card (Figure 9).



Figure 9. Calibration process using the special card and Tobii controller software

Wearing the Tobii Glasses 2 which was connected to the Tobii controller software, after the calibration process, the operator (Mr. Grebely Csaba) was mandated to proceed conducting his regular tasks in hay lining using the tractor (CLAAS ARES 567 ATZ) and the attached lining tool (CLAAS LINER 450T) along about 6600 working seconds. Thereafter; the analysis process was started on the recorded video using Tobii Pro Lab software.

After accomplishing the analysis process, the resulted data was exported by the same software to MS Excel sheet. The samples were normalized in accordance to the mentioned normalization formula.

The exported results (Table. 2) showed:

- 1- The sample reference in the original video (column 1).
- 2- The sample number (X) (column 2).
- 3- The tool snap times in (X) sample (column 3).
- 4- The normalization factor (N) for the sample (X) (column 4).
- 5- The Normalized tool snap times (X*N) (column 5).
- 6- The generated heat map for the sample (X) (column 6).

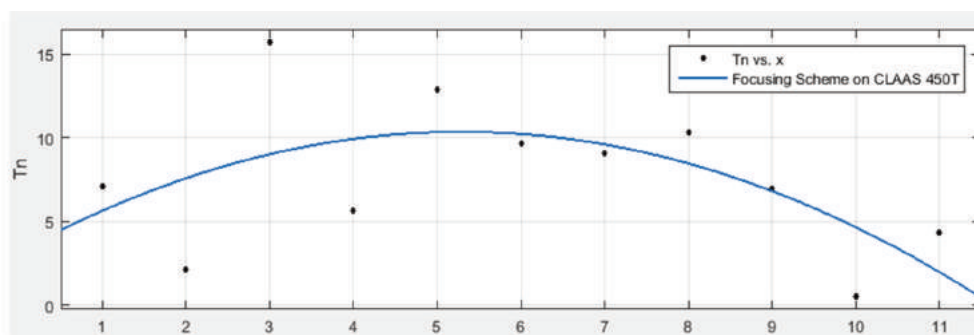
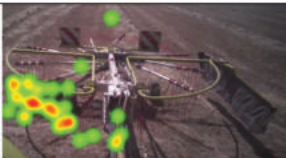
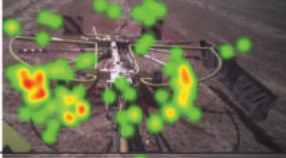
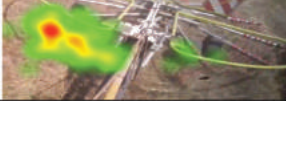


Figure 10. Curve fitting of results

Table 2. Experiment results

Sample Reference	X value	Tool Snap time (Sec)	N Factor	Time (weighted) (Sec)	Generated Heat map
8	1	7.09	1.00	7.09	
9	2	2.15	1.00	2.15	
10	3	15.17	1.00	15.17	
11	4	5.67	1.00	5.67	
12	5	15.38	0.83	12.82	
13	6	9.37	1.03	9.61	
14	7	9.04	1.00	9.04	
15	8	12	0.86	10.29	
16	9	6.94	1.00	6.94	
17	10	0.53	1.00	0.53	
18	11	4.89	0.89	4.35	

Thereafter; the curve fitting operation is conducted using the MATLAB Curve Fitting Toolbox™, the resulted curve (Figure 10) was processed selecting the Linear model (Poly 2) which generates a polynomial equation with the second degree and using Bisquare robust method.

The resulted model and the goodness of fit is shown in (Fig. 11), which gave the final equation:

$$F(x) = -2.814x^2 - 1.21x + 10.21$$

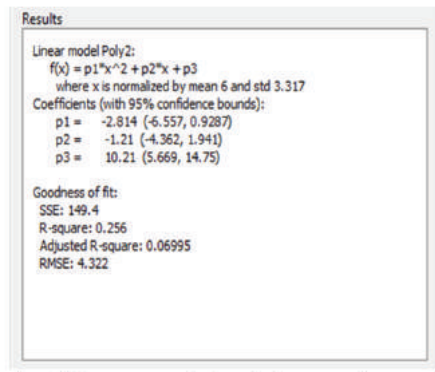


Figure 11. Resulted linear model and the goodness of fit parameters

Discussion

The results showed very accurate and dependable data of the operator's gaze on selected area of interest. The used equipment and supporting software packages easily defined the time in which the operator paid his attention to the attached lining tool during working time in the lining operation.

The analysis of the recorded sample from lining agricultural operation showed that; clearly; the operator focusing scheme is decreasing along working hours which is related to the increment of physical and mental load as the time of the agricultural operation conducting.

4. Conclusions

The methodology used to generate deterministic results which are validated, verified and dependable to represent the operator's behaviour of the focusing scheme inside the workplace (tractor cabin).

The variety of filters and options available under the scope of the analyser software capability is found convenient to come over expected challenges during further research activities such as in-field experiments and outdoors activities.

Such generated results confirmed the feasibility of investing the followed methodology in studying more AOIs inside the tractor cabin to feed the design and/or development processes of the tractor cabin with valuable input data beside the conventional user experience feedback and continual research and development channels.

Additionally; the physical load is expected to be reduced by installing a video screen to the dashboard broadcasting live videos of the lining attached tool. And is expected as well to spare the time and physical effort spend on by the operator for checking the parameters of the tractor and the attention planned track direction.

Usability of research results

Increasing the efficiency and effectiveness of any agricultural or industrial operations that involves human operator – workplace

interaction will be the main benefit of implementing this research methodology. Therefore, a limit is expected to be set for having the break time and scheduling the working days or hours based on deterministic data.

Current cabin designs are subjected to be enhanced with interactive guides and/or equipment for operators at the time in when and/or where it is expected to be needed because of the resulted numbers showing a decrement of focusing scheme.

Additionally, this research methodology is expected to be efficient comparison tool between prototypes of new cabin designs, workload of different operations, operating different vehicles etc, based on deterministic measures.

Future research

This research methodology is proposed to be developed for producing deterministic safety related measures to feed operator's workplace and operation design with the necessary inputs. Which might be dependable to produce the safety or risk assessment reports for certain vehicle or operation design.

References

- [1] Li G., Haslegrave C. M.: 1999. Seated work postures for manual, visual and combined tasks. *Ergonomics*, Vol. 42. No. 8. pp. 1060-1086. <http://dx.doi.org/10.1080/001401399185144>
- [2] Kroulik M., Chyba J., Brant V.: 2015. Measurement of tensile force at the fundamental tillage using tractor's built-in sensor and external sensor connected between machines and their comparison. *Agronomy Research*, Vol. 13. No. 1. pp. 95-100.
- [3] Young K., Regan M.: 2007. Driver distraction: A review of the literature. In: I.J. Faulks, M. Regan, M. Stevenson, J. Brown, A. Porter & J.D. Irwin (Eds.). *Distracted driving*. Sydney, NSW: Australasian College of Road Safety, pp. 379-405.
- [4] Hsiao H., Whitestone J., Bradtmiller B., Whisler R., Zwiener J., Lafferty C., Kau T. Y., Gross M.: 2005. Anthropometric criteria for design of tractor cabs and protection frames. *Ergonomics*, Vol. 48. pp. 323-53. <http://dx.doi.org/10.1080/00140130512331332891>
- [5] Matthews, J.: 1977. The ergonomics of tractors. *ARC Research Review*, Vol. 3. pp. 59-65.
- [6] Kaminaka M.S.: 1985. Research needs in the American agricultural equipment industry. *Applied Ergonomics*, Vol. 16. No. 3. pp. 217 – 220.
- [7] Liljedahl J. B., Turnquist P. K., Amith D. W., Hoki, M.: 1996. *Tractors and Their Power Units*. pp. 226 – 231 (St. Joseph, MI: American Society of Agricultural Engineers).
- [8] Casey S. M., Kiso J. L.: 1990. The acceptability of control locations and related features in agricultural tractor cabs. In *Proceedings of the Human Factors Society 34th annual meeting* (Santa Monica, CA: Human Factors Society). pp. 743 – 747.
- [9] Sheridan T. B.: 1992. *Telerobotics, automation, and human supervisory control*. MIT Press.
- [10] Endsley M. R.: 1996. *Automation and situation awareness*. *Automation and Human Performance: Theory and Applications*, CRC Press. 163–181.
- [11] Fukunaga A., Rabideau G., Chien S., Yan D.: 1997. Towards an application framework for automated planning and scheduling. *Aerospace conference*. In *Proceedings, IEEE*.
- [12] Scheduling S., Dissanayake G., Nebot E. M., Durrant-Whyte, H.: 1999. An experiment in autonomous navigation of an underground mining vehicle. *IEEE Transactions on Robotics and Automation*, Vol. 15. No. 1. pp. 85–95. <http://dx.doi.org/10.1109/70.744605>
- [13] Shen S., Neyens D. M.: 2017. Assessing drivers' response during automated driver support system failures with non-driving

tasks. *Journal of Safety Research*, Vol. 61. pp. 149–155.
<http://dx.doi.org/10.1016/j.jsr.2017.02.009>

[14] **Louw T., Merat N.:** 2017. Are you in the loop? Using gaze dispersion to understand driver visual attention during vehicle automation. *Transportation Research Part C*, Vol. 76. pp. 35-50.
<http://dx.doi.org/10.1016/j.trc.2017.01.001>

[15] **Magó L.:** 2016. Working hours demand of transportation tasks in foil covered field vegetable production technology. *Hungarian Agricultural Engineering*, Vol. 29. pp. 28-31.
<http://dx.doi.org/10.17676/HAE.2016.29.28>

[16] **Kramer A.:** 1990. Physiological metrics of mental workload: A review of recent progress. In D. Damos, (Ed.). 2015. *Multiple-task Performance*, London, Taylor & Francis. pp. 279-328.

[17] **De Waard D.:** 1996. The measurement of drivers' mental workload (Doctoral dissertation). University of Groningen, Haren, Netherlands.

[18] **Brookhuis K., De Waard D.:** 2010. Monitoring drivers' mental workload in driving simulators using physiological

measures. *Accident Analysis and Prevention*, Vol. 42. pp. 898-903. <http://dx.doi.org/10.1016/j.aap.2009.06.001>

[19] **Marquart G., Cabrall C., Winter J.:** 2015: Review of eye-related measures of drivers' mental workload. *Procedia Manufacturing*, Vol. 3. pp. 2854 – 2861.
<http://dx.doi.org/10.1016/j.promfg.2015.07.783>

[20] **Sporrong H., Palmerud G., Kadefors R., Herberts, P.:** 1998. The effect of light manual precision work on shoulder muscles-an EMG analysis. *Journal of Electromyography and Kinesiology*, Vol. 8. pp. 177-184.
[http://dx.doi.org/10.1016/S1050-6411\(97\)00032-1](http://dx.doi.org/10.1016/S1050-6411(97)00032-1)

[21] **Saxby D. J., Matthews G., Warm J. S., Hitchcock E. M., Neubauer, C.:** 2013. Active and passive fatigue in simulated driving: discriminating styles of workload regulation and their safety impacts. *J. Exp. Psychol. Appl.* Vol. 19. No. 4. pp. 287–300. <http://dx.doi.org/10.1037/a0034386>

[22] **Gonçalves J., Bengler K.:** 2015. Driver State Monitoring Systems– Transferable knowledge manual driving to HAD, AHFE.



THE ROLE OF DIGITALIZATION IN THE AGRICULTURAL 4.0 – HOW TO CONNECT THE INDUSTRY 4.0 TO AGRICULTURE?

Author(s):

I. Kovács – I. Husti

Affiliation:

Institute of Engineering Management, Szent István University, Páter K. u. 1., Gödöllő, H-2103, Hungary

Email address:

kovacs.imre@gek.szie.hu, husti.istvan@gek.szie.hu

Abstract

In this time, many authors have reached to the conclusion that development of digital technology and applications are regarded as an important factor in their economic growth and development in the agricultural production. The improvement of mechanization of field work, machinery and equipment is a continuous process. We are witnessing the spread and agricultural use of the more and more modern equipment, which reflects to the technical and technological level of the area. The current paper is analyzing the connections between the tasks of the Agricultural 4.0 and Industry 4.0. In our study we systematize the following area: Industry 4.0, “Smart Farming”, Internet of Things (IoT), Cloud Computing, and Big Data.

Keywords

Industry 4.0, Agricultural 4.0, Smart Farming.

1. Introduction

Hungary is a historical agricultural country. This country produces corn, sunflower, wheat, pork, fruit, milk and many other foods. Agriculture, rural area and farmers are of particular importance when it comes to digitalism modernization reform. Our ability to handle these three problems properly has a great problem on Hungary’s development for the future [1]. In this time, many authors have reached to the conclusion that development of digital technology and applications are regarded as an important factor in their economic growth and development in the agricultural production. The improvement of mechanization of field work, machinery and equipment is a continuous process. We are witnessing the spread and agricultural use of the more and more modern equipment, which reflects to the technical and technological level of the area [2].

2. From Industry 4.0 to Agricultural 4.0

Industry 4.0 is a name for the current trend of automation and data exchange in manufacturing technologies. It includes cyber-physical systems, the Internet of Things and cloud computing. Industry 4.0 creates what has been called a „Smart Factory”. Within the modular structured smart factories, cyber-physical systems monitor physical processes, create a virtual copy of the physical world and make decentralized decisions. Over the

Internet of Things, cyber-physical systems communicate and cooperate with each other and with humans in real time, and via the Internet of Services, both internal and cross-organizational services are offered and used by participants of the value chain [3].

Cloud computing is a kind of computing method based on the internet, which enables shared software and hardware information to be delivered to computers and other equipment on demand. The end users do not need to know basics of the “cloud” or have professional knowledge concerning this, or control directly. All they need to know is what kind of resource they actually require and how to receive relevant service through the internet. Cloud computing describes a new way of adding, using and exchanging IT service based on the internet which involves providing dynamic, expandable and most of the time virtualized resources by using the internet. Generally speaking, cloud computing has the following five features: on-demand service, internet access, resource polling, rapid elasticity and calculability [4].

IoT in this way some sensors connect the internet, so as to operate certain programs and realize remote control. The central computer can Smart Agriculture Based on Cloud Computing and IoT realize concentrated management and control of machine, equipment and personnel based on the internet and improve production and life through more detailed and dynamic means. This is useful for integration and harmony between human society and the physical world and is regarded as the third wave of information industry development following computer and internet. Major IoT technologies include radio frequency identification technology, sensor technology, sensor network technology and internetwork communication, all of which have been involved in the four links of IoT industrial chain, namely, identification, sensing, processing and information delivery [3].

In terms of definitions, Agriculture 4.0, in analogy to Industry 4.0, stands for the integrated internal and external networking of farming operations. This means that information in digital form exists for all farm sectors and processes; communication with external partners such as suppliers and end customers is likewise carried out electronically; and data transmission, processing and analysis are largely automated. The use of Internet-based portals can facilitate the handling of large volumes of data, as well as networking within the farm and with external partners [4]. Other terms frequently used are “Smart Agriculture” and “Digital Farming”. It is based on the emergence of smart technology in agriculture. Smart devices consist of sensors, actuators and communication technology.

3. The Main Stations of Agricultural Development

Agriculture 1.0

Situation in the early 20th century. A labour-intensive system of agriculture with low productivity. It was able to feed the population but required a vast number of small farms and a third of the population to be active in the primary agricultural production process.

Agriculture 2.0

This phase of farming began in the late 1950s when agronomic management practices like supplemental nitrogen and new tools like synthetic pesticides, fertilizers and more efficient specialized machines allowed to take advantage of relatively cheap inputs, thus dramatically increasing yield potential and growing returns to scale at all levels [5].

Agriculture 3.0

“Precision Farming” started once military GPS-signals were made available for public use.

Precision Farming entails solutions for:

- Guidance: early adopters in the mid-1990s were using GPS-signals for manual guidance. They built further on technology used in aerial spraying. The first automatic steering solutions appeared in the late 90s. During the 2000s, guidance accuracy was improved to 5 cm.
- Sensing & control: during the 1990s, combine harvesters were equipped with yield monitors based on GPS location. The first automatic Variable Rate Application (VRA) started at the same time. Low fertiliser prices and high technology costs initially limited adoption of variable rate technology. In the early days, VRA was based on soil sampling input, but performance improved drastically based on data gathered by yield monitors.
- Telematics: Telematics is a technology used to monitor vehicle fleets. It appeared in the early 2000s, and was inspired by the transportation industry. It is based on cellular technology and allows the optimisation of the logistics processes on the farm (Figure 1).
- Data Management: Farming software has become widely available since the birth of the PC in the early 80s.

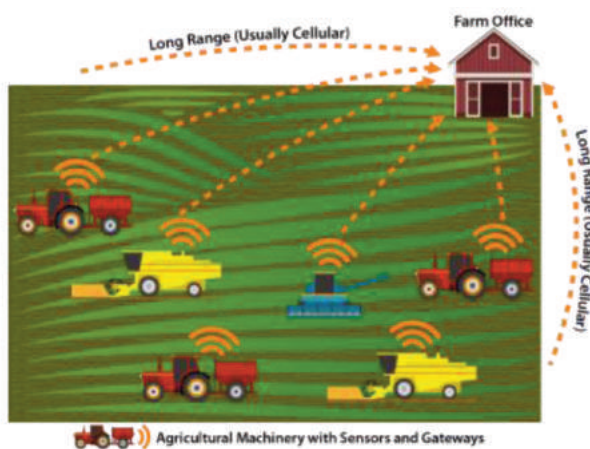


Figure 1. Precision farming [6]

Agriculture 3.0 can be seen as the gradual introduction of more and more advanced and mature Precision Farming technologies.

The focus is moved from pure efficiency in terms of cutting costs to profitability which can be seen as objectively and creatively seeking ways to lower costs and enhance quality or develop differentiated products.

Agriculture 4.0

A new boost in precision agriculture can be observed around the early 2010s based on the evolution of several technologies:

- Cheap and improved sensors and actuators
- Low cost micro-processors
- High bandwidth cellular communication
- Cloud based ICT systems
- Big Data analytics

As of the 2010s, smart technologies are also increasingly fitted as standard features on tractors, combine harvesters and other equipment, like [4]:

- Smart control devices (on-board computers)
- Many sensors for the operation of the machine and the agronomic process
- Advanced automation capabilities (guidance, seed placement, spraying, etc)
- Communication technology (telematics) embedded in the vehicle.

This evolution happens in parallel with similar evolutions in the industrial world, where it is marked as “Industry 4.0”, based on a vision for future manufacturing. Accordingly, the term “Agriculture 4.0” is often used in farming. Agriculture 4.0 paves the way for the next evolution of farming consisting of unmanned operations (for example BoniRob) and autonomous decision systems. Agriculture 5.0 will be based around robotics and (some form of) artificial intelligence [7].

By Harold et al. [7] the digital agriculture offers new opportunities through the ubiquitous availability of highly interconnected and data intensive computational technologies as part of the so-called Industry 4.0.

Digital Agriculture can leverage the smart use of data and communication to achieve system optimization. The tools that enable digital agriculture are multiple and varied, and include cross-cutting technologies such as computational decision and analytics tools, the cloud, sensors, robots, and digital communication tools (Table 1). In addition, field-based activities are enabled by geo-locationing technologies such as Global Positioning Systems (GPS), geographical information systems, yield monitors, precision soil sampling, proximal and remote spectroscopic sensing, unmanned aerial vehicles, auto-steered and guided equipment and variable rate technologies.

Animal-focused technologies include radio frequency identification (RFID chips) and automated (robotic) milking and feeding systems, among others. Controlled-environment agriculture (greenhouses, indoor farms, etc.) is also increasingly enabled by digital technologies such as sensors and robots. Digital agriculture can potentially accumulate large amounts of data, and analytical capabilities that facilitate the effective employment of these data are key implementation factors.

Agriculture will follow other industrial sectors in that the benefits from digital technologies will materialize and become a source of increased production efficiencies once ubiquitously available data are effectively employed [8]. In a global economic environment, a nation’s agricultural competitiveness and ability to sustain critical natural resources will be strongly tied to its ability to innovate in these aspects of the production system. The question is not whether the global agricultural industry should adopt digital technologies, but how this adoption process can occur in an environment that encourages it to fully capitalize on the potential production gains.

Table 1. Enabling technologies for digital agriculture [7]

Production environment	Type of technology	Purpose and benefits
Cross-cutting technologies	Computational decision tools	Use data to develop recommendations for management and optimize multitudes of farm tasks
	The cloud	Provide efficient, inexpensive, and centralized data storage, computation, and communication to support farm management
	Sensors	Gather information on the functioning of equipment and farm resources to support management decisions
	Robots	Implement tasks with efficiency and minimal human labour
	Digital communication tools	Allow frequent, real-time communication between farm resources, workers, managers, and computational resources in support of management
	Geo-locationing (GPS, RTK)	Provide precise location of farm resources (field equipment, animals, etc.), often combined with measurements (yield, etc.), or used to steer equipment to locations
Field	Geographic information systems	Use computerized mapping to aid inventory management and to make geographical crop input prescriptions (fertilizer, etc.)
	Yield monitors	Employ sensors and GPS on harvesters to continually measure harvest rate and make yield maps that allow for identification of local yield variability
	Precision soil sampling	Soil at high spatial resolution (in zones) to detect and manage fertility patterns in fields
	Unmanned aerial systems	Use small, readily deployed remote-control aerial vehicles to monitor farm resources using imaging UAS
	Spectral reflectance sensing	Measure light reflectance of soil or crop using satellite, airplane, or UAS, imaging, or field equipment-mounted sensors, to make determinations on soil patterns, crop
	Auto-steering and guidance	Reduce labour or fatigue with self-driving technology for farm equipment (including robots); can also precisely guide equipment in fields to enable highly accurate crop input placement and management
Livestock	Variable rate technology	Allow continuous adjustment of application rates to precisely match localized crop needs in field areas with field applicators for crop inputs (chemicals, seed, etc.)
	On-board computers	Collect and process field data with specialized computer hardware and software on tractors, harvesters, etc., often connected to sensors or controllers
	Radio frequency ID	Transmit identity data with tags attached to production units (mostly animals) that allow data collection on performance as well as individualized management
	Automated milking, feeding, and monitoring systems	Perform milking or feeding operations automatically with robotic systems, often combined with sensors that collect basic biometric data on animals, thereby reducing labour needs and facilitating individualized animal management

4. Two digital areas of agricultural machinery – The tools of geo-locationing by John Deere

The StarFire 3000 receiver (Figure 2.) picks up satellite signals from the Global Positioning System GPS and has the capability to use GLONASS satellites (Russian navigation satellite system, similar to GPS) to maintain guidance performance even in shaded conditions and other unpredictable environments. Moreover, the receiver is designed to utilize satellites as low as 5 degrees above the horizon. Due to the improved satellite availability, the StarFire 3000 provides a more reliable position. John Deere terrain compensation technology with the StarFire 3000 receiver provides the capability to detect the roll, pitch, and yaw of the vehicle. So the receiver can compensate accordingly to ensure true vehicle position with respect to the ground throughout the field [9].



Figure 2. An John Deere 6150R with the StarFire 3000 Receiver (The photo has been made by the authors)

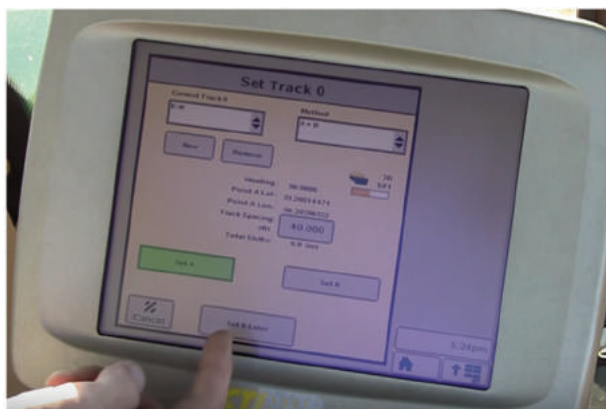


Figure 3. Set the A-B line for the AutoTrack on the GreenStar 3 2630 Display (The photo has been made by the authors)

A variety of John Deere precision applications can be ran on the GreenStar 3 2630 Display (Figure 3) with a StarFire 3000 receiver regardless if it is planting or harvesting season, or for any application in between. The GreenStar 3 2630 display supports the following activations [9]:

- AutoTrac: with the GreenStar 3 2630 display coupled with an AutoTrac activation can provide automatic guidance with integrated AutoTrac, AutoTrac Controller, or AutoTrac Universal.
- Pivot Pro: brings all the benefits of AutoTrac to applications needing automated tracking in circle mode.

- Section Control: reduces input cost by automatically turning implement sections off in previously covered areas and turning them back on precisely to decrease skips.
- RowSense: provides the best in automatic guidance, by pairing up row feeler data with satellite positioning data, when harvesting row crops with a combine or self-propelled forage harvester.
- iTEC Pro: automates end row functions to reduce operator stress and increase efficiency, while consistently managing headland space.
- Machine Sync: provides combine harvest automation, harvest logistics, coverage map sharing, and guidance line sharing functionality.

5. Data exchanges standards in the digital farming by AgGateway

For the agricultural machinery industry, it has been of vital importance that the end customer, the farmer, can decide freely among individual products, and can combine machinery of different manufacturers. This has been achieved via uniform interface standards e.g. the three-point hitch or the ISOBUS connection between tractor and implement (Figure 4).



Figure 4. The data relationship between the tractor and implements with Isobus [9]

The Agricultural Industry Electronics Foundation (AEF) and AgGateway are considered the key players to promote interoperability in the primary agricultural production chain. Since decades ISO-11783 (ISOBUS) is the de-facto standard between tractors and implements of different brands. The AEF an independent international organization, has been founded for the implementation and further enhancement of ISOBUS. But over time its work is expanded to include other important areas such as Electric Drives, Camera Systems, Farm Management Information Systems, High speed ISOBUS and Wireless In-field Communication, developing guidelines and transferring the gained knowledge to ISO level [11].

6. Conclusions

Agriculture has a long and proud past history in applying digital systems including farming operations. Although there have been significant strides forward in improving the leading of farm managers there are still areas for improvement.

Agriculture differs from industry in several aspects but smart technologies can also be used in agricultural production. In the development of technical elements of crop production the development of digital played a dominant role in the past few years. The focus of the digital development of power and working machines was on the more precisely determination of the location

of machine-relations. The data flow between data collector sensors and the central processing unit is regulated by international standards during the operations. All data collected during the operations can be evaluated by using the modular built resource planning systems. GPS controlled agricultural robots work in plant production and in animal husbandry. Smart farming makes use of GPS services, machine to machine (M2M) and Internet of Things (IoT) technologies, sensors and big data to optimize crop yields and reduce waste. Company leaders and senior executives need to understand their changing environment, challenge the assumptions of their operating teams, and relentlessly and continuously innovate [12].

References

- [1] **Toth, L. Horvath, B. Fulop, Zs., Fogarassy, Cs.:** 2017. Climate Regulation of Rearing-Related Building – Evaluating the Factors Related to the Energy Requirement of Heating/Cooling, and Analysis of Alternative Solutions. *YBL Journal of Built Environment*, Vol. 5. No. 1. 73-83. <http://dx.doi.org/10.1515/jbe-2017-0006>
- [2] **Magó L.:** 2002. Economically Reasonable Using of Different Power Machines According to the Farm Sizes. *Hungarian Agricultural Engineering, Periodical of the Committee of Agricultural Engineering of the Hungarian Academy of Sciences*, Vol. 15. pp. 79-82.
- [3] **TongKe F.:** 2017. Smart Agriculture Based on Cloud Computing and IOT. *Journal of Convergence Information Technology*, Vol. 8. No. 2. pp. 210-216. <http://dx.doi.org/10.4156/jcit.vol8.issue2.26>
- [4] **CEMA.:** 2017a. Digital Farming: what does it really mean? Link: <http://www.cema-agri.org/page/digital-farming-what-does-it-really-mean>
- [5] **Bártfai Z., Blahunka Z., Faust D., Ilosvai P., Nagy B., Szentpétery Zs., R Lefánti R.:** 2010. Synergic effects in the technical development of the agricultural production. *Mechanical Engineering Letters*, Szent István University.
- [6] **Romeo S.:** 2016. Enabling Smart Farming through the Internet of Things Current Status and Trends. Principal Analyst – Beecham Research, Sensing Technologies for Effective Land Management Workshop, Bangor University. Link: <http://www.nrm-lee.ac.uk/documents/5.SaverioRomeoSmartFarming.pdf>
- [7] **Harold E., M., Woodard J., Glos M., Verteramo L.:** 2016. *Digital Agriculture in New York State: Report and Recommendations*. Cornell University, Ithaca, N Y.
- [8] **Borocz M., Szoke L., Horvath B.:** 2016. Possible climate friendly innovation ways and technical solutions in the agricultural sector for 2030. *Hungarian Agricultural Engineering*, Vol. 29. pp. 55-59. <http://dx.doi.org/10.17676/HAE.2016.29.55>
- [9] **John Deere.:** 2017. *Agricultural Management Solutions (AMS)*. Link: <https://www.deere.co.uk/en/agricultural-management-solutions/receivers-displays/greenstar-3-display-2630/>
- [10] **TeeJet.:** 2017. *ISOBUS and ISO 11783 Solutions*. Link: <http://teejet.it/hungarian/home/products/application-control-and-equipment/isobus-and-iso-11783-solutions.aspx>
- [11] **Husti I., Daróczy M., Kovács I.:** 2017. Messages from “Industry 4.0” to agriculture Szent István University, Engineering Management Institute, Gödöllő, Hungary (in print).
- [12] **CEMA.:** 2017a. *Connected Agricultural Machines in Digital Farming*. Link: <http://www.cema-agri.org/publication/connected-agricultural-machines-digital-farming>



SYMMETRY-BASED STUDY OF QUASI-ONE-DIMENSIONAL SYSTEMS RELEVANT TO SOLAR CELL APPLICATIONS

Author(s):

I.R. Nikolényi – Cs. Mészáros

Affiliation:

Department of Physics and Process Control, Szent István University, Páter K. u. 1., Gödöllő, H-2100, Hungary

Email address:

nikolenyi.istvan@gek.szie.hu, meszaros.csaba@gek.szie.hu

Abstract

The importance of nanorods and nanotubes are presented in the field of solar cell developments. The investigations of nanostructured related efficiency- increasing processes in external fields are more invited. A group theoretical method for the study of electron states of semiconductors can be relevant to solar energy too is proposed. For further applications a possible extension is raised up.

Keywords

carrier multiplication, vertically aligned nanowire array, line groups, projective representations, magnetic field

1. Introduction

Quasi –one-dimensional systems (Q1D), namely carbon nanotubes (CNT), ZnO nanowires and nanorods and conjugated polymers (CP) have great interests on the field of study of solar cell applications nowadays thanks to the results of Nanotechnology. One of the main ones is the detectability of the so-called Carrier Multiplication process (CM) (or Multiply Exiton Generation one) in some CNT structures, for example in photodiodes [1], or in (6,5) chirality tubes [2], in which a single falling photon can create two or more electron-hole pairs (excitons). With the help of this process the so-called and referencia-considered Shockley-Quisser (SQ) theoretical limit [3] can be overcome. However the CM has been observed in bulk semiconductors since 1950s [4] the contribution of CM for efficiency-increasing is significant in the solar spectrum in quantum-confined semiconductor nanocrystals (in bulk semiconductors this contribution is insignificant) namely in quantum dots – the possible applicability in solar energetics can be originated from Nozik [5] – furthermore in the other type of Q1D nanorods (for example PbSe) [4, 6] and graphene [2, 7-8]. The CM effect in CNTs - due to the fact that they have no direct bulk counterparts- is also important in the understanding the fundamental processes responsible for the effect itself in the case of those nanocrystals at which the effect is enhanced related to their bulk counterparts. This is an open question yet [2]. Another aspect of the importance of the usage of Q1D materials in solar cells is in their technology known as vertically aligned nanowire array. With the help of its oriented geometry high carrier collection efficiency can be reached [9]. Xu et al. [10] gave a

generalized theoretical limit-for efficiency - maintaining the same detailed balance principle on which stand the Shockley and Quisser's results- for nanostructured solar cells and proved its equality to the case of the usage of optical concentrators in Shockley and Quisser's article (42%). Authors also gave examples for published efficiencies of the vertically aligned nanowire-based PV cells (in Figure 1b in their paper). For CNTs array (Figure 1.) as absorbent Bierman et al. [11] reported a solar thermophotovoltaic device and discussed the implications of surpassing the SQ limit. For ZnO nanowire arrays an important example is given by Bi et al. [12] for MEH-PPV/ZnO hybrid solar cell. Further solar cell applications are presented in Peng and Qin's [13] review (Figure 2).

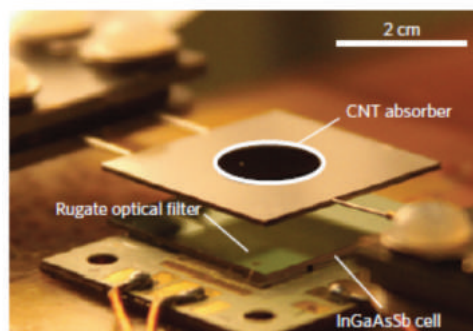


Figure 1. Array of CNTs as solar absorbent in a solar thermophotovoltaic device [11]

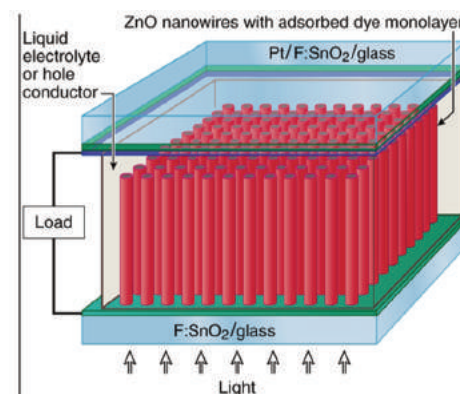


Figure 2. Schematic diagram of the nanowire-based dye-sensitized solar cell [13]

However the increasing of power efficiency is not the only reason for developments, this is the case when solar cells are needed to be installed onto uneven surfaces. For this installations the CP based solar cells are suitable against to the traditional Si-based ones. However the efficiency of polymer solar cells are much lower than Si-solar cells there are some cases when this type of solar cells gives the only result for using solar cells for example installation onto top of tents or onto the surfaces of rucksacks or onto the surfaces of human body thank to their flexibility.

2. Symmetry-based study of 01d solar cell materials

The above mentioned Q1D materials for solar cell applications have special space symmetry described by the so-called line group. Line groups are algebraical groups of Euclidean symmetries leaving invariant a straight line conventionally the z-axis. For the concreteness let us see polymers: they are built up from monomers. Monomers have own symmetry: rotations, mirrors and their combinations leaving the z-axis invariant. This is the one of the 7 possible point groups, namely: "... C_n (successive rotations C_n by $2\pi/n$ around z-axis), S_{2n} , C_{nh} , C_{nv} , D_n (which combine C_n with rotation by π/n followed by horizontal mirror reflection, horizontal and vertical mirror plane and rotation U by π around x-axis, respectively) and D_{nd} and D_{nh} (vertical mirror reflection combined with S_{2n} and C_{nh})..." [14]. But (identical) monomers are regularly repeated along the z-axis (regularly arrangement) and a monomer can achieved from the previous one not by pure translation but by screw axis or glide plane (generalized translations). Every line group can be set up a factorized form: $L=ZP$, where Z the set of generalized transformations and P the point group of the monomer. The generalized translations are needed to be combined with point group operations for getting an algebraical group at the end of procedure. There are infinitely many line groups gathered into 13 families. For example for polyacetylen- it was the one of the first CP for solar cells and it is under theoretical studies nowadays too [15] - the line group is $L2_1/mcm$ and this belongs to the 13th family. The capital L refer to the line group structure, 2_1 means that the generalized translation in this case a rotation by π around z-axis followed by a translation $a/2$, the half of the translation unit along z-axis (the symmetry element of it is a glide plane) the point symmetry group consists of a σ_h horizontal mirror (in the $z=0$ plane) and a σ_v vertical one (in the plan containing the polymer), their products and powers. This point group is D_{2h} . [16]. For getting the line group structure of CNTs we need to follow the so-called rolling up procedure of graphene sheet with identifying carbon atoms by the so - called chiral vector (Figure 3-6) [17].

We wish to study these materials in the presence of external uniform magnetic field. The reasons of our choice are the following: solar cells are under investigations in the presence of external magnetic field both experimenetally and theoretically nowadays [18-22]. However, there are no symmetry-based considerations of solar cells using Q1D materials in external magnetic field to our knowledge. In the field of study of quantum confined nanostructures, namely quantum dots (QD), quantum wells (QW) [23], superlattices (SL) [24] for solar cell applications have great importance but the investigation of CM processes in the presence of external magnetic field has no already received enough attention yet. Beside these facts some important research work have been already published about Q1D materials in constant external magnetic field. For example Trencsényi et al. [25] analyzed the bond connected hexagon chain structures of polyphenylene type of materials placed in perpendicular field to the surface containing the system. This structure is of some CP like PPV whose derivates (for example MEH-PPV as above,

MDMO-PPV) are the one of the most frequently applied materials at polymer based solar cells. For the future applications the Dzyaloshinsky and Kats's [26] result about magnetic field induced order (superconductivity) in Q1D materials might be decisive.

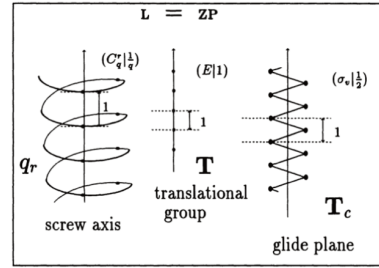


Figure 3. The types of generalized translations of line groups [16]

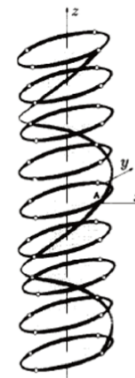


Figure 4. The so-called orbits of the line groups. [16]

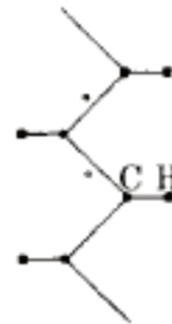


Figure 5. The structure of trans-polyacetylene [16]

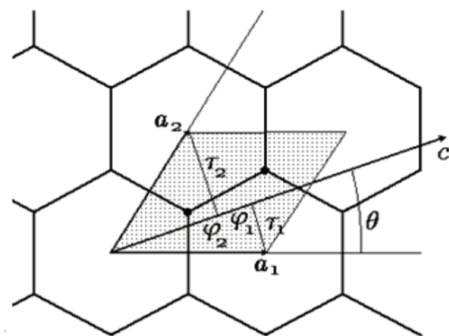


Figure 6. The elementary cell (shaded) and the chiral vector c and angle θ of graphene [17]

Our considerations are based on Tronc and Smirnov's [27] symmetry methods worked out for various semiconductor types

in the presence of external uniform magnetic field. The usages of symmetry methods mean a powerful tool for generating the so-called (optical) selection rules for transitions between electron states allowed by the symmetry of the systems. The symmetry method name means that we have to deal with the symmetry group of the Hamilton operator (Hamiltonian) of the system, with a group of operators representing some coordinate transformation which commute with Hamiltonian. The main problem in the field of study of an electron being in a crystal potential in the presence of external magnetic field that however a uniform field does not destroy the translational invariance of the system physically the operators of pure geometrical translations did not commute with Hamiltonian and these operators do not belong to the symmetry group of Hamiltonian. Brown [28] showed that multiplying with Peierls's phase factor they will have already been commute with it. In this case the representation of the usual translation group will become projective and the symmetry group form a so-called ray group. In the other way Zak [29, 30] defined an operator group (not a ray group) which is homomorphic to the usual translation group and commute with Hamiltonian. of the electron immersed to a crystal in magnetic field. This two constructions will be the same in the finite case and called by Magnetic Translation Group (MTG). But this method do not treat with point symmetry operations and its application for concrete semiconductor structure can be problematic. For this difficulty Tronc and Smirnov [27] gave a method. (A group-theoretical extension for the case of all the admissible rotations, reflections and time reversal is given by Tam [31] too.) Let us see the „General Considerations” of Tronc and Smirnov [27] (sec 2.) in more detail:

The Schrödinger equation for an electron in the crystal potential $V(r)$ placed in external magnetic field:

$$H\Psi_{j,n}(\mathbf{r}) = E_j\Psi_{j,n}(\mathbf{r}), \quad (1)$$

$$H = \frac{1}{2m} \left(\mathbf{p} + \frac{e}{c}\mathbf{A} \right)^2 + V(\mathbf{r}) + \frac{e}{mc}\hat{\mathbf{S}}\mathbf{B}, \quad (2)$$

where H is the Hamiltonian, \mathbf{A} is the vector potential of the magnetic field, \mathbf{p} is the momentum operator ($=i\hbar \text{grad}$), $\hat{\mathbf{S}}$ the spin operator, j the eigenvalue index and n enumerates the eigenstates of the same energy.

Let us choose the form of vector potential in the symmetric gauge:

$$\mathbf{A} = \frac{1}{2}[\mathbf{B}\times\mathbf{r}]. \quad (3)$$

Let be a general element of the symmetry group of the crystal $\mathbf{g}=(R|\mathbf{a})$, which labels the rotation R as the coordinate transformation followed by the translation \mathbf{a} . The „symmetry element” expression means that $V(r)$ crystal potential do not changes under this operation. This is the same case at the last term of the Hamiltonian since does not depend on \mathbf{r} . The action of the symmetry element of the crystal on the geometrical space vectors can be written in the form: $\mathbf{r} \rightarrow \mathbf{g}^{-1}\mathbf{r} = R^{-1}(\mathbf{r}-\mathbf{a})$. From the fact that the scalar product of two vectors does not change under orthogonal transformations and after the acting of operation \mathbf{g} the transformation R^{-1} „can be raised up” from the expressions for \mathbf{p} and \mathbf{A} , the change in the expression of the Hamiltonian is solely:

$$\mathbf{A} \rightarrow \mathbf{A}(\mathbf{r}-\mathbf{a}). \quad (4)$$

At this time the Hamilton operator in the Schrödinger equation acts on $\Psi_{j,n}(\mathbf{g}^{-1}\mathbf{r})$. But this change can be reached in the starting Schrödinger equation with a gauge transformation too. Since $\mathbf{B} = \text{rot}\mathbf{A} = \text{rot}(\mathbf{A} + \text{grad} f(\mathbf{r}))$, where $f(\mathbf{r})$ an arbitrary function of coordinates if add to \mathbf{A} the gradient of:

$$f(\mathbf{r}) = \frac{1}{2}([\mathbf{B}\times\mathbf{a}]\mathbf{r}), \quad (5)$$

$$\mathbf{A} + \text{grad} f(\mathbf{r}) = \mathbf{A}(\mathbf{r}-\mathbf{a}). \quad (6)$$

According to the teaching of quantum mechanics the Schrödinger equation remain unchanged if we carry out at the same time a transformation on the wave function:

$$\Psi_{j,n}(\mathbf{g}^{-1}\mathbf{r}) = \exp(-i\frac{e}{2\hbar c}[\mathbf{B}\times\mathbf{a}]\mathbf{r}) \quad (8)$$

$$\sum_m C_{mn}(\mathbf{g}) \Psi_{j,m}(\mathbf{r}).$$

Thus to every \mathbf{g} symmetry element of the crystal belongs a $C(\mathbf{g})$ matrix which represents it. From this procedure one can see the structure of the elements of the symmetry group of the Hamiltonian: after the geometrical transformation $\mathbf{r} \rightarrow \mathbf{g}^{-1}\mathbf{r}$, where $\mathbf{g}=(R|\mathbf{a})$ and $R\mathbf{B}=\mathbf{B}$, we have to carry out a gauge transformation with $f(\mathbf{r}) = -f(\mathbf{r})$, since $\mathbf{A}(\mathbf{r}-\mathbf{a}+\mathbf{a})=\mathbf{A}(\mathbf{r})$ remain unchanged and we returned to the starting Hamiltonian. The elements of this group labeled by \mathbf{g}^* . the group itself labelled by G^* . G^* contains magnetic translations as subgroup. Tronc and Smirnov [27] pointed out that for the \mathbf{g}^* . elements the representation of matrices are projective

$$\bar{\mathbf{g}}_2^* \mathbf{g}_1^* = \omega(\mathbf{g}_2, \mathbf{g}_1) \bar{\mathbf{g}}_3^*, \quad (9)$$

$$C(\mathbf{g}_2)C(\mathbf{g}_1) = \omega(\mathbf{g}_2, \mathbf{g}_1)C(\mathbf{g}_2\mathbf{g}_1), \quad (10)$$

and

$$\omega(\mathbf{g}_3, \mathbf{g}_2) \omega(\mathbf{g}_3\mathbf{g}_2, \mathbf{g}_1) = \omega(\mathbf{g}_3, \mathbf{g}_2\mathbf{g}_1) \omega(\mathbf{g}_2, \mathbf{g}_1). \quad (11)$$

This method has other solutions for obtaining the so-called irreducible representations (IR) for the symmetry group of the Hamiltonian of bulk materials than MTG theory's ones. For example in the case of two symmetry operations with lattice translations are in $(\mathbf{a}_1, \mathbf{a}_3)$, where \mathbf{a}_3 is in the direction of magnetic field do not commute in contrast with the theory of MTG.

The authors applied their results of their model namely the symmetry groups of bulk semiconductors with the wurtzite and zinc blende structure and for the related nanostructures as well such as SLs, QWs and QDs under magnetic field directed parallel or perpendicular to some symmetry elements (symmetry axis, mirror plane).

From the viewpoint of our research the most interesting results are about Q1D rods and tubes related to bulk materials with wurtzite structure specially for the ZnO nanorods and nanotubes [32]. Their space symmetry are described by the so-called rod groups a subperiodic (1-periodic) subgroups of 3-periodic 3-dimensional space groups [33]. We can get a rod group from the related space group by keeping translations only in the direction of z -axis. The order of rotations or screw axis can only be 1, 2, 3, 4 and 6. The point symmetry of them is the same as ones of their space groups [34]. For generating optical selection rules conventional group theoretical methods can be used just by referring to the corresponding space groups – for example the so-called little group method known as subgroup one [27, 32]. But this method for CNTs whose space symmetry described by general line groups – rod groups are considered as special line groups- due to the lack of bulk counterparts were mentioned at the beginning of this paper cannot be used, there are no „global” space groups related to their space symmetries. It seems to us that

this is an essential open problem yet. At this point can become relevant the mathematical study of projective representations of line groups which one is almost completely missing in the literature. (This idea is suggested by the second author of this paper.) A short description are in the Evarestov's book [34].

3. A possible extension of Tronc and Smirnov's method

Since the Tronc and Smirnov [27] method contains the theory of MTGs- but came to another result for generating IR of symmetry group of Hamiltonian- can be raised naturally the extension of it to the case when external electric field is present too. This type of generalization of the theory of MTG is given by Ashby and Miller [35], in which the Hamiltonian contains space and time periodic potentials. too (However Tronc and co-workers discussed the power of the electric field on the symmetry of ZnO nanorods and tubes and referred to Ashby and Miller [35] too did not considered the cases of time-varying fields). For the solar cell applications would be essential to study the case of the light wave falling onto the semiconductor. If so a perturbing term of this form:

$$\mathcal{K} = \frac{eE}{m} \left(\mathbf{p} + \frac{eA}{c} \right) \frac{1}{2i\omega} [\boldsymbol{\varepsilon} \exp(i\omega t) - \boldsymbol{\varepsilon}^* \exp(-i\omega t)], \quad (12)$$

where „m” is the free electronic mass, ω is the frequency of the radiation, E is the magnitude of the electric field, and $\boldsymbol{\varepsilon}$ is the unit vector in the direction of the field will appear in the Hamiltonian [36].

Our task is to find translation-type operators commuting with the perturbed Hamiltonian which translations are in not purely in the space but in the time too according to Ashby and Miller's [35] ideas. Arising from these ones the time-periodicity leads to the restrictions for possible magnitude of the electric field and because of this fact we have to proceed carefully.

4. Conclusions

However the Q1D materials have a great importance in the efficiency-increasing developments of solar cells but the added external magnetic field investigations of them have no enough attention. The investigations of CM processes are hoped to extend for the case of the presence of external magnetic field. The Tronc and Smirnov's symmetry method is a usefool tool for studying solar cells using Q1D materials under external uniform magnetic field. For more general cases as of the CNTs the research of the mathematical theory of projective representations of line groups would be fruitful. For further solar cell applications the extension for the case of falling electromagnetic wave onto the semiconductors would be a possible way.

References

- [1] Gabor N. M., Zhong Z., Bosnick K., Park J., McEuen P. L.: 2009. Electron-hole pair generation in carbon-nanotube photodiodes, *Science*, Vol. 325. pp. 1367-1371. <http://dx.doi.org/10.1126/science.1176112>
- [2] Wang S. Khafizov M., Tu X., Zheng M., Krauss T. D.: 2010. Multiple exciton generation in single-walled carbon nanotubes, *Nano Letters*, Vol. 10. pp. 2381-2386. <http://dx.doi.org/10.1021/nl100343j>
- [3] Shockley W., Quisser J.H.: 1961. Detailed balance limit of efficiency of p-n junction solar cells. *J.Appl.Phys.* Vol. 32. pp. 510-519. <http://dx.doi.org/10.1063/1.1736034>
- [4] Padilha L. A., Stewart J. T., Sandberg R. L., Bae W. K., Koh W. K., Pietryga J.M., Klimov V.I.: 2013. Carrier Multiplication in Semiconductor Nanocrystals: Influence of Size,

- Shape, and Composition. *Accounts of Chemical Research* Vol. 46. pp.1261-1269. <http://dx.doi.org/10.1021/ar300228x>
- [5] Nozik A. J.: 2002. Quantum dot solar cells. *Physica E: Low-dimensional Systems and Nanostructures*, Vol. 14. No. 1-2. pp.115-120. [http://dx.doi.org/10.1016/S1386-9477\(02\)00374-0](http://dx.doi.org/10.1016/S1386-9477(02)00374-0)
- [6] Sandberg R. L., Padilha L.A., Qazilbash M.M., Bae W. K., Schaller R.D., Pietryga J. M., Stevens M. J., Baek B., Nam S.W., Klimov V. I.: 2012. Multiexciton dynamics in infrared-emitting colloidal nanostructures probed by a superconducting nanowire single-photon detector. *ACS Nano*, Vol. 6. No. 11. pp. 9532-9540. <http://dx.doi.org/10.1021/nn3043226>
- [7] Tielrooij K. J., Song J.C.W., Jensen S.A., Centeno A., Pesquera A., Elorza A. Z., Bonn M., Levitov S., Koppens F. H. L.: 2013. Photoexcitation cascade and multiple hot-carrier generation in graphene. *Nature Physics*, Vol. 9. pp. 248-252. <http://dx.doi.org/10.1038/NPHYS2564>
- [8] Cirloganu C. M., Padilha L. A., Lin Q., Makarov N. S., Velizhanin K. A., Luo H., Robel I., Pietryga J. M., Klimov V. I.: 2014. Enhanced carrier multiplication in engineered quasi-type-II quantum dots, *Nature Communications*, Vol. 5. pp. 1-8. <http://dx.doi.org/10.1038/ncomms5148>
- [9] Tang Y. B., Chen Z. H., Song H. S., Lee C. S., Cong H. T., Cheng H. M., Zhang W. J., Bello I., Lee S. T.: 2008. Vertically Aligned p-Type Single-Crystalline GaN Nanorod Arrays on n-Type Si for Heterojunction Photovoltaic Cells, *Nano Letters*, Vol. 8. No. 12. pp. 4191-4195. <http://dx.doi.org/10.1021/nl801728d>
- [10] Xu Y., Gong T., Munda J. N.: 2015. The generalized Shockley-Queisser limit for nanostructured solar cells. *Scientific Reports*, Vol. 5. pp. 1-9. <http://dx.doi.org/10.1038/srep13536>
- [11] Bierman D., Lenert A., Chan W. R., Bhatia B., Celanovic I., Soljagic M., Wang E. N.: 2016. Enhanced photovoltaic energy conversion using thermally based spectral shaping, *Nature Energy*, Vol. 1. pp. 1-7. <http://dx.doi.org/10.1038/nenergy.2016.68>
- [12] Bi D., Wu F., Yue W., Qu Q., Cui Q., Qiu Z., Liu C., Shen W., Wang M.: 2011. Improved performance of MEH-PPV/ZnO solar cells by addition of lithium salt. *Solar Energy*, Vol. 85. pp. 2819-2825. <http://dx.doi.org/10.1016/j.solener.2011.08.016>
- [13] Peng Q., Qin Y.: 2011. ZnO nanowires and their application for solar cells, *Nanotechnology and Nanomaterials*. <http://dx.doi.org/10.5772/17923>
- [14] Damnjanović M.: 2014. Symmetry of quasi one-dimensional systems: line groups and applications. *Europhysics News*, Vol. 45. No. 3. pp. 27-30. <http://dx.doi.org/10.1051/epn/2014305>
- [15] Tímár M., Barcza G., Gebhard F., Legeza Ö.: 2017. Optical phonons for Peierls chains with long-range Coulomb interactions. *Physical Review B*, Vol. 95. pp. 085150. <http://dx.doi.org/10.1103/PhysRevB.95.085150>
- [16] Milošević I., Živanović R., Damnjanović, M.: 1997. Symmetry classification of stereoregular polymers, *Polymer* Vol. 38. No. 17. pp. 4445-4453. [http://dx.doi.org/10.1016/S0032-3861\(96\)01042-7](http://dx.doi.org/10.1016/S0032-3861(96)01042-7)
- [17] Damnjanović M., Milošević I., Vuković T., Sredanović R.: 1999. Symmetry and lattices of single-wall nanotubes. *Journal of Physics.A: Mathematical and General*, Vol. 32. pp. 4097-4104. <http://dx.doi.org/doi.org/10.1103/PhysRevB.60.2728>
- [18] Madougou S., Made F., Boukary M. S., Sissoko G.: 2007. I-V characteristics for bifacial silicon solar cell studied under a magnetic field. *Advanced Materials Research*, Vols. 18-19. pp. 303-312. <http://dx.doi.org/10.4028/www.scientific.net/AMR.18-19.303>
- [19] Zerbo I., Zougrana M., Sourabie I., Ouedraogo A., Zouma B., Bathiebo D. J.: 2015. External Magnetic Field Effect on Bifacial Silicon Solar Cell's Electric Power and Conversion Efficiency. *Turkish Journal of Physics*, Vol. 39. pp. 288-294. <http://dx.doi.org/10.3906/fiz-1505-10>

- [20] **Zoungrana M., Zerbo I., Ouédraogo F., Zouma B., Zougmore F.:** 2012. 3D modelling of magnetic field and light concentration effects on a bifacial silicon solar cell illuminated by its rear side. IOP Conference Series: Materials Science and Engineering, Vol. 29. pp. 1-12. <http://dx.doi.org/10.1088/1757-899X/29/1/012020>
- [21] **Erel S.:** 2002. The effect of electric and magnetic fields on the operation of the solar cell. Solar Energy Materials&Solar Cells, Vol.71. pp. 273-280. [http://dx.doi.org/10.1016/S0927-0248\(01\)00088-5](http://dx.doi.org/10.1016/S0927-0248(01)00088-5)
- [22] **Erel S.:** 2008. Comparing the behaviours of some typical solar cells under external effects. Teknoloji, Vol. 11. No. 3. pp. 233-237.
- [23] **Barnham K. W. J., Ballard I., Connolly J. P., Ekins-Daukes N. J., Kluftinger B. G., Nelson J., Rohr C.:** 2002. Quantum well solar cells. Physica E: Low-dimensional Systems and Nanostructures, Vol. 14. No. 1-2. pp. 27-36. [http://dx.doi.org/10.1016/S1386-9477\(02\)00356-9](http://dx.doi.org/10.1016/S1386-9477(02)00356-9)
- [24] **Courel M., Rimada J.C., Hernández L.:** 2011. AlGaAs/GaAs superlattice solar cell. Progress in Photovoltaics, Vol. 21. No. 3. pp. 276-282. <http://dx.doi.org/10.1002/pip.1178>
- [25] **Trencsényi R., Gulácsi K., Kovács E., Gulácsi Z.:** 2011. Exact ground states for polyphenylene type of hexagon chains. Ann. Der Phys, Vol. 523. No. 8-9. pp. 741-750. <http://dx.doi.org/10.1002/andp.201100022>
- [26] **Dzyaloshinskii I. E., Kats E. I.:** 2012. Magnetic field induced order in quasi-one-dimensional systems. Physics Letters A, Vol. 376. No. 32. pp. 2206-2208. <http://dx.doi.org/10.1016/j.physleta.2012.05.034>
- [27] **Tronc P., Smirnov V. P.:** 2007. Symmetry of electron states in semiconductor structures under a magnetic field. Physica Status Solidi (b), Vol. 244. No. 6. pp. 2010-2021. <http://dx.doi.org/10.1002/pssb.200642446>
- [28] **Brown E.:** 1964. Bloch Electrons in a Uniform Magnetic Field. Physical Review, Vol. 133. No. 4A. pp. 1038-1044. <http://dx.doi.org/10.1103/PhysRev.133.A1038>
- [29] **Zak J.:** 1964. Magnetic translation group. Physical Review Journals Archive, Vol. 134. pp. 1602-1606. <http://dx.doi.org/10.1103/PhysRev.134.A1602>
- [30] **Zak J.:** 1964. Magnetic translation group II. Irreducible representations. Physical Review Journal Archive, Vol. 134. pp. 1607-1611. <http://dx.doi.org/10.1103/PhysRev.134.A1607>
- [31] **Tam W. G.:** 1968. Invariance groups of the Schroedinger equation for the case of uniform magnetic field II. Physica, Vol. 42. pp. 557-564. [http://dx.doi.org/10.1016/0031-8914\(69\)90160-8](http://dx.doi.org/10.1016/0031-8914(69)90160-8)
- [32] **Tronc P., Stevanović V., Milošević I., Damnjanović M.:** 2006. Symmetry properties of ZnO nanorods and nanotubes. Physica Status Solidi (b), Vol. 243. No. 8. pp. 1750-1756. <http://dx.doi.org/10.1002/pssb.200541382>
- [33] **Milošević I., Stevanović V., Tronc P., Damnjanović M.:** 2006. Symmetry of zinc oxide nanostructures. Journal of Physics: Condensed matter, Vol. 18. pp. 1939-1953. <http://dx.doi.org/10.1088/0953-8984/18/6/010>
- [34] **Evarestov R. A.:** 2015. Theoretical Modelling of Inorganic Nanostructure, Springer, Berlin Heidelberg.
- [35] **Ashby N., Miller S. C.:** 1965. Electric and magnetic translation group. Physical Review Journals Archive, Vol. 139. No. A428. pp. 428-436. <http://dx.doi.org/10.1103/PhysRev.139.A428>
- [36] **Roth L. M., Lax B., Zwerdling S.:** 1959. Theory of optical magneto-absorption effects in semiconductors. Physical Review Journals Archive, Vol. 114. No. 1. pp. 90-104. <http://dx.doi.org/10.1103/PhysRev.114.90>



GROUNDWATER DYNAMICS AND RECHARGE TRENDS IN SEMI-ARID IRRIGATED LANDS OF NIGERIA

Author(s):A. Sobowale¹ – A. A. Ramalan² – O. J. Mudiare² – M. A. Oyeboode²**Affiliation:**¹Department of Agricultural and Bioresources Engineering, Federal University of Agriculture, P.M.B. 2240 Abeokuta 110001, Nigeria.²Department of Agricultural Engineering, Ahmadu Bello University, Zaria, Nigeria**Email address:**

sobowalea@funaab.edu.ng, ramalanaa@aol.com, ojmudiare@yahoo.com, muyideenoyebode2004@yahoo.com

Abstract

Groundwater dynamics and recharge trends were evaluated for three years (2008 – 2011) to elucidate the daily, monthly and seasonal response to climate and irrigation. Observed water levels ranges between 120 – 1180 mm, below ground level (b.g.l.) in the identified soil profiles in the area; a good correlation of water level exist in the area despite differing soil profile types and non-uniform irrigation regime in the dry season. Analysis for trend, change and randomness reveals high diurnal variations in the cool dry season, hot dry season and wet season. Exponential smoothing model was found to adequately predict groundwater recharge and discharge in the area. A new cropping schedule was proposed to forestall low crop yields caused by the new groundwater regime.

Keywords

groundwater dynamics, recharge trends, water level changes, randomness test

1. Introduction

Shallow groundwater tables have been shown to provide a portion of crop water needs [1]; this suggests that irrigation water demand could be reduced under a conjunctive use of available water resources. According to [2], water scarcity is a major occurrence in arid and semi-arid regions of the world; the vagaries of the weather and climate change realities have placed all resources, agricultural activities and ecosystem services under severe stress. The food security implication of this development is quite enormous especially in developing countries like Nigeria where the agricultural production system is predominantly rain-fed [3]. Utilization of shallow groundwater for crop cultivation experienced a boom in Nigeria following the initiation of the National Fadama Development Project in 1991; this led to the national mapping of shallow groundwater zones in the country and a radical development of valley bottoms for dry season farming to boost food security [4][5]. These efforts were meant to compliment the initial efforts of establishing large scale irrigation schemes following the Sahelian drought of 1970s; many of the schemes so establish were bedevilled with serious problems such as huge maintenance cost, salinization, poor irrigation water management, weak cost recovery and reduction of river flows

(climate change). While the successes recorded at that time were unprecedented, they were however, short lived and continuity was a huge challenge leading to many of the schemes becoming dilapidated and/or abandoned in subsequent years [6]. The climate change problem has tremendous effect on water availability on all the irrigation schemes located in semi-arid northern Nigeria leading to the need to develop and apply water-saving practices, e.g., improving the canal system, using water saving irrigation technology and adjusting cropping patterns in order to achieve sustainable agricultural development and river basin environmental equilibrium [7, 8]. The most efficient and adaptable water saving measure to the region is the development of conjunctive use of both surface water and groundwater in the irrigation schemes; irrigation return flows could be reused where there are adequate drainage structures and a monitoring programme for groundwater. Over the years, groundwater irrigation has made substantial contribution to agriculture and food security, and has lifted many millions of households out of poverty [9]. The FAO estimated that more than one-third of the world's 303 million ha irrigated area is served by groundwater; over 70 % of this is in Asia [10].

An understanding of groundwater dynamics and recharge trends in irrigated lands is therefore imperative for implementing a conjunctive water use system in semi-arid regions; literature suggests that diurnal fluctuations of groundwater on irrigated lands are principally induced by three main factors: evaporation, barometric pressure and tidal actions; other factors include topography, soil type, land use, water management practices and anthropogenic impacts [11-13]; all these are made possible by the hydrodynamic balance caused by the interactions between atmospheric, surface and subsurface water systems represented by the hydrological cycle. The study of groundwater dynamics in agricultural lands is a vital requirement for an efficient management of water resources; several approaches have been highlighted in literatures [14]. The flow of water within confined and unconfined aquifers is complex and may require extensive data and detailed modelling to understand. However, relatively simple data, such as water levels in a carefully designed network of monitoring wells, can be combined with estimates of rainfall input to provide key indications of groundwater dynamics and recharge.

The objectives of this research was to evaluate the dynamics of groundwater and to elucidate recharge trends in the largest irrigation scheme in the semi-arid region of Nigeria with a view to providing inputs for the development of a conjunctive water

management system as an adaptation to climate change realities in Sub Saharan Africa (SSA).

2. Materials and Methods

The study was conducted at the Irrigation Research station (IRS), Kadawa, within the West Branch of the Kano River Irrigation Project located between Longitude 8° 25' 47" and 8° 26' 12" and

Latitude 11° 38' 30" and 11° 38' 51"; Table 1 shows the hydraulic characteristics of soils at the study site. The experimental farmland belong to Sudan savannah agro-ecological zone of Nigeria characterized by a uni-modal rainfall regime, with mean annual rainfall between 700 mm – 800 mm that is always erratic, poorly distributed and falls between June and October of each year, evaporation is also high with diurnal variations as reported by [15].

Table 1. Hydraulic characteristics of soils at sampling points [17]

Sn.	Piezometer Code	Soil Profile Description	Void Ratio	Porosity	Degree of Saturation	Specific Yield Sy
1	Pa3/F3-4/1	Deep soils, loamy sands over sandy	0.187	0.158	0.987	0.829
2	Pa3/F3-5/2	clay loam, well drained with	0.206	0.171	0.993	0.821
3	Pa3/F3-7/3	Aeolian drift over colluvial/alluvial soils as parent material.	0.204	0.169	0.978	0.809
4	Pal/F3-4/1	Moderately deep soils underlain by	0.179	0.153	0.998	0.846
5	Pal/F3-5/2	iron pan, loamy sand over sandy	0.169	0.145	0.994	0.849
6	Pal/F3-7/3	loam, well drained soils with Aeolian drift parent material.	0.203	0.169	0.995	0.826
7	PI/F3-4/1	Shallow soils, loamy sands (30 mm	0.137	0.121	0.943	0.823
8	PI/F3-5/2	to 100 mm depth) underlain by iron	0.179	0.152	0.995	0.843
9	PI/F3-6/3	pan. Well drained with Aeolian drift parent material.	0.211	0.175	0.995	0.821
10	Pab/F3-5/1	Deep soils, loamy sands over sandy	0.200	0.167	0.997	0.829
11	Pab/F3-6/2	clay between 30–100 mm. Poorly	0.219	0.179	0.994	0.814
12	Pab/F3-7/3	drained with Aeolian drift over colluvial/alluvial soils as parent material.	0.135	0.119	0.998	0.879
13	Pb/F3-4/1	Loamy sands within 30 mm over	0.100	0.091	0.945	0.854
14	Pb/F3-4/2	sandy clay loams with	0.099	0.089	0.979	0.889
15	Pb/F3-4/3	colluvial/alluvial parent material.	0.150	0.131	0.991	0.861

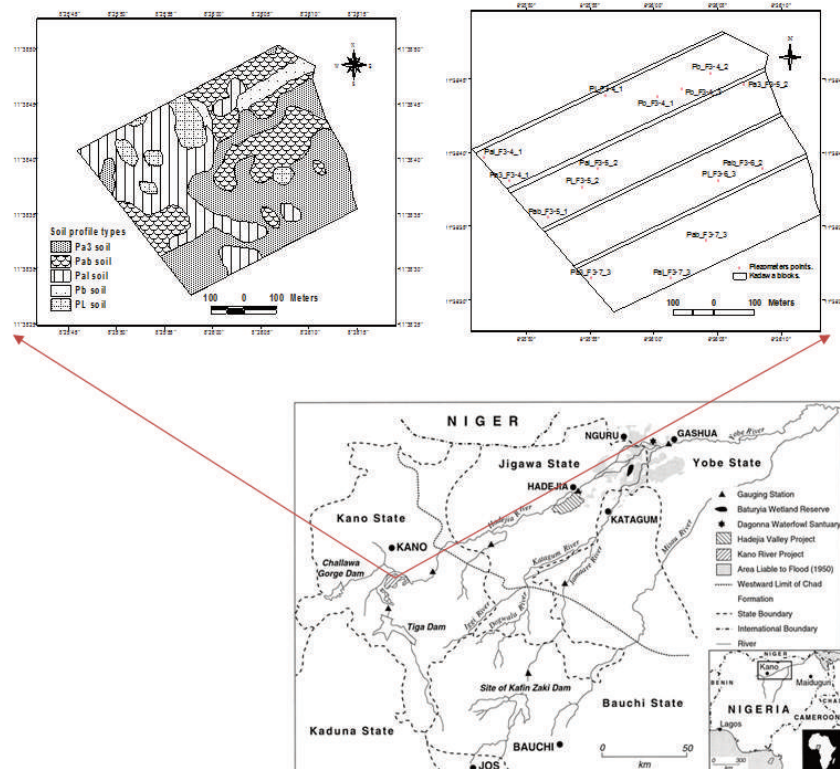


Figure 1. Locations of the Study site

Data collection and Analysis

Groundwater level monitoring was carried out daily for three years (2008/2009, 2009/2010, and 2010/2011) at 15 locations using randomly installed piezometers in three replicates in each identified soil profile types shown in Figure 1; in order to minimize sampling errors, double measurements of groundwater levels was implemented using a combination of an automatic water level dipper and an improvised float gauge. The data obtained were subjected to statistical analysis using TREND® v1.0.2 software to detect trend, change and randomness in the time series; the tests include: Mann-Kendall test and Spearman's Rho test (non-parametric test for trend), Linear Regression test (parametric test for trend); Distribution-Free CUSUM test (non-parametric test for step jump in mean), Cumulative Deviation test

and Worsley Likelihood Ratio test (parametric test for step jump in mean); Rank-Sum test (non-parametric test for difference in median from two data periods) and Student's t test (parametric test for difference in mean from two data periods); Median Crossing test, Turning Points test, Rank Difference test (non-parametric test for randomness) and Autocorrelation test (parametric test for randomness). Groundwater recharge and discharge on the farmland were computed on a spread sheet (Microsoft Excel®) using water level fluctuation (WLF) method [16]; the resulting groundwater recharge and discharge hydrographs were analysed for trends and subjected to goodness of fit to evaluate possible prediction of groundwater recharge and discharge in the area using moving average and exponential smoothing methods.

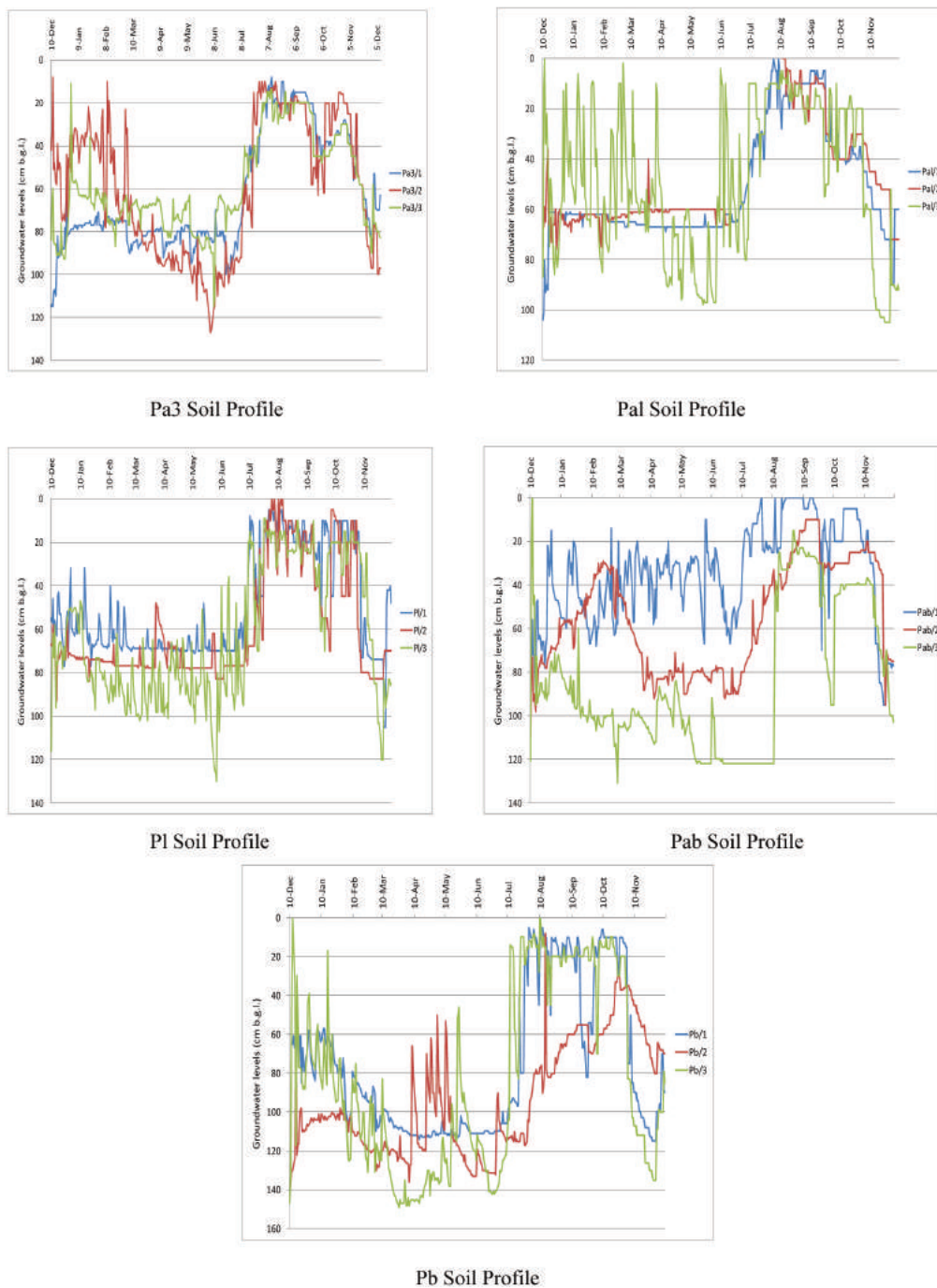


Figure 2. Groundwater trend in all soil profile types in the study area

3. Results and Discussion

Trend of Groundwater level

The groundwater regime at the IRS farmland reveals high diurnal variations that were found to be dependent on season. Groundwater level changes rapidly in response to events of irrigation in the dry season and rainfall in the wet season. This observed behaviour was due to the continuous cropping practiced on the farmland throughout the year; it was observed that water levels were generally high (near ground surface) in the wet months, worthy of note was the observation that most parts of the farmland is completely waterlogged in the month of July, August, September and some parts of October making the field suitable for lowland rice production at those periods. Slight variations in groundwater levels were observed in all the soil profile types found at the site; observed water levels ranges between 120 – 840 mm, 90 – 740 mm, 80 – 880 mm, 170 – 940 mm and 190 – 1180 mm below ground level (b.g.l.) in the Pa3, Pal, Pl, Pab and Pb soil profiles respectively. Figure 2 present the observed groundwater level trends at the study locations.

It was generally observed that the water table was lowest (deep) in Pb soil profile within the period of study; this part of the land also gave the least diurnal variation. This might be due to the land use in that part of the farm as it remained fallow in the period of study; some of the local farmers interviewed explained that the area was abandoned due to suspected salt build up leading to low crop yield from that part of the field. An examination of the soil characteristics revealed that this portion of the farmland lies towards the direction of groundwater flow hence was always waterlogged for most parts of the year. Contrary to farmers' opinion, [15] reported that there was no salt build up in this part of the farmland.

Correlation analysis reveals that there was a good correlation in observed groundwater levels among the 15 piezometers regardless of differing soil profile types and non-uniform irrigation regime in the dry season. Strong correlation was observed among the piezometers replicated in the same soil profile types, this shows that groundwater levels in all the soil profile types on the farmland can be predicted by simple linear regression regardless of the season; this information is very pertinent for the development of a regional groundwater model for the area. Some cases of poor correlations were also observed; this is however of no significant consequences. When the data was analysed on annual basis, no observable trend was identified; however, exploratory data analysis (EDA) show that the groundwater levels reveal both periodic and linear trend as shown in Figure 2; these can be easily understood by seasonal analysis. Seasonal decomposition of the data was carried out based on the identified seasons in the area namely; cool dry season (108 days), hot dry season (73 days) and wet season (183 days).

Cool dry season

The mean water level in the cool dry season was 720 mm, 750 mm, 700 mm, 760 mm and 870 mm b.g.l. in Pa3, Pal, Pl, Pab and Pb soil profiles respectively. The tests for trend (Mann-Kendall, Spearman rho, and Linear Regression) reveal that there was a statistically significant trend at $\alpha < 0.01$ level in Pl, Pab, and Pb soil profiles, respectively. The Pa3 profile however displayed a significant trend at $\alpha < 0.05$ level while there was no significant trend of groundwater level observed in Pal soil profile. The implication of these observations of increasing groundwater level trend is that it can lead to the twin menace of waterlogging and soil salinization. Waterlogging brings about changes in cropping schedules and reduces the agricultural potentials of irrigated lands. Soil salinity on the other hand influences agricultural

productivity due to reduced crop yield which has direct consequences on food security. The results compares favourably with that reported by [18], where over 8.4 million hectares of irrigated lands in semi-arid regions of India has been affected by soil salinity and alkalinity, out of which about 5.5 million hectares are waterlogged.

Hot dry season

The hot dry season has a mean water level of 770 mm, 620 mm, 740 mm, 800 mm and 1080 mm b.g.l. in Pa3, Pal, Pl, Pab and Pb soil profiles, respectively. There was a statistically significant trend at $\alpha < 0.01$ level in Pa3 and Pab soil profiles, respectively; no significant trend was observed in Pal, Pl and Pb soil profiles in the hot dry season. The tests for step jump in mean (Distribution Free CUSUM, Cumulative Deviation and Worsley Likelihood Ratio) show a statistically significant step jump in all the soil profiles, it was observed generally that water levels had higher values at the beginning of the season than latter part of the season implying that the water levels are subject to change throughout the season in all the soil profiles. The tests for randomness (Median Crossing, Turning Points, Ranked Difference and Autocorrelation) revealed that the water level data do not come from a random process at $\alpha < 0.01$ level. The tests for step jump in mean (Distribution Free CUSUM, Cumulative Deviation and Worsley Likelihood Ratio) show a generally statistically significant step jump in all the soil profiles at $\alpha < 0.01$, it was observed that water levels had higher values at the beginning of the season than latter part of the season in Pa3 profile implying that the water levels are subject to change; it was equally observed that the mean water level was lower at the beginning of the season than towards the end in Pab, Pal, Pb and Pl soils. The tests for randomness (Median Crossing, Turning Points, Ranked Difference and Autocorrelation) revealed that variations in the water level in this season do not come from a random process at $\alpha < 0.01$ level.

Wet Season

The mean water level in the 172 days of the wet season was 420 mm, 360 mm, 400 mm, 490 mm and 600 mm in Pa3, Pal, Pl, Pab and Pb soil profiles respectively. The tests for trend (Mann-Kendall, Spearman rho, and Linear Regression) reveal that there was a statistically significant trend at $\alpha < 0.01$ level in all the soil profiles. The tests also revealed that all the profiles reveal a decreasing trend of groundwater levels. The tests for step jump in mean (Distribution Free CUSUM, Cumulative Deviation and Worsley Likelihood Ratio) show a statistically significant step jump in all the soil profiles at $\alpha < 0.01$; it was also observed generally that water levels had higher values at the beginning of the season than latter part of the season implying that the water levels has a rising profile as the rains (which is solely responsible for the rise at this time) increase in amount and intensity. This suggests that groundwater levels in the wet season could be fairly predicted from rainfall amounts in the wet season using a linear model. The tests for randomness (Median Crossing, Turning Points, Ranked Difference and Autocorrelation) revealed that the water level data do not come from a random process at $\alpha < 0.01$ level.

Implications for crop planning

A salient outcome of the water level studies in the area is the need for change in the cropping schedule on the farmland. Some crops planned for the area is no longer feasible because of the new groundwater regime; farmers who are still adhering to the old

cropping schedule are experiencing low crop yield. Adequate root zone depth is essential for good crop productivity and access to soil air; the pore spaces in the soil have now been filled with water indicating very poor land drainage caused by deteriorating drainage system on the farmland. The use of tile drains is suggested for the area.

The following crops are suggested for cropping on the farmland: Wet season (Rice); Cool dry season (Wheat, Potatoes,

Onions, Pepper, Tomatoes, Vegetables and Maize); Hot dry season (Maize, Onions, Cowpea, Tomatoes and Vegetables). These are crops that could be supported by the groundwater regime observed on the farmland; however, further studies need to be carried out to confirm these suggestions.

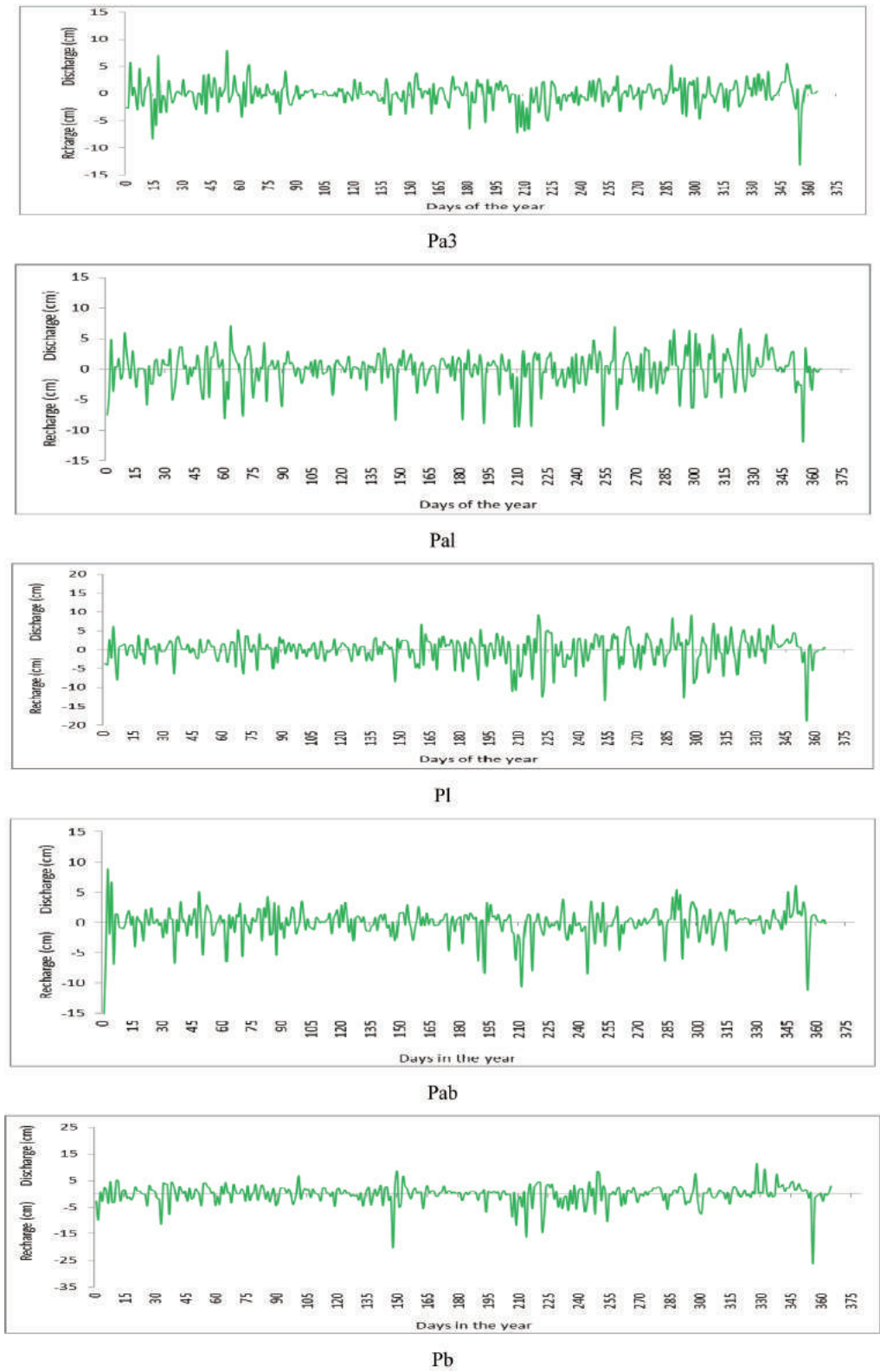


Figure 3. Groundwater recharge and discharge trend at the study site

Groundwater recharge and discharge prediction

The W.L.F analysis was based on the premise that groundwater rises as a result of recharge water arriving at the water table while groundwater discharge takes place when water flows away from storage which is evident by the reduction of water level. Figures 3 presents the hydrological time series of mean daily groundwater recharge and discharge from the five soil profile types on the farmland. The pattern displayed is very similar to that observed in the groundwater levels presented earlier. Groundwater recharge ranges between 10 mm – 60 mm as the case may be on a daily basis, this variation in recharge and discharge was found to oscillate about zero in all the soil profile types. Stemming from visual inspection of these time series plots, no visible trend can be seen in the 1095 days of data in all the soil profiles. However, all of them exhibit cyclical variation which is an indication that the series has only a periodic component; the implication is that days of recharge are immediately followed by days of discharge.

Predicting recharge and discharge in this scenario was no doubt a daunting task. Attempts were made to fit the data series without any good success, simply because the values in the daily series were very small and make analysis very problematic. The data series showed an evidence of a partial fit when moving average was considered; this method of forecasting did not account for some data points in the series, hence was not accepted as having a good fit. When exponential smoothing was considered, a better fit for the data with insignificant residuals was obtained as shown in figure 4. This better fit is indicative of the fact that values of groundwater recharge and discharge can easily be predicted when previous values are known and $\alpha = 0.2$. The equation of fit was:

$$Re_{t+1} = \alpha Ra_t + (1 - \alpha) Re_t \quad (1)$$

Where Re is predicted recharge or discharge at time t or $t+1$ in cm, Ra is the actual value of recharge or discharge at time t in cm

and α is a constant ($0.01 < \alpha < 0.3$).

4. Conclusion

Groundwater dynamics and recharge trends at the Irrigation Research Station, Kadawa within the Kano River Irrigation Project had been evaluated for three years. The results revealed a very high diurnal variation of groundwater level trend in the period of study; statistical tools for trend indicate significant trend at $\alpha < 0.01$ level in Pl, Pab, and Pb soil profiles, respectively in the cool dry season while groundwater level changes rapidly in response to irrigation in the dry season and rainfall in the wet season as a result of intensive cropping on the farmland. Water levels ranges between 120 – 840 mm, 90 – 740 mm, 80 – 880 mm, 170 – 940 mm and 190 – 1180 mm below ground level (b.g.l.) in the Pa3, Pal, Pl, Pab and Pb soil profiles respectively. There was a good correlation of groundwater levels at the monitoring locations regardless of differing soil profile types and non-uniform irrigation regime in the dry season indicating that groundwater levels can be predicted by simple linear regression. There is also the need to change the cropping schedule as crops planned for the farmland are no longer feasible because of the new groundwater regime; the old cropping schedule should be discontinued because of low crop yield. The following crops are suggested for cultivation on the farmland: Wet season (Rice); Cool dry season (Wheat, Potatoes, Onions, Pepper, Tomatoes, Vegetables and Maize); Hot dry season (Maize, Onions, Cowpea, Tomatoes and Vegetables). These are crops that could be supported by the groundwater regime observed on the farmland; however, further studies need to be carried out to confirm these suggestions. Prediction of groundwater recharge in the area was found to be possible using exponential smoothing method which gave minimal prediction errors. A very good fit was obtained between actual and predicted groundwater recharge in the area.

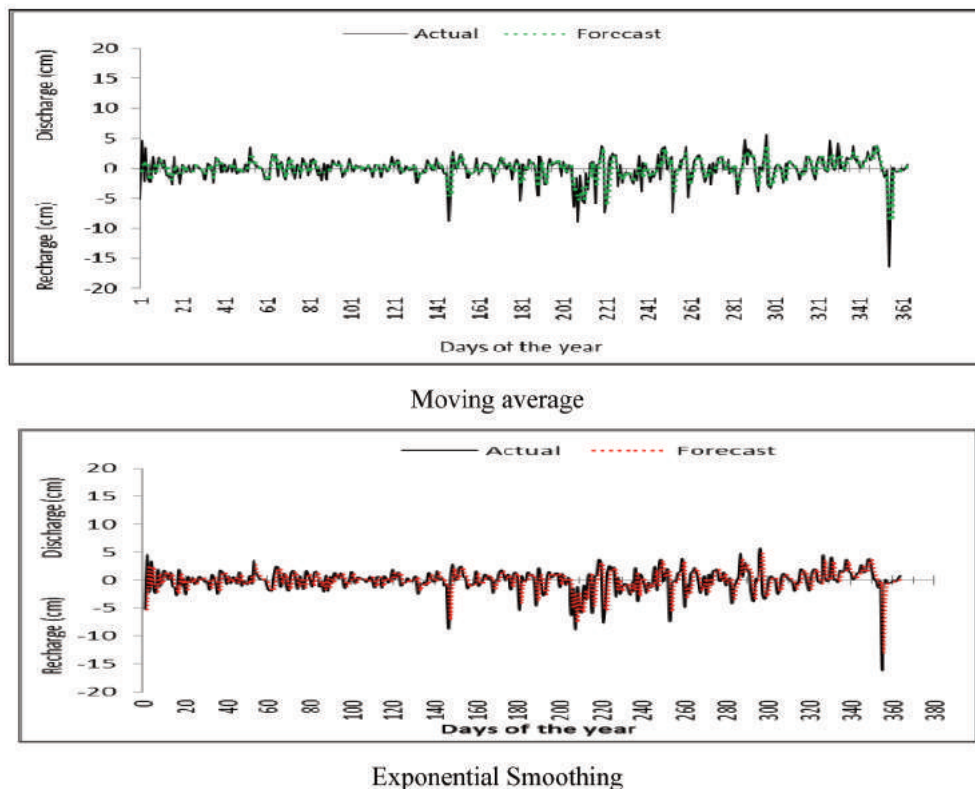


Figure 4. Actual and forecasted recharge and discharge at the study site

Acknowledgement

The researchers are grateful to the management of Irrigation Research Station, Kadawa, for the use of their facilities. All the technicians and field staff that contributed in data gathering are gratefully acknowledged. Special thanks to Mr. Jeremiah Wuya, Mr. Eddy Emmanuel and Late Malam Tijani for their invaluable contributions.

References

- [1] **Babajimopoulos C., Panoras A., Georgoussis H., Arampatzis G., Hatzigiannakis E., Papamichail D.:** 2007. Contribution to irrigation from shallow water table under field conditions. *Agricultural Water Management*, Vol. 92. No. 3. pp. 205-210.
<https://doi.org/10.1016/j.agwat.2007.05.009>
- [2] **Han, D., Song X., Curell M. J., Cao G., Zhang Y., Kang Y.:** 2011. A survey of groundwater levels and hydrogeochemistry in irrigated fields in the Karamay Agricultural Development Area, northwest China: Implications for soil and groundwater salinity resulting from surface water transfer for irrigation. *Journal of Hydrology*, Vol. 404. No. 3-4. pp. 217-234.
<https://doi.org/10.1016/j.jhydrol.2011.03.052>
- [3] **Sobowale, A., Sajo S. O., Ayodele O.E.:** 2016. Analysis of Onset and Cessation of Rainfall in Southwest Nigeria: Food Security Impact of Variability in the Length of Growing Season. *Hungarian Agricultural Engineering*, Vol. 30. pp. 23-30.
<http://dx.doi.org/10.17676/HAE.2016.30.23>
- [4] **Aboyeji O. S.:** 2016. Hydro-period dynamics of some inland valley agroecosystems in southwest Nigeria. *African Geographical Review*, Vol. 35. No. 3. pp. 294-305.
<https://doi.org/10.1080/19376812.2016.1168308>
- [5] **Tijani M. N., Obayelu A. E., Sobowale A., Olatunji A.S.:** 2014. Welfare Analysis of Smallholder Farmers by Irrigation Systems and Factors Affecting their Production Outputs in Nigeria, Sustainability of Water Quality and Ecology, Vol. 3-4. pp. 90-100. <https://doi.org/10.1016/j.swaqe.2014.12.002>
- [6] **Sangari D. U.:** 2006 An Evaluation of Water and Land Uses in the Kano River Project, Phase I, Kano State. *J. Appl. Sci. Environ. Mgt*, Vol. 11. No. 2. pp. 105-111.
<http://dx.doi.org/10.4314/jasem.v11i2.55002>
- [7] **Xu X., Huang G., Qu Z., Pereira L. S.:** 2010. Assessing the groundwater dynamics and impacts of water saving in the Hetao Irrigation District, Yellow River basin. *Agricultural Water Management*, Vol. 98. pp- 301–313.
<https://doi.org/10.1016/j.agwat.2010.08.025>
- [8] **Akande O. K., Olagunju R. E., Aremu S. C., Ogundepo E. A.:** 2018. Exploring Factors Influencing of Project Management Success in Public Building Projects in Nigeria. *YBL Journal of Built Environment*, Vol. 6. No. 1. pp. 47-62.
<http://dx.doi.org/10.2478/jbe-2018-0004>
- [9] **Siebert S., Burke J., Faures J. M., Frenken K., Hoogeveen J., Doll P., Portmann F. T.:** 2010. Groundwater use for irrigation – a global inventory. *Hydrol. Earth Syst. Sci*, Vol. 14. pp. 1863–1880. <http://dx.doi.org/10.5194/hess-14-1863-2010>
- [10] **Shah T.:** 2014. Groundwater Governance and Irrigated Agriculture. TEC Background Paper No. 19, Global Water Partnership, Stockholm, Sweden.
- [11] **Petheram C., Dawes W., Grayson R., Bradford A., Walker G.:** 2003. A sub-grid representation of groundwater discharge using a one-dimensional groundwater model. *Hydrol. Process*, Vol. 17. pp. 2279–2295.
<https://doi.org/10.1002/hyp.1332>
- [12] **Wang S., Song X., Wang Q., Xiao G., Liu C., Liu J.:** 2009. Shallow groundwater dynamics in North China Plain. *J. Geogr. Sci*. Vol. 19. pp. 175-188.
<https://doi.org/10.1007/s11442-009-0175-0>
- [13] **Vircavs V., Jansons V., Veinbergs A., Abramenko K., Dimanta Z., Anisimova I., Lauva D., Liepa A.:** 2011. Modeling of groundwater level fluctuations in agricultural monitoring sites. In: Lambrakis N., Stournaras G., Katsanou K. (eds) *Advances in the Research of Aquatic Environment*. Environmental Earth Sciences. Springer, Berlin, Heidelberg.
https://doi.org/10.1007/978-3-642-19902-8_25
- [14] **Jiménez-Martínez J., Candela L., Molinero J., Tamoh K.:** 2010. Groundwater recharge in irrigated semi-arid areas: quantitative hydrological modelling and sensitivity analysis. *Hydrogeology Journal*, Vol. 18. pp. 1811–1824.
<https://doi.org/10.1007/s10040-010-0658-1>
- [15] **Sobowale, A., Ramalan A. A., Mudiare O. J., Oyebode M. A.:** 2015. Evaluation of chloride mass balance and recharge in agricultural lands in Nigeria. *Agric. Eng. Int.: CIGR Journal*, Vol. 17. No. 2. pp. 11-22.
- [16] **Healy R. W., Cook P. G.:** 2002. Using groundwater levels to estimate recharge. *Hydrogeology Journal*, Vol. 10. 91–109.
<https://doi.org/10.1007/s10040-001-0178-0>
- [17] **Sobowale, A., Ramalan A. A., Mudiare O. J., Oyebode M. A.:** 2014. Groundwater recharge studies in irrigated lands in Nigeria: Implications for basin sustainability. *Sustainability of Water Quality and Ecology (SWAQE)*, Vol. 3–4. 124–132.
<https://doi.org/10.1016/j.swaqe.2014.12.004>
- [18] **Singh A, Panda S. N.:** 2012. Effect of saline irrigation water on mustard (*Brassica Juncea*) crop yield and soil salinity in a semi-arid area of North India. *Experimental Agriculture*, Vol. 48. pp. 99–110.
<https://doi.org/10.1017/S0014479711000780>



POSSIBILITIES OF IMPROVING PV/T SYSTEM EFFICIENCY

Author(s):

Sz. Bódi¹ – P. Víg² – I. Farkas²

Affiliation:

¹Mechanical Engineering Doctoral School, Szent István University, Páter K. u. 1. Gödöllő, H-2100, Hungary

²Department of Physics and Process Control, Szent István University, Páter K. u. 1. Gödöllő, H-2100, Hungary

Email address:

bodi.szabolcs@gamf.uni-neumann.hu, vig.piroska@gek.szie.hu, farkas.istvan@gek.szie.hu

Abstract

Photovoltaic/thermal hybrid collectors (PV/T) simultaneously are able to produce electrical energy and thermal energy as such unit combines a photovoltaic module with a thermal solar collector. In this paper, we are focusing on the liquid cooled PV/T systems. The paper overviews the energetics models of the PV/T collectors. Furthermore, it is planned to examine the possibilities for development of the photovoltaic thermal resistance network models for different PV/T collector arrangements.

Keywords

hybrid collector, efficiency, heat flow network, solar energy, influencing factors

1. Introduction

At present our world has to face energy problems. Environment is burdened by pollutants emitted by burning traditional energy carriers. In our world heat energy is obtained mostly by burning fossil energy sources (gas, oil, coal) [1]. The so called greenhouse effect is related to the excessive carbon-dioxide emission. Earth average temperature is increasing as the Earth's long-wave length radiation decreases significantly because of the formed polluter envelope [2]. Because of the increasing amount of gases causing greenhouse effect and because of other environment pollution, it is more and more necessary to use renewable energy sources (solar energy, wind energy, geothermal energy, biomass, sea and river energy) [3]. Concerning the use of solar energy, our country's climatic conditions are favourable. In case of architectural constructions, passive solar energy is utilized. In case of utilization of active solar energy, electrical and heat energy are obtained. The former is obtained by photovoltaic systems, the latter is obtained by solar collectors. Heat transfer at high temperature is realized with concentrator collectors.

Photovoltaic-thermal collectors (PV/T) are systems that generate electric energy and heat energy simultaneously, as photovoltaic modules are combined with traditional solar collectors (Figure 1).

A PV/T system consists of a PV module, with a heat exchanger behind it. In order to cool the PV module and extract the useful heat, a cooler fluid (water or air) is circulated in the heat exchanger.

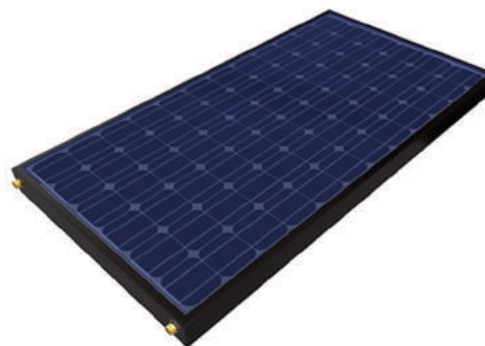


Figure 1. Layout of a PV/T collector

Photovoltaic PV systems absorb solar radiation and convert it into electricity. This is especially advantageous where electrical network is not available. Solar-thermal collectors absorb the solar radiation, and in order to produce heat energy, they convert it into heat with the heat converter fluid (water or air).

Solar radiation conversion efficiency of commercial PV modules is about 5-20%. It means that 80% of the incident solar radiation in the PV module is converted into heat. The generated waste heat is partially lost in the atmosphere, contributing to global warming, and the remaining heat increases the temperature of the PV cells. Cooling is proposed because of the increasing temperature of the cells. This is especially important in case of crystalline silicon cells as at high temperature the electrical conversion efficiency of the cells decreases below the nominal value.

PV/T systems are innovative solutions for increasing solar energy conversion efficiency. The circulating cold fluid maintains the temperatures of the cells as it extracts heat from the module, so it maintains the PV efficiency at an appropriate level. The heat extracted by the fluid is lead through pipes to low temperature applications, such as to industrial or agricultural sectors for drying, apartment heating, domestic water heating [4].

PV/T collectors generate more energy on unit surface than the adjacent solar collectors and PV modules. According to the collecting refrigerant, there are two types of PV/T collectors: water-cooling collectors (Figure 2) and air-cooling collectors [5]. Besides these, concentrating PV/T collectors (CPV/T) are also developed, which use lens or mirrors, and circulating liquid, in order to avoid the high operation temperature of the PV [6].

Water PV/T systems are used for heating buildings, for producing domestic hot water, where the need for running water is high. PV/T systems are more and more frequently combined

with heat pumps. It seems to be a useful application to preheat the flowed air in PV/T and BIPV/T (Building Integrated PV/T) systems, especially during the heating season, but also during the summer season [7].

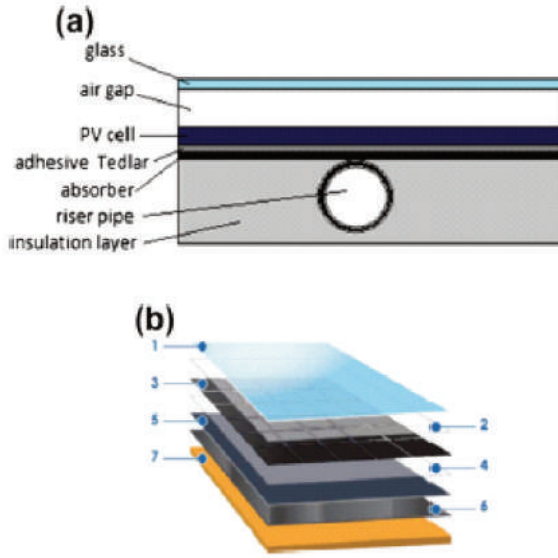


Figure 2. PV/T water systems [6]

To test the operation of the PV/T system, to determine its parameters, to compare measured and simulated results, we need to set up a suitable energy model for the given purpose, the most important ones being discussed below.

2. Energetic models used for PV/T collectors

In this paper we present the most often used energetic models in the investigation of photovoltaic (PV) modules, solar collectors and PV/T collectors. In order to present properly the models it is necessary to define the parameters which influence the efficiency of the PV/T collectors.

PV/T collectors are designed according to two basic aspects: the thermal efficiency or the photovoltaic efficiency is considered to be more important.

Thermal efficiency of PV/T collectors:

$$\eta_t = \frac{Q_h}{A_K \cdot I} \quad (1)$$

Thermal performance of PV/T flat-plate collectors:

$$Q_h = \dot{m}c_p(T_{out} - T_{in}) \quad (2)$$

The determination of the heat abstraction factor (FR) is:

$$F_R = \frac{Q_h}{A_K \cdot [I \cdot \tau \cdot \alpha - U_L \cdot (T_{in} - T_w)]} \quad (3)$$

F' factor varies with the material, for water in our study:

$$F' = \frac{1}{U_L} \frac{1}{W \left[\frac{1}{U_L(D_o + (W - D_o)F)} + \frac{1}{C_b} + \frac{1}{\pi D_i h_{wm}} \right]} \quad (4)$$

Thermal efficiency:

$$\eta_t = \frac{F_R \cdot A_K \cdot [I \cdot \tau \cdot \alpha - U_L \cdot (T_{in} - T_w)]}{A_K \cdot I} \quad (5)$$

Photovoltaic efficiency:

$$\eta_v = \eta_{ref} \cdot [1 - \beta_{pv} \cdot (t_{pv} - t_{ref})] \quad (6)$$

where: η_{ref} is the efficiency measured in Standard Test Conditions (STC), β_{pv} is the temperature coefficient of the module, t_{pv} is the cell temperature, t_{ref} is the reference temperature, which is defined during the measurement of the temperature coefficient, which is 25 °C in case of STC.

Total efficiency of PV/T systems:

$$\eta_0 = \eta_t + \eta_v \quad (7)$$

The modelling system should be applied to the local conditions, that is, environmental characteristics have to be input as mathematical functions. For the investigation of the efficiency of the PV/T module and for the calculation of energy generation, we have to develop a proper mathematical model. With this model we can realize the effect of the environmental characteristics on the investigated parameters [8].

Our aim is to develop a model, based on Physics, which presents the operation of the system, taking into consideration the mass flow, the inlet liquid temperature, the ambient temperature, the solar radiation and other parameters. Physical models of the processes can be shown with partial differential equations or equation systems. In this way we can present the dynamic properties of solar energy systems.

Experiments and measurements have to be performed to determine the parameters and physical constants of the models. This is a difficult and long task in case of complex systems, and there are only approaching methods for equation solutions.

The physically based models relates to determine the heat and mass transfer in the system (e.g. solar collector) with several approaches and neglections.

Depending on the mass flow and temperature of the inlet working fluid, the ambient temperature and solar radiation, the Hottel-Whillier model gives the temperature distribution of the flowing working fluid along the collector.

UL is the linear function of TC – TW variable. This model is called a quadratic efficient model. The useful amount of heat per unit of time generated by the collector, divided by the amount of heat per unit of time of the incident solar radiation on the surface of the collector is called the efficiency of the collector.

Where T_c [°C] is the outlet temperature of the liquid, T_w [°C] is the ambient temperature of the collector.

Flat-plate collectors are approached by the Hottel-Whillier or quadratic model. The operation of solar systems are modeled by softwares (e.g. TRNSYS, TRANSOLAR). Beside a direct numeric method it is possible to solve the obtained equation system by using indirect methods as well [8].

Buzás et al. [9] developed a model to describe the behavior in time of the flat-plate collectors. On the base of the energy balance of the solar collector.

The heat transfer process in the collector can be described with the following energy balance equation:

$$\frac{[\text{accumulated energy}]}{\text{time}} = \frac{[\text{incoming energy}]}{\text{time}} + \frac{[\text{exhaust energy}]}{\text{time}} \quad (8)$$

Total energy:

$$E = U^* + K + P \quad (9)$$

where $dK/dt = 0$ and $dP/dt = 0$, as the collector does not move, $dE/dt = dU^*/dt$.

With the enthalpy change of the system, the internal change of energy can be considered the same in case of change of solid and liquid systems ($dU^*/dt \sim d\text{Enthalpy}/dt$) [9].

The operation of artificial neural networks (NN) is based on biologic neural networks. Neuron is the operational and structural unit of the nervous system, a cell that can adopt, process and transmit information to glands, muscles, nerve cells with biochemical reactions.

The artificial neural network is the network of neurons. In case of practical problems, neural networks are able to help only in solving part tasks, they cannot be applied by themselves. Hybrid systems are used more and more often in case of complex tasks, during which NN is combined with other artificial intelligence methods (e.g. combination of NN and genetic algorithm), so several part tasks are solved with the most appropriate method [10].

Heat flow network modelling is based on that in a properly small part of material conductivity properties are considered constant. Dividing the model that describes the whole system into parts, we can construct the continuum as the interconnection of concentrated units of conductive resistances [11].

We can determine the average temperature of layers (nodes) if we group the whole structure according to its materials and layers. In the model we connect the nodes with heat transfer resistances and we assign the heat capacity to the nodes of the network [8].

3. Optimize the efficiency of PV/T collector using a heat-flow model

In a hybrid solar/solar collector, the electric efficiency can be increased by cooling the collector surface while gaining heat from the system. Therefore, the possibilities for optimizing the efficiency of a liquid cooled PV/T collector are discussed below for a heat-flow model. The aim to be achieved is to study a PV/T hybrid system that increases the efficiency of the system by reducing the temperature of the cell by increasing the electrical power and reducing the thermal radiation losses.

The cooling of the panels can be solved by means of cold water circulation or using a heat sink that is either pre-installed in the PV/T module or can be retrofitted to the rear of the module.

The temperature of the photovoltaic panel (PV) depends dynamically on the changes in the incident sunlight. Under realistic operating conditions, the PV panel temperature is subject to wind direction and wind speed fluctuation as well as randomly changing ambient temperature. In indoor experiments, we cannot properly implement these parameters, so we will set up a heat-flow model that includes the effects of the module's structure, its components and atmospheric conditions.

The thermal model to be set up has the following parts: it consists of an RC circuit to model the panel's thermal response. Secondly, it will be necessary to analyse radiation heat losses and to assess the convective heat transfer losses. We can consider the electrical equivalence of the thermal mechanisms of the PV panel so that the thermal resistance corresponds to the electrical resistance and the thermal capacity of the electrical capacity. On the PV panel layers, conductive heat transfer can be determined using these parameters [12].

The optical properties of solar cells limit the thermal efficiency of the PV/T collector since the selective heat absorber used for solar collectors does not match the heat absorbing emission of solar cells. Radiation losses can be reduced by using a casing that has a spectrally selective low emission factor in the infrared spectrum.

The balance equation can be solved for each layer of the module using the heat flow model. Numerically we can solve the energy equilibrium equation in the direction of flow of y water and in the x-direction perpendicular to which all layers are not continuously distributed to N_x and N_y nodes. We can solve the energy equation for all finite volumes (Figure 3).

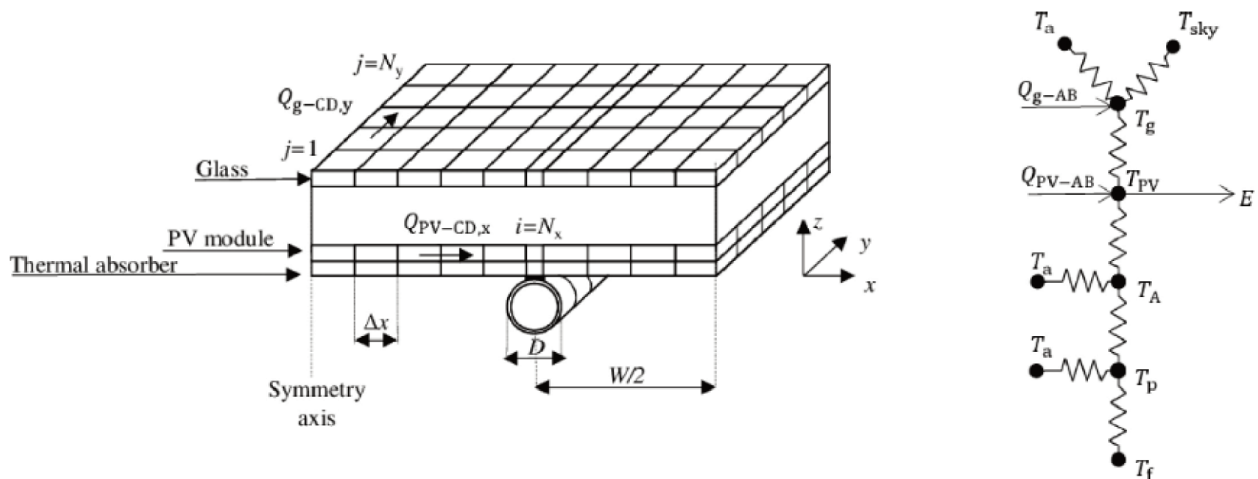


Figure 3. Sketch of the discretization used for the thermal analysis (left) and network of thermal resistances on the x-z plane between the layers of the PVT module (right) [13]

Conversion efficiency, i.e., the efficiency of converting incident sunlight into electricity is reduced by increasing the operating temperature of the cell. The heat absorbing energy balance can be written to any i, j node, as well as the heat transfer due to heat losses on the rear side of the panel. The convection at the rear of the panel and the thermal conductivity through the insulating layer is taken into account by the heat resistance. From the Energy Balance Equation, we can calculate the energy equilibrium equation for the fluid and the equilibrium equation for the cooling

pipe energy. Then we can calculate the output instantaneous electrical power as well as the thermal and electrical efficiency [13].

4. Conclusion

The heat transfer processes in the PV/T collectors to be tested can be written using the heat flow model to determine the thermal or electrical efficiency of the system and the parameters influencing

the efficiency. We can improve efficiency through various procedures, e.g. cold water circulation, reduction of radiation losses, etc. By comparing the simulation results with the results of the measurements, we can draw conclusions about the efficiency of the system, its structural design, its material properties, and further research and development goals which can be the basis for writing articles, conference presentations and development projects.

Nomenclature

A_k	surface of the module	m^2
C_b	thermal conductivity	W/mK
c_p	specific heat	J/kgK
D_o	outer diameters of the pipe	mm
D_i	inner diameters of the pipe	mm
F	collector tubing efficiency	-
F'	factor varies with the material	-
F_R	heat abstraction factor	-
h_{wm}	heat transfer coefficient of the liquid	W/m^2K
I	intensity of the incident radiation	W
\dot{m}	mass flow	kg/s
K	kinetic energy	J
P	potential energy	J
Q_h	available thermal performance	W
T_C	outlet temperature of the liquid	$^{\circ}C$
T_w	ambient temperature of the solar collector	$^{\circ}C$
t_{in}	input temperature	$^{\circ}C$
t_{pv}	cell temperature	$^{\circ}C$
t_{ref}	reference temperature	$^{\circ}C$
t_{out}	output temperature	$^{\circ}C$
t_w	ambient temperature	$^{\circ}C$
U^*	internal energy	J
U_L	total heat loss rate	W/K
W	distance between the rows of the coil of pipes	m

Greek letters

α	absorption characteristics of glazing	-
β_{pv}	temperature coefficient of the module	$\%/^{\circ}C$
η_0	total efficiency	-
η_v	photovoltaic efficiency	-
η_t	thermal efficiency	-
τ	transmittance characteristics of glazing	-

References

[1] **Horvath B., Borocz M., Zsarnoczai S., Fogarassy Cs.:** 2016. Long-term Green Innovation Opportunities Within the Hungarian District Heating Sector Towards 2030. *YBL Journal of Built Environment*, Vol. 4. No. 1. pp. 12-24. <http://dx.doi.org/10.1515/jbe-2016-0002>

[2] **Fekete I., Farkas I.:** 2012. Thermal analysis of shell-structured solar collectors. *Electrotehnica, Electronica, Automatica*, Vol. 60. No. 2. pp. 43-48.

[3] **Farkas I.:** 2003. Solar energy in agriculture. *Mezőgazda Kiadó*, Budapest, Hungary.

[4] **Koech R. K., Arusei G. K., Yegon G. K., Tonui J. K., Rotich S. K.:** 2014. Photovoltaic/Thermal (PV/T) System as Innovative Solution to Increase Solar Energy Conversion Efficiency. *International Journal of Emerging Technology and Advanced Engineering*, Vol. 4. No. 10. pp. 717-722.

[5] **Kim J. H., Park S. H., Kang J. G., Kim J. T.:** 2014. Experimental performance of heating system with building-integrated PVT (BIPVT) collector. *Energy Procedia*, Vol. 48. pp. 1374-1384. <http://dx.doi.org/10.1016/j.egypro.2014.02.155>

[6] **Tripagnagnostopoulos Y.:** 2014. Hybrid Photovoltaic/Thermal Collectors. University of Patras, Patra, Greece, pp. 1-50.

[7] **Zondag H. A.:** 2008. Flat-plate PV-Thermal collectors and systems: A review. *Renewable and Sustainable Energy Reviews*, Vol. 12. pp. 891-959. <http://dx.doi.org/10.1016/j.rser.2005.12.012>

[8] **Háber I. E., Farkas I.:** 2016. Combining CFD simulations with blockoriented heatflow-network model for production of photovoltaic energy production. *Journal of Physics: Conference Series*, Vol. 268. No. 1. pp. 1-7. <http://dx.doi.org/10.1088/1742-6596/268/1/012008>

[9] **Géczy-Víg P., Farkas I.:** 2007. Possibilities of ANN modelling for thermal behaviour of a solar system. *Proceedings of the International Conference on Research and Teaching of, Nitra, Slovakia, June 5-6, 2007*, pp. 22-27.

[10] **Buzás J., Farkas I., Bíró A., Németh R.:** 1998. Modelling and simulation aspects of a solar hot water system, *Mathematics and Computers in Simulation*, Vol. 48. No. 1. pp. 33-46. [http://dx.doi.org/10.1016/S0378-4754\(98\)00153-0](http://dx.doi.org/10.1016/S0378-4754(98)00153-0)

[11] **Fürjes P., Dúcsó C., Vízváry Z., Bársony I.:** 2006. Transient Heat Conduction Effects in Deformed Microstructures. *Proceedings of Eurosensors XX, Göteborg, Sweden, Vol. 2*. pp. 164-165.

[12] **Armstrong S., Hurley W. G.:** 2010. A thermal model for photovoltaic panels under varying atmospheric conditions. *Applied Thermal Engineering*, Vol. 30. pp. 1488-1495. <http://dx.doi.org/10.1016/j.applthermaleng.2010.03.012>

[13] **Guarracino I., Mellor A., Ekins-Daukes N. J., Markides C. N.:** 2016. Dynamic coupled thermal-and electrical modelling of sheet-and-tube hybrid photovoltaic/thermal (PVT) collectors. *Applied Thermal Engineering*, Vol. 101. pp. 778-795. <http://dx.doi.org/10.1016/j.applthermaleng.2016.02.056>

CONTENTS OF NO 33/2018

ANALYSIS OF THE TOWED AGRICULTURAL MACHINERY MANUFACTURERS IN EUROPE P. Kiss – J. Hajdú – L. Máthé – J. Dobos – L. Magó Szent István University, Faculty of Mechanical Engineering, NARIC, Institute of Agricultural Engineering5	THE ROLE OF DIGITALIZATION IN THE AGRICULTURAL 4.0 – HOW TO CONNECT THE INDUSTRY 4.0 TO AGRICULTURE? I. Kovács – I. Husti Institute of Engineering Management, Szent István University, Páter K. u. 1., Gödöllő, H-2103, Hungary38
ALTERNATIVE UTILIZATION OPTIONS IN MULTI-FUNCTION COMPOSTING TECHNIQUES M. Czikkely – Zs. Tóth – Cs. Fogarassy Assistant lecturer, Doctoral candidate, Climate Change Economics Research Centre, Faculty of Economics and Social Sciences, Szent István University, Hungary Faculty of Economics and Social Sciences, Szent István University, Hungary Associate Professor, Director of Climate Change Economics Research Centre, Faculty of Economics and Social Sciences, Szent István University, Hungary11	SYMMETRY-BASED STUDY OF QUASI-ONE-DIMENSIONAL SYSTEMS RELEVANT TO SOLAR CELL APPLICATIONS I.R. Nikolényi – Cs. Mészáros Department of Physics and Process Control, Szent István University, Páter K. u. 1., Gödöllő, H-2100, Hungary43
DEVELOPMENT OF BIOMASS-BASED PYROLYSIS CHP (R + D) V. Madár – I. Bácskai – A. Dhaundiyal – L. Tóth Szent István University, Faculty of Mechanical Engineering, Cső-Montage Ltd. and Pyrowatt Ltd. National Agricultural Research and Innovation Centre, Institute of Mechanical Engineering Szent István University, Faculty of Mechanical Engineering17	GROUNDWATER DYNAMICS AND RECHARGE TRENDS IN SEMI-ARID IRRIGATED LANDS OF NIGERIA A. Sobowale – A. A. Ramalan – O. J. Mudiare – M. A. Oyebode Department of Agricultural and Bioresources Engineering, Federal University of Agriculture, P.M.B. 2240 Abeokuta 110001, Nigeria. Department of Agricultural Engineering, Ahmadu Bello University, Zaria, Nigeriay.....48
INFLUENCE OF MOISTURE AND CURRENT FREQUENCY ON ELECTRICAL POTENTIAL OF SORGHUM GRAINS (SORGHUM BICOLOUR (L.) MOENCH) J. Audu – O. J. Ijabo – J. O. Awulu Dept. of Agric. & Environmental Engineering, College of Engineering, University of Agriculture, Makurdi, Nigeria24	POSSIBILITIES OF IMPROVING PV/T SYSTEM EFFICIENCY Sz. Bódi – P. Víg – I. Farkas Mechanical Engineering Doctoral School, Szent István University, Páter K. u. 1. Gödöllő, H-2100, Hungary Department of Physics and Process Control, Szent István University, Páter K. u. 1. Gödöllő, H-2100, Hungary55
THE CHANGE ON OPERATOR’S FOCUSING SCHEME INSIDE A MULTI-TASKING OFF-ROAD VEHICLE ALONG WORKING HOURS I. Szabó – M. Hushki – Z. Bártfai – L. Kátai Faculty of Mechanical Engineering, Institute of Mechanics and Machinery, Szent István University, Páter K. u. 1., Gödöllő, H-2103, Hungary.....30	

HUNGARIAN

AGRICULTURAL

ENGINEERING

